Featured in Physics

FLASH: New intersection of physics, chemistry, biology, and cancer medicine

Marie-Catherine Vozenin*

Radiotherapy and Radiobiology Sector, Radiation Therapy Service, University Hospital of Geneva and Laboratory of Innovation in Radiobiology Applied to Radiotherapy (LiRR), University of Geneva, Geneva, Switzerland

Billy W. Loo, Jr.

Department of Radiation Oncology and Stanford Cancer Institute, Stanford University School of Medicine, Stanford, California 94305, USA

Sami Tantawi

SLAC National Accelerator Laboratory, Menlo Park, California 94025, USA

Peter G. Maxim

Department of Radiation Oncology, University of California, Irvine, Irvine, California 92697-2695, USA

Douglas R. Spitz

Free Radical and Radiation Biology Program, Department of Radiation Oncology, University of Iowa, Iowa City, Iowa 52242, USA

Claude Bailat

Institute of Radiation Physics/CHUV, Lausanne University Hospital, Switzerland

Charles L. Limoli

Department of Radiation Oncology, University of California, Irvine, California 92697-2695, USA

(published 19 September 2024)

Ultrahigh dose rate, FLASH radiotherapy has emerged as one of the most promising innovations over the past decade in the field of radiation oncology, with the potential to eradicate radiation resistant primary tumors and improve the therapeutic outcome for cancer patients. FLASH is based on delivering radiation doses at ultrahigh dose rates (UHDR; >40 Gy/s), more than 1000 times faster than irradiation at conventional dose rates (CONV). The experimental evidence demonstrating the differential effect of dose rate modulation on tumors and normal tissue is reviewed. Preclinical data consistently show that the antitumor efficacy of cytotoxic doses is not dependent on dose rate, but in normal tissues UHDR significantly reduces normal tissue toxicities compared to CONV, as observed *in vivo*. These observations define the FLASH effect. The FLASH effect has been reported to occur when using single or hypofractionated dose regimens in several experimental animal models (mice, rat, zebrafish, pig, and cats) and in multiple organs (lung, skin, gut, and brain) by numerous groups worldwide. Note that the FLASH effect has been demonstrated with electron, photon, and hadron (proton and heavier ion) beams. The current status and future technological development are reviewed, with an emphasis on critical beam parameters, future beam modalities, and prerequisites for safe clinical translation in terms of dosimetry, radioprotection, and treatment planning systems. Mechanistic investigations at the physicochemical and biological levels are presented, as are strategies to support and initiate clinical translation. This comprehensive review provides multidisciplinary radiation scientists with a road map of the technological, physical, chemical, biological, and clinical considerations that have made FLASH topical. These considerations are presented with a realistic and practical backdrop of the limitations and challenges that lie ahead.

DOI: 10.1103/RevModPhys.96.035002

*Contact author: marie-catherine.vozenin@hug.ch

CONTENTS

I. INTRODUCTION

Since the discovery of x rays by Wilhelm Conrad Roentgen in 1896, ionizing radiation has been used for more than a century to treat cancer. While the anticancer benefits of ionizing radiation were immediately pondered, the discovery of normal tissue toxicity occurred in 1904 when Pierre Curie described the first radiation-induced complications on the forearm of his wife, Marie Curie. These two fundamental yet antagonistic principles suggest that radiation-induced cancer kill always comes at the cost of normal tissue damage. They still form the basis of radiation oncology and define the concept of the therapeutic index (i.e., the enhanced kill of tumors versus normal tissue sparing). Strategies to achieve a therapeutically exploitable difference in the radiation sensitivity of tumors versus normal tissue have evolved tremendously in recent years. After the discovery of ionizing radiation, the next major breakthrough came from the French school of radiotherapy (circa 1930), when researchers discovered that daily doses of radiation (fractionation) over several weeks greatly improved the patient's chance for a cure, i.e., eradication of the disease within the limits of tolerable side effects.

Since then, the technology has advanced tremendously (Fig. 1), and radiotherapy (RT) is now often prescribed with curative intent. It remains one of the most powerful and cost-effective tools in the fight against cancer, with more than half of all cancer patients treated at some point in the management of their disease (Rosenblatt *et al.*, 2013; Atun *et al.*, 2015; Lievens, Borras, and Grau, 2015; Pistenmaa *et al.*, 2018). Over the past decade, technological and biological advances have transformed RT into a precise and personalized treatment; nevertheless, the treatment of many tumors is still restricted by normal tissue complications and the frequent development of metastasis that ultimately kills patients. Therefore, enhancing the differential effect of RT by selective targeting of tumors, enhancing tumor radiosensitization, and/or enhancing normal tissue protection has been and remains the overarching goal for radiobiologists and oncologists.

In this context, our teams conceptualized and implemented a novel approach in RT based upon the delivery of radiation at ultrahigh dose rates (UHDRs), a new modality termed FLASH. FLASH is potentially paradigm shifting, with multiple benefits that include the capability to simultaneously eliminate targeting uncertainty from physiological tumor or organ motion and effectively kill tumors while minimizing normal tissue complications. This combination of benefits has now been collectively termed the FLASH effect, and thus far it has been demonstrated almost exclusively using *in vivo* models. The FLASH effect occurs when the overall irradiation time is extremely short (a few hundred milliseconds or less) and/or when delivered at an UHDR (a mean dose rate above 40 Gy/s). However, this definition has proven to be overly simplistic (Montay-Gruel *et al.*, 2019; Vozenin, Hendry, and Limoli, 2019). The full characterization of FLASH is much more complex and still incompletely understood as it involves several interdependent physical beam parameters [as recently reviewed by Schneider *et al.* (2022)]. Recent analyses show that, besides average dose rate, the instantaneous dose rate and the overall time of irradiation are critical parameters as well.

In addition, regarding a pulsed electron beam structure, the dose per pulse, number of pulses, pulse width, interspacing (i.e., the repetition frequency), and total duration of exposure can modulate the biological outcome. Despite major differences in the macrostructure and microstructure between various FLASH beams that impact tissue dose deposition, the FLASH effect has been found in preclinical mouse models using electrons, protons, carbon ions, and photons (x rays) (Farr *et al.*, 2022). This finding suggests that the most important physical parameter is probably the overall time of exposure, at least when small volumes of tissue are irradiated. It also suggests the existence of a common biological parameter and/or profile that will constitute the molecular determinant(s) of the FLASH effect.

The excitement surrounding FLASH lies in its unexpected differential effect on tumors versus normal tissue. At a given cytotoxic dose for tumors, FLASH ameliorates a wide range of normal tissue complications compared to conventional dose rate radiotherapy (CONV), resulting in an increase in the therapeutic index. The biological factors contributing to the FLASH effect are covered in the Secs. III and IV. Additionally, in terms of its biological superiority, FLASH promises to be a powerful tool to overcome the confounding effects of organ motion owing to the nearly instantaneous delivery of the dose (Maxim, Keall, and Cai, 2019; Maxim, Tantawi, and Loo, 2019). The relevant technological developments required for medical applications and the medical physics considerations are presented and discussed in Sec. II. Dosimetry, diagnostics, and beam monitoring

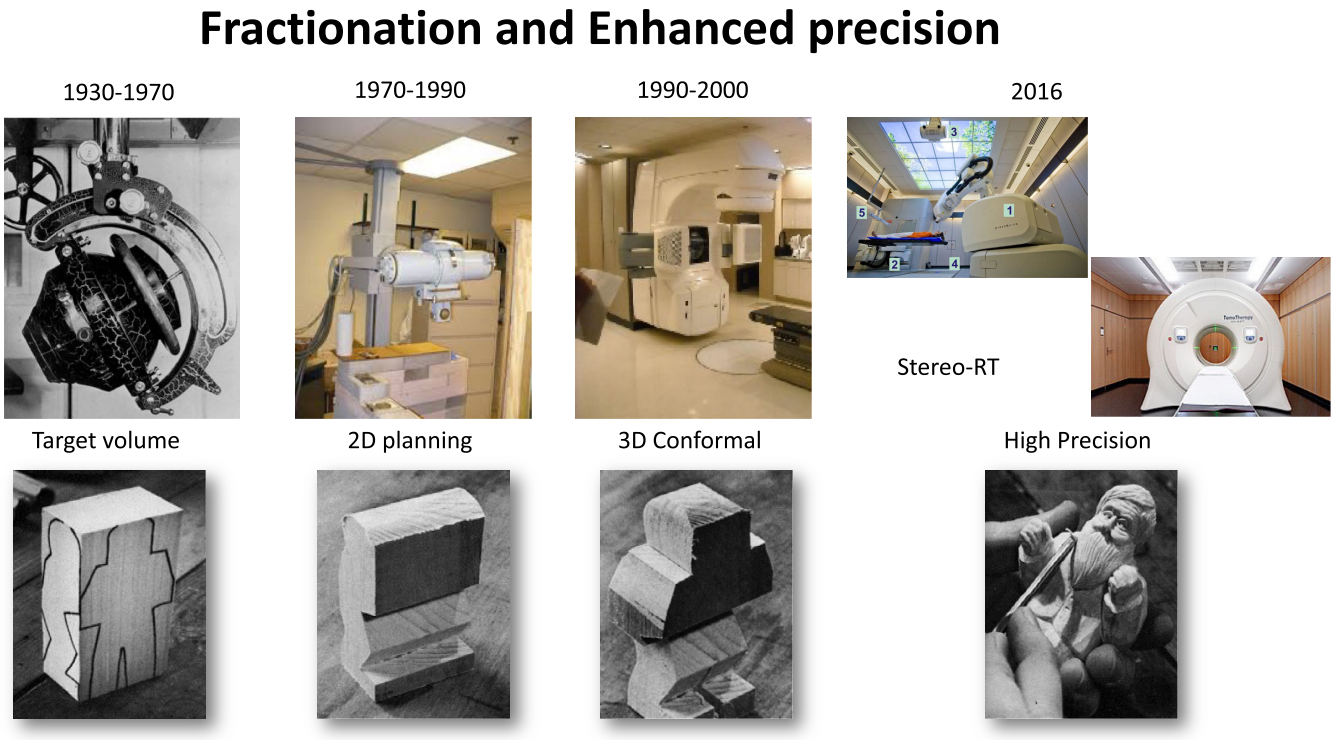

FIG. 1. One hundred years of evolution in radiotherapy to optimize the therapeutic index and differential effect is based on fractionation of the dose and enhanced precision.

considerations are important for moving the field of FLASH forward and are included in the Supplemental Material (207). To date, the FLASH effect has been investigated by numerous groups around the world [recently reviewed by Kacem, Almeida *et al.* (2022), Vozenin, Bourhis, and Durante (2022), and Limoli and Vozenin (2023)], mainly while using mouse models (wild type, genetically engineered, and immunocompetent and immunocompromised). Most of those studies were performed using well characterized radiobiological systems developed over the past 50 years to investigate the biological basis of normal tissue complications that occur in acute (gut and the hematopoietic system) and late-responding organs (lung, skin, and brain). We emphasize that *in vivo* experimentation has to date been the only robust way to validate the FLASH effect, while the critical physical parameters required to trigger the FLASH effect are still being optimized for various modalities, as discussed in Sec. II. The preponderance of data published to date demonstrates that FLASH does not spare tumors *in vivo*, thus reinforcing the idea that tumor kill is dose rate independent, unlike normal tissue responses. In addition, the FLASH effect has primarily been studied using single high dose irradiation, and only just recently with hypofractionated regimens (Montay-Gruel *et al.*, 2021; Liljedahl *et al.*, 2022). However, studies investigating the benefits of FLASH using conventional fractionation are scarce (Limoli *et al.*, 2023). Noteworthy too is that the FLASH effect (normal tissue sparing and tumor kill) has been demonstrated in multiple species, including rats, cats, and dogs, whereas the normal tissue protection component has been shown to occur also in zebrafish and pigs. These findings are further reviewed in Secs. III and V. Last, investigations of human cells, tissues, and samples are still scarce and individual sensitivity to FLASH remains to be investigated, as recently suggested by Chabi *et al.* (2021). In addition, and despite many positive findings, we also note that a few studies have reported the absence of the FLASH effect using synchrotron photon (Smyth *et al.*, 2018), proton (Beyreuther *et al.*, 2019), and electron (Venkatesulu *et al.*, 2019) beams. This emphasizes the necessity of understanding the conditions (both physical and biological parameters) capable of producing the FLASH effect to promote the safe and reliable transfer of these strategies into the clinic.

With a dose modifying factor (DMF) of FLASH versus CONV ranging from 1.1 to 1.5, given the consistent nature of the FLASH effect across multiple tissues and species along with the magnitude of the benefits observed in various preclinical studies, FLASH has sparked the imagination and interest of radiation scientists and oncologists worldwide. It is now recognized as one of the most promising approaches to resolve normal tissue toxicity, enhance the therapeutic index of RT, eliminate organ motion uncertainty, and possibly overcome radioresistance; see Fig. 2.

The field is progressing rapidly toward the clinic, with trials using electron FLASH (eFLASH) and proton FLASH (pFLASH) in domestic animals (Vozenin *et al.*, 2019; Konradsson *et al.*, 2021; Velalopoulou *et al.*, 2021; Rohrer Bley *et al.*, 2022; Børresen *et al.*, 2023), one feasibility study in a single patient (Bourhis *et al.*, 2019), and a therapeutic trial (IMPULSE) started with a 9 MeV electron beam. Low-energy electron beams limit clinical applications to superficial tumors, whereas a feasibility study treating bone metastases in cancer patients with protons has been published (FAST-01 trial NCT04592887) (Mascia *et al.*, 2023). The use of protons provides additional opportunities (albeit not

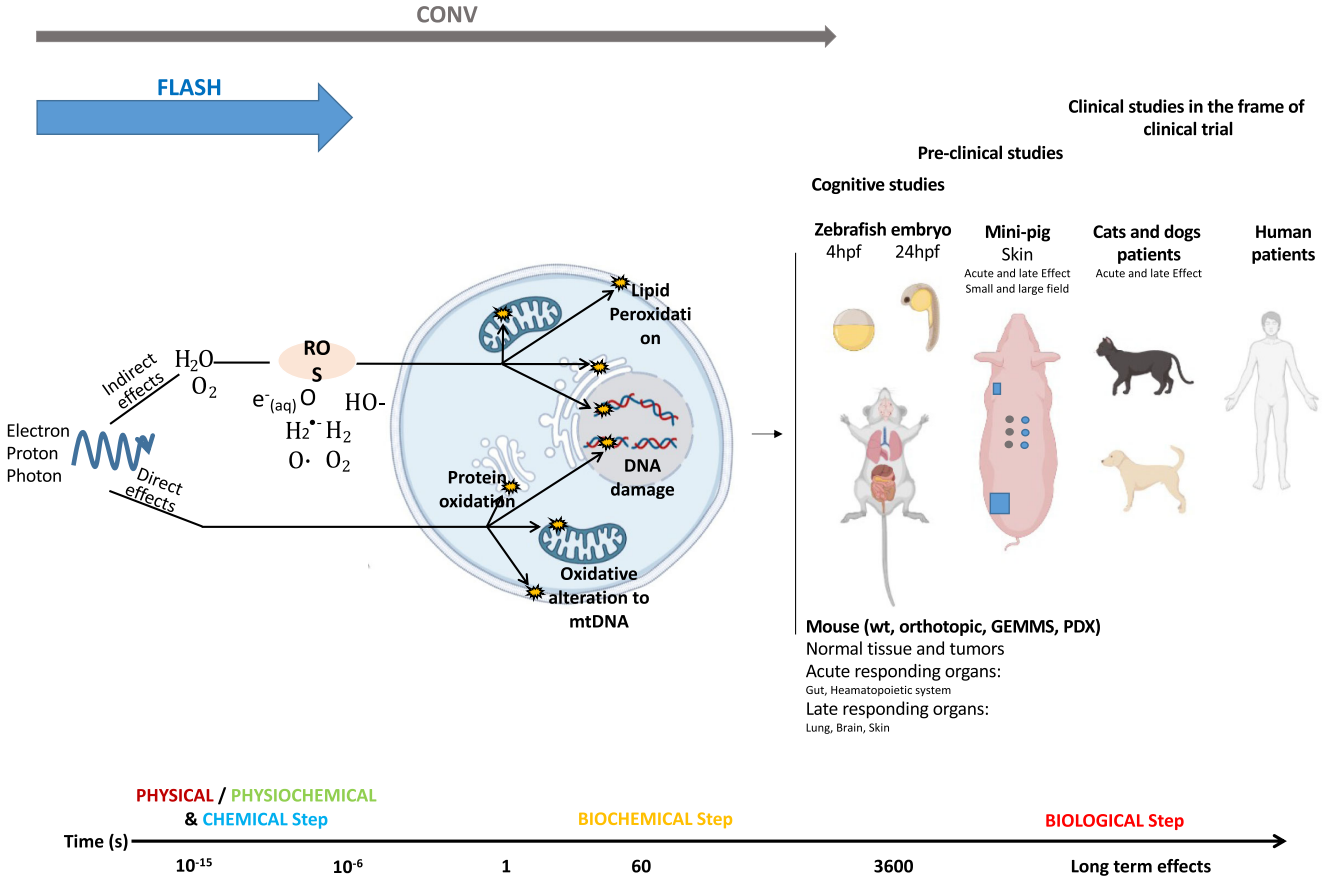

FIG. 2. FLASH effect: from beams to tissues. The main interest of FLASH lies in its differential impact on tumors vs normal tissue, where at a given cytotoxic isodose for tumors FLASH spares normal tissue. This effect has been named the FLASH effect and has been validated primarily using intermediate energy electron beams capable of delivering high doses in a short period of time (<200 ms). The FLASH effect has now been reproduced with photon and proton beams, and the initial physicochemical events occurring immediately after FLASH irradiation are being investigated. In the meantime, the FLASH effect has been demonstrated in many experimental animal models, mainly involving mice and zebrafish, but also in preclinical experiments performed with minipigs, as well as in early clinical trials performed with cat and dog patients suffering from spontaneous cancer. The first human patient with cutaneous lymphoma has been treated twice with electron FLASH, and the first clinical trial on metastasis of extremities was completed with proton FLASH.

without caveats) to hasten clinical translations of FLASH, as reviewed by Diffenderfer *et al.* (2022). Protons allow for a more accurate control of dose deposition profiles, coupled with a degree of dose conformality that can be achieved by superimposing the Bragg peak over the tumor volume. Combining the well-known advantages of proton beams to enhance the therapeutic ratio (Lomax *et al.*, 1999) with their capability of delivering ultrahigh dose rates to deep-seated tumors has distinct advantages but also involves overcoming other technological constraints (as discussed in Sec. II). Last, the current state of the field suffers from the lack of FLASH enabled systems and, as detailed throughout this review, each type of beam (electron, photon, and proton) has its specific limitations. With this backdrop, we have organized our review to systematically highlight the physical, chemical, biological, and clinical implications unique to specific FLASH beams (see Fig. 3), thereby providing unique and comprehensive insight into this rapidly evolving and interesting field.

II. RADIATION BEAMS: TYPES AND FLASH CAPABILITY

The future development of new accelerators will be essential for exploring and understanding the FLASH effect along with ensuring global and cost-effective clinical applications. Whereas the high dose rates required for producing the FLASH effect can in principle be achieved using present technologies, the size, weight, and power needed make the machine large, expensive, and difficult to operate; the FLASH effect would not be compatible with most current hospital radiation therapy shielded rooms. Research and development (R&D) on linear accelerators (linacs) and their associated radio-frequency (rf) systems to push for higher gradient, higher efficiency, and cost-effective, compact systems has been and continues to be the subject of intense effort for high-energy physics applications; the ten-year road map for this R&D in the U.S. was detailed in 2017. Many R&D efforts dedicated to advancing each of the modalities described in this review and transforming the modalities into practical

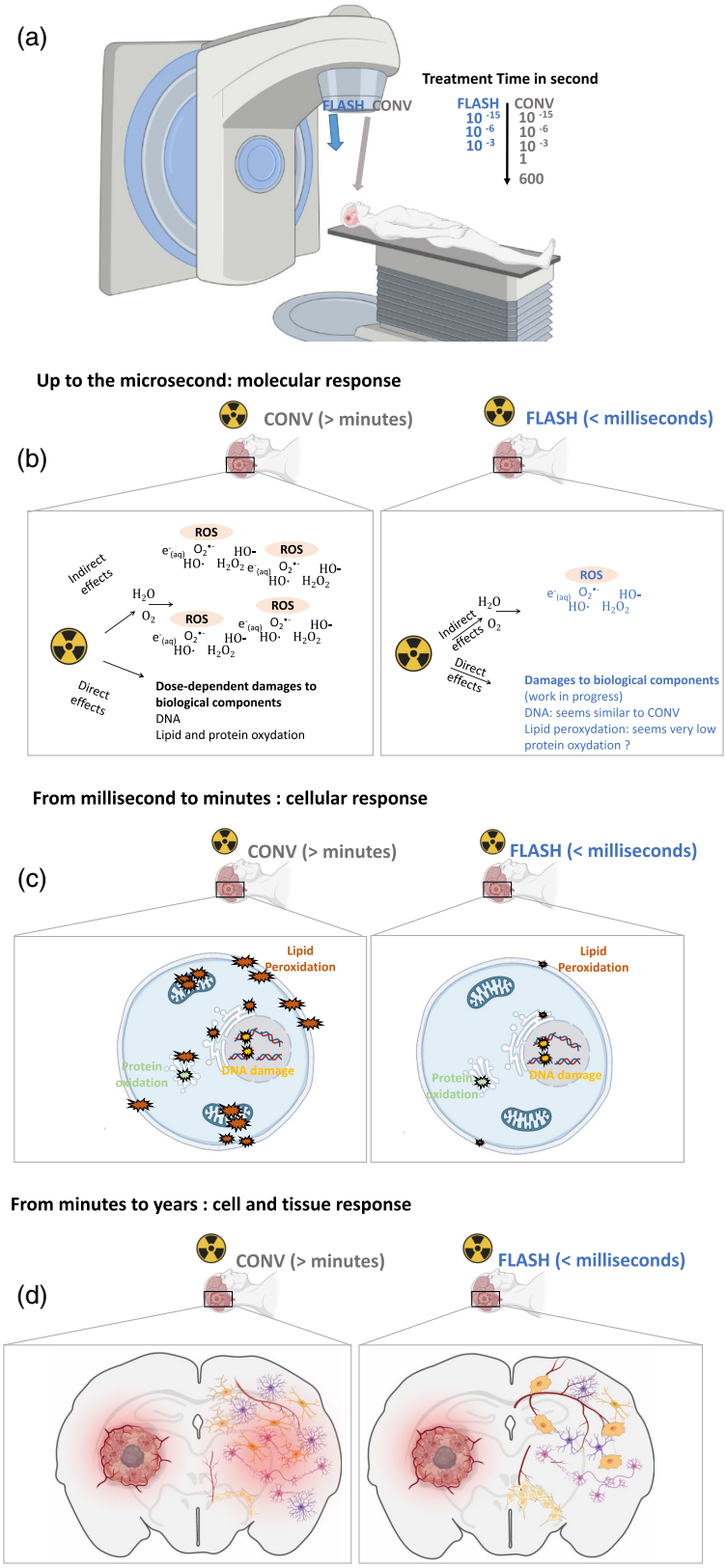

FIG. 3. The FLASH effect is a matter of time. (a) Comparative time frame to deliver 10 Gy with FLASH and CONV; see Secs. II and V. (b) Impact of FLASH and CONV at the molecular level; see Sec. IV. (c) Impact of FLASH and CONV at the cellular level; see Secs. III and IV. (d) Impact of FLASH and CONV at the cellular and tissue level; see Secs. III–V.

technologies to fit with a typical hospital RT facility are capitalizing on these advances. In what follows, we provide a summary of the various devices available today and perform a comprehensive comparison of the various technologies, highlighting the similarities and differences and specific advantages and disadvantages to emphasize priorities for future technological developments. Note that for currently available and emerging FLASH technology excellent reviews have recently been published (Farr, Parodi, and Carlson, 2022; Schulte *et al.*, 2023). Of note, because it is not well understood exactly what beam parameters are required to produce the FLASH effect, we distinguish UHDR systems by whether they have been validated by published results of biological experiments demonstrating FLASH effects.

A. Electron FLASH beams

Electron linear accelerators producing electron beams in the MeV energy range (up to about 20 MeV) are commonly used in radiation therapy and can be considered a mature technology. They can be used directly for the treatment of superficial targets (such as skin tumors) at conventional dose rates, limited primarily by typical clinical dose monitoring systems, and ultrahigh dose rate electron irradiation is readily achievable simply by direct treatment with the electron beam at the full current capability of existing accelerators. While this approach is limited to superficial tumors in human patients (up to a few centimeters), MeV energy electrons can penetrate the depth of small-animal models such as mice.

As such, the Kinetron (CGR-MeV, France, which was later bought by PMB/Alcen, France) was the device used in the seminal paper by Favaudon *et al.* (2014), who demonstrated the FLASH effect. Dismantled in 2020, the Kinetron was initially funded by the European Union after the Chernobyl disaster in 1986; Ponette *et al.* (1996) used it to investigate pulsed radiolysis and the biological impact of pulsed beams *in vitro*. The Kinetron was a pulsed electron beam with a beam energy of 4 to 5 MeV, and its main experimental interest was its flexibility, as it could be operated in conventional RT modes (dose rate < 0.03 Gy/s, dose per pulse $\sim 10^{-3}$ Gy), high dose rate and ultrahigh dose rate modes with a pulse output reproducibility better than 5% (Lansonneur *et al.*, 2019). The flexibility of the accelerator was driven by an adjustable triode electron gun that is able to provide peak beam currents of 10–250 mA, pulse widths of 0.1–2.2 μs, at full width at half maximum (FWHM), and macropulse repetition frequencies (PRFs) of 10–250 Hz (Favaudon *et al.*, 2019; Lansonneur *et al.*, 2019). Under typical treatment conditions, this flexibility enabled the linac to achieve average dose rates between 10^{-1} and 10^{6} Gy/s under single-pulse usage.

Built in 2013 to explore the biological and clinical interest of FLASH, the Oriatron eRT6 (PMB-Alcen, Peynier, France) was a functional replicate of the Kinetron. It is also an electron linac that allows output control based on fine control over several beam parameters of interest, including the number of electron pulses, the PRF (5–200 Hz), and the pulse width (0.5–4 μs) (Jaccard *et al.*, 2017, 2018; Petersson *et al.*, 2017; Jorge *et al.*, 2019). The eRT6 beam energy is nominally 6 MeV, and it can be adjusted to achieve a dose per pulse of 14 Gy (Jaccard *et al.*, 2017; Petersson *et al.*, 2017). For example, Petersson *et al.* achieved average dose rates on the order of 10^{-2} to 10^{3} Gy/s, which corresponds to an intrapulse (instantaneous) dose rate of 10^{2} to 10^{7} Gy/s, and a dose per pulse of 10^{-4} to 10^{1} Gy, assuming a pulse width of 1.8 μs and a PRF of 100 Hz. Additionally, the eRT6 delivers ultrahigh dose rates at the standard 100 cm source-to-surface distances (SSDs) in a field size of 1.6–20 cm and has a therapeutic (R80) range of 1.8 to 2.3 cm. For now, the Oriatron/eRT6 can be considered the reference for investigating the FLASH effect, as most of the experimental studies published (>15 publications to date in many organs and animal models) have been produced with it. In most instances, these studies have been performed by pushing the dose rates to the maximum achievable for the eRT6 at single-pulse widths of 1.8 μs. However, as summarized (Fig. 4), irradiating at such high dose rates is probably not required to produce a robust FLASH effect, as proton-UHDR systems (see Sec. II.C) have been found to deliver the FLASH effect over millisecond timescales (i.e., lower mean dose rates). Nonetheless, as apparent in this review, unvalidated systems should strive for short-duration treatment times with microsecond pulse widths such that single dose (or multiple dose) studies can be designed with the highest likelihood of achieving a robust *in vivo* FLASH effect under a given set of experimental conditions.

To date the first dose rate escalation study was published by Montay-Gruel *et al.* (2017) and was performed using whole-brain irradiation of mice, in which neurocognition was employed to validate the sparing outcome; see Fig. 5. This study identified a threshold for maximal neuroprotection at dose rates above 100 Gy/s and when the dose was delivered in up to 10 pulses (1.8 μs width) at a frequency of 100 Hz (a 10 Gy dose was delivered in less than 90 ms). This study was later reproduced in zebrafish embryos (Kacem *et al.*, 2022).

These types of dose escalation studies are of the utmost importance for safe clinical implementation. They will ultimately be required to critically characterize the FLASH effect under variable irradiation geometries and biological conditions.

In Oxford, England, an in-house-developed 6 MeV electron linear accelerator is used for FLASH radiation studies (Ruan *et al.*, 2021; Moon, Petersson, and Olcina, 2022). The main components, for example, the diode gun and the traveling-wave waveguide, were taken from an Elekta SL75 clinical linear accelerator (Elekta AB, Stockholm, Sweden). The accelerator has a fixed horizontal beamline, with the beam exiting through a thin output window (10 μm thick beryllium-copper foil) and a scatter filter (usually a 30 μm thick titanium foil) into an *in vivo* or *in vitro* experimental area where the temperature and CO_2 level can be controlled (Berne *et al.*, 2021). The collimator system allows for any field shape and size ≥5 cm in diameter. The electron pulses have a width of ~3.4 μs, with a PRF ranging from 25 to 300 Hz (Berne *et al.*, 2021). The dose per pulse varies from 4 mGy to 5 Gy at an SSD of around 63 cm, which corresponds to a variable average dose rate of 0.1 Gy/s to 1.5 kGy/s. The FLASH-sparing efficacy of this device has been validated (Ruan *et al.*, 2021).

PITZ-DESY (Stephan *et al.*, 2022) is a superconducting photoinjector in Zeuthen, Germany, with an energy of up to

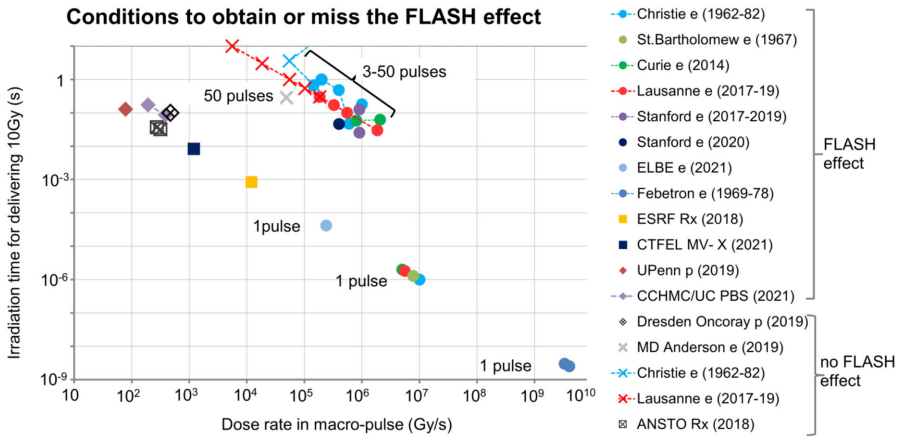

FIG. 4. Summary the temporal dosimetry characteristics of the published experimental data describing the FLASH effect *in vivo* (Hendry *et al.*, 1982; Favaudon *et al.*, 2014; Loo *et al.*, 2017; Montay-Gruel *et al.*, 2017, 2018, 2019; Schueler, Trovati *et al.*, 2017; Vozenin, Hendry, and Limoli, 2019; Diffenderfer *et al.*, 2020; Levy *et al.*, 2020) or *in vitro* (colored dots) (Town, 1967; Berry *et al.*, 1969; Epp *et al.*, 1972; Michaels *et al.*, 1978), those that have not been able to observe the FLASH effect (black or gray dots) (Smyth *et al.*, 2018; Beyreuther *et al.*, 2019; Venkatesulu *et al.*, 2019), and the dose rate deescalation studies showing the range in which the FLASH effect is lost (colored crosses). The horizontal axis denotes the dose rate per pulse for electrons (e) and protons (p) or in a single stripe [as described by Montay-Gruel *et al.* (2018)] for synchrotron radiation (Rx). The vertical axis corresponds to the total irradiation time needed for delivering 10 Gy at the average dose rate quoted by the authors of the respective publications. The parameters for other dose values have been changed accordingly. Courtesy of Dr. J. F. Germond. Adapted from Montay-Gruel *et al.*, 2021.

22 MeV that is now available for radiobiological studies and will be upgraded to 250 MeV in the frame of a project called FLASHLab. The temporal structure of the beam is highly versatile. The bunch trains and repetition rate can be adjusted up to 1 ms in length and from 0.1 to 1 MHz, while the frequency of the trains can reach 10 Hz. Typically, 1 to 1000 bunches can be delivered in 1 ms and, depending on their charge, bunch length can range from 0.1 to 60 ps. Each bunch can be guided to create microbeams that can be scanned over the target in a manner comparable to pencil-beam scanning in proton therapy but has the additional advantage of being able to deliver the treatment in 1 ms.

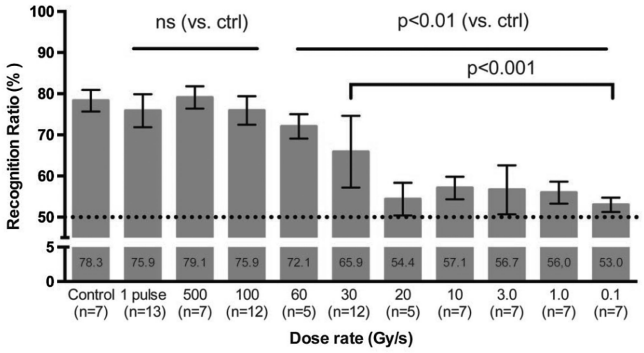

FIG. 5. Neuroprotection demonstrated by the evaluation of the recognition ratio two months after irradiation for groups of mice (n = number of mice) that received 0 Gy (control) and 10 Gy whole-brain irradiation with an average dose rate of 0.1, 1.0, 3, 10, 20, 30, 60, 100, or 500 Gy/s, or with a single 1.8 μs electron pulse (one pulse). Bars represent mean values and whiskers indicate the standard deviations. Dose rates above 60 Gy/s or delivery times <167 ms were required for maximum neuroprotection at a dose of 10 Gy in this model. From Montay-Gruel *et al.*, 2017.

Because of the biological results obtained using the first two linacs of intermediate energy, companies involved in the manufacturing of intraoperative electron radiation therapy electron linacs became interested and modified their devices to deliver FLASH dose rates in preclinical and subsequent clinical settings. The Mobetron (IntraOp, Sunnyvale, CA) is a pulsed linac with electron beam energies of 6–9 MeV. The clinical applications include intraoperative radiation therapy and dermatologic treatments. This system can operate in CONV and UHDR modes and produces electron beams of 9 MeV in CONV mode and 6–9 MeV in UHDR mode. The CONV mode operates under standard clinical settings. In contrast, the UHDR beams can be fine-tuned for both energies. The pulse width can be varied from 0.5 to 4 μs, and the PRF varies from 5 to 120 Hz. The control system monitors the synchronization of each pulse to ensure repeatability across the range of pulse widths and records each delivered pulse. While the commissioning of the Mobetron was described recently by Moeckli *et al.* (2021), validation of the FLASH effect was reported by Valdes Zayas *et al.* (2023).

The eFlash (SIT, Sordina IORT Technologies) is a dedicated research accelerator for FLASH RT. The system works in electron mode only, and it is designed to produce UHDR with two different nominal energies: 5 and 7 MeV, 7 and 9 MeV, or 10 and 12 MeV. The eFlash can produce a dose rate of up to 1500 Gy/s with the 10 cm applicator at an SSD of 100 cm. The dose rate can be varied by modifying several parameters, which can be controlled independently. In addition to the electron gun peak current, the pulse duration can be varied from 0.5 to 4 μs. The PRF can be adjusted from 1 to 350 Hz in 1 Hz increments; however, the maximum power is limited to 250 Hz due to the solid-state modulator limits. Circular field dimensions can be adjusted from 1 to 12 cm. The beam collimation system consists of a set of PMMA cylindrical applicators, which can be directly mounted to the

radiant head. The internal diameters range from 10 to 120 mm, with a 5 mm wall thickness. The SSD can be adjusted according to the applicator diameter size to guarantee optimal beam flatness and symmetry values. The eFLASH has been designed to produce both FLASH and conventional dose rates. A dual dose monitoring system measures the output to allow an adequate fluence reading within a broad range for FLASH and conventional modes. In the UHDR modality, the electron beam output is monitored by means of two toroidal inductors, while the monitor chambers are positioned outside the beamline. In contrast, in the conventional mode the monitor chambers are inserted along the beamline. The toroidal inductors provide a fast and robust signal up to a few milliamperes of beam current thanks to their sensitivity of 10 V/A. With this dual dose monitoring system, a high signal-to-noise ratio is obtained in every operational mode. The occurrence of the FLASH effect remains to be verified.

The FLASHKNiFE (PMB-Alcen, France) has been developed as an upgrade of the Oriatron/eRT6 dedicated to the implementation of clinical trials in IORT settings. Designed to produce UHDR with nominal energies of 6–10 MeV, the FLASHKNiFE is expected to produce average dose rates up to 350 Gy/s at a depth of 30 mm at an SSD of 30 cm. The treatment time can be modulated from 0.5 μs to several minutes.[1] Circular applicators will be used to modify the size of the field and optimize the beam flatness and symmetry.

RadiaBeam Technologies is also working on the development of accelerator systems called flexible linac for electrons and x rays (FLEX). These systems are designed to explore novel applications such as FLASH. Unlike traditional accelerators, FLEX is a new *S*-band traveling-wave linac capable of ramping energy from 2 to 9 MeV in a single 16 μs rf pulse and should be capable of delivering a peak beam power of up to 3.6 MW, which is highly suitable for exploring many FLASH parameters (Kutsaev *et al.*, 2021).

Other investigators have adapted existing clinical linacs (clinacs) for electron FLASH experiments (Schueler, Trovati *et al.*, 2017; Lempart *et al.*, 2019; Rahman *et al.*, 2021). Such modified linacs have been used successfully to deliver electron beams at dose rates exceeding 200 Gy/s, with the caveat that the small field size and short SSD are suited only for small animals. Schueler, Trovati *et al.* (2017) were the first to successfully deliver ultra-high-dose rates using a modified Varian clinac 21EX (Schueler, Trovati *et al.*, 2017). After extensive tuning, they achieved 220 Gy/s (a pulse dose rate of 1.7×10^6 Gy/s at 1 cm depth) at the location of the light field mirror, which was chosen so that depth-dose and field size characteristics remained suitable for small-animal experiments (Schueler, Trovati *et al.*, 2017). Compared to the aforementioned commercial preclinical systems, the higher beam energy (∼8–20 MeV) of clinacs leads to improved dose homogeneity, although limited to small field sizes and fewer beam parameter choices. Simmons *et al.* used the FLASH linac configuration of Schueler, Trovati *et al.* (2017) to demonstrate less brain toxicity with FLASH after whole-brain irradiation in mice (Simmons *et al.*, 2019). The primary parameter that varied between the FLASH and the conventional dose rate beam was the overall delivery time in that study. Both beams used a pulse width of 5 μs, with a dose per pulse of 1.75 Gy and pulse dose rate of 3.5×10^5 Gy/s, delivering FLASH irradiations at average dose rates of either 200 or 300 Gy/s for 20 and 16 MeV beams, respectively, and 0.13 Gy/s for conventional irradiation (for both 16 and 20 MeV beams). This was achieved by modulating the PRF, which were set to 108 Hz for the 20 MeV FLASH beam or 180 Hz for the 16 MeV FLASH beam, and for the CONV beam by delivering five trains of two to three pulses (at a PRF of 180 Hz), each separated by 60 s, for a total delivery time of 240 s. Later the transformation of a Varian clinac was further optimized by Rahman, Ashraf *et al.* (2021) to be both reversible and able to irradiate small and large subjects (Rahman *et al.*, 2021). With a circular beam size of 1 cm to open field, the researchers were able to achieve a dose rate of >238 Gy/s and a dose per pulse of up to 0.81 Gy. While several dosimetry and chemistry papers have been produced by the group (Cao *et al.*, 2021; Rahman *et al.*, 2021, 2023), no biological validation has yet become available but Varian (a Healthineers company; Palo Alto, CA) launched production of FLASH capable clinical linacs including FLASH TrueBeam (Dal Bello *et al.*, 2023).

Lempart *et al.* (2019) proposed a scheme to achieve an average dose rate of 30–300 Gy/s (dose per pulse = 0.1–1.9 Gy, PRF = 200 Hz) on an Elekta Precise linac ($E \sim 8$ MeV), depending on the measurement point within the treatment head. Whereas no formal biological validation of the FLASH effect has been published with this device, the system was subsequently improved to treat veterinary canine patients, now with a 10 MeV beam achieving doses per pulse of 2.2 and 1 Gy, corresponding to average dose rates of 440 and 200 Gy/s, at SSDs of 70 and 100 cm, respectively (Konradsson *et al.*, 2021; Børresen *et al.*, 2023).

In summary, electron FLASH beams are available, but their major limitation is their relatively low penetration and their scattered dose distribution in tissues. Therefore, other treatment devices or techniques are needed for FLASH to be clinically useful for deep-seated tumors.

B. Photon FLASH beams

While medical linear accelerators initially produce an electron beam, the majority of treatments are delivered using x rays generated by bremsstrahlung conversion of the electron beam; see Fig. 6. For the initial electron beam, electrons over the energy range of several MeV deposit dose superficially and scatter widely, whereas corresponding x rays produced by the same beam penetrate much more deeply and maintain a consistent transverse profile with a depth such that they can be collimated to produce sharp dose gradients where desired. Indeed, in clinical radiation therapy key physical beam characteristics impacting the quality of treatment plans include a falloff of radiation dose with depth into the tissue (depth-dose profile) and lateral spreading of the beam (transverse profile). Nevertheless, even with x rays the dose along the beam path continuously decreases with depth, thereby contributing a substantial dose outside the desired target region for deeply situated targets.

[1]See https://www.pmb-alcen.com/en/flashknife-flash-radiotherapy-system.

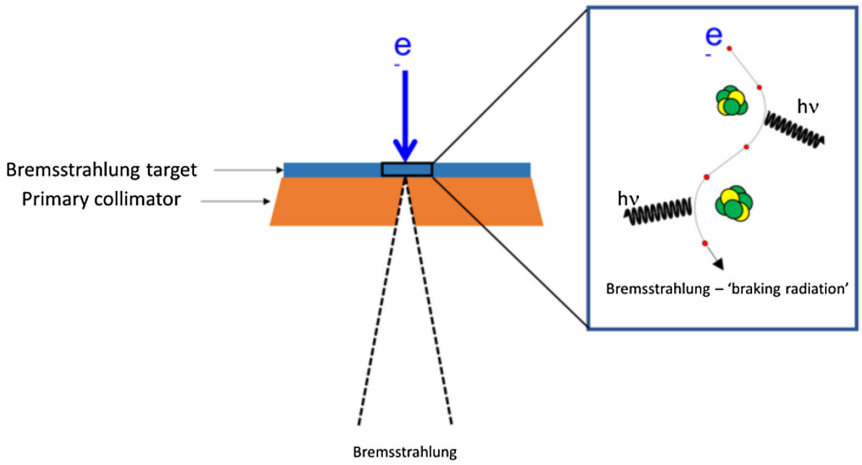

FIG. 6. Bremsstrahlung production. Electromagnetic radiation is produced by a sudden slowing down or deflection of charged particles (electrons) passing through matter near the strong electric fields of atomic nuclei.

Today photon beams remain the most used modality in radiation oncology. X rays are produced by electrons striking a high atomic number target and interacting with the atoms of the target material. In RT, the electron energies are in the range of megaelectron volts, which can be achieved in medical linear accelerators. Through the interactions with the atoms of the target materials, the electrons are decelerated and lose energy by creating bremsstrahlung (braking radiation) and heat. The rate of energy loss per unit length is defined by the stopping power of the material and is split between the bremsstrahlung and heat. The challenge of x-ray UHDR radiation generation by bremsstrahlung stems from the low efficiency of bremsstrahlung x-ray production. Higher electron beam currents (>100 times) than that produced by current clinical linacs are required to achieve x-ray dose rates compatible with the FLASH effect, thus requiring a new class of accelerator; furthermore, at such currents conventional strategies for the mitigation of heating of the x-ray conversion target may be inadequate. Therefore, to achieve the FLASH effect with photon RT, one must build a linac with extremely high beam currents to overcome the low efficiency of converting electron beam energy to photons through the bremsstrahlung process of hitting a target made of high Z material (atomic number). This high average beam current over a short period of time needs to be $\gtrsim 300$ times a typical medical linac used for this purpose. Hence, the accelerator needs to be redesigned to operate at a much higher repetition rate. Consequently, the rf sources and associated modulators would need to provide these powers as well. A paradigm shift in the art is required to make these devices fit a typical hospital RT facility.

These limitations make UHDR photons difficult to produce. Synchrotron light sources represent a solution for providing high brightness xray beams without using bremsstrahlung conversion. The first demonstration of the FLASH-sparing effect with UHDR x-ray beams was performed at the European Synchrotron Research Facility (ESRF; Grenoble, France) using broad beam irradiation, where the dosimetry was optimized by our late colleague Dr. Elke Bauer-Krisch (Brauer-Krisch *et al.*, 2015; Montay-Gruel *et al.*, 2018). One of the most significant advances in the field of radiation research is the evolution and adoption of synchrotron x rays in medical research. Several key features make synchrotron radiation appealing for FLASH research. These include high brightness or brilliance, which is a measure of the synchrotron radiation power. Typically the higher the brilliance value, the stronger the emitted beam. In contrast to conventional RT, the synchrotron beam allows the irradiation of a sample with parallel microbeams. Owing to the utilization of high beam currents, synchrotron radiation results in high photon fluxes (dose rates) that allow the irradiation of the samples on millisecond timescales. Dose rates in excess of 10 000 Gy/s can be achieved. The energy of the synchrotron beam is tunable and in the keV range, which has the advantage of low secondary electron (Compton) scattering, but has the disadvantage of steep depth-dose curves (Pelka, 2008). Reduced cognitive impairments in mice after whole-brain irritations have been shown (Montay-Gruel *et al.*, 2018). Using an average dose rate of 37 Gy/s and a field height of 17 mm diameter, Montay-Gruel *et al.* (2018) were able to deliver the radiation in 0.27 s; these beam parameters were similar to those reported by Favaudon using electron beams. Quasicontinuous x rays on the ID17 biomedical beamline of the third-generation 6 GeV synchrotron were used. The ID17 wiggler gap was set to 24.88 mm to maximize the photon flux, and aluminum and copper attenuators were inserted to produce the standard microbeam irradiation (MRT) spectrum, with the maximum intensity at 102 keV. A dose rate in each 50 μm slice of 67 Gy/(s mA) was measured at 2 cm depth using the pinpoint ionization chamber (PTW 31014). During the experiment, the current was 178 mA, leading to an in-slice dose rate of 12 000 Gy/s and a mean dose rate (considering overall delivery time to the whole brain) of 37 Gy/s. The achievable dose rates range from 8000 to 16 000 Gy/s using a PRF of 355 MHz (Brauer-Krisch *et al.*, 2015). A limitation is the field size of 1–3 mm height and 40 mm width; thus, larger targets need to be scanned to achieve adequate coverage (Prezado *et al.*, 2012). The nominal energy spectrum of this beam is between 30 and 600 keV with a mean energy of ~105 keV (Laissue *et al.*, 2013), but for most preclinical trials the energy is lowered to

100 keV and an average dose rate of 40 Gy/s. Medical applications of synchrotrons are currently supported by the results brought by MRT (Eling *et al.*, 2019; Montay-Gruel *et al.*, 2022). Although MRT *de facto* combines UHDR and spatial fractionation (at the micrometric scale) (Griffin *et al.*, 2020), the respective additive and/or synergic value of combining UHDR and spatial fractionation is a topical field of investigation and is outside the scope of this review (Prezado, 2021; Schneider *et al.*, 2022). In addition, the accessibility and cost of synchrotron facilities are the major drawbacks for the development of x-ray FLASH beams unless compact sources for clinical MRT become available, such as the line-focus x-ray tube developed recently (Winter *et al.*, 2020). In addition, Bazalova-Carter and Esplen (2019) suggested using Monte Carlo simulations and indirect experimental validation to show that an unfiltered 160 kVp continuous 3 and 6 kW x-ray beam delivered by the Comet MXR-160/22 and MXR-165 x-ray tubes would be able to deliver dose rates up to 150 Gy/s at the surface of a water phantom. However, a result of only 40 Gy/s at 2 mm in depth (Bazalova-Carter and Esplen, 2019) was achieved, then further optimized to reach 140 Gy/s (Cecchi *et al.*, 2021). Rezaee, Iordachita, and Wong (2021) used a rotating-anode x-ray tube and high-power 115 kW x-ray tube (RAD-44 by Varex Imaging Corp.) that was theoretically (such as via a MC simulation) able to produce 40 Gy/s at 2 cm. They also implemented parallel-opposed x-ray tubes to reach a 5% dose uniformity at 8–12 mm and recently published the first biological report (Miles *et al.*, 2023).

1. Megavoltage xFLASH

Optimization of the conversion target is also ongoing. Liu *et al.* (2023) performed UHDR irradiations with a 10 MV x-ray beam generated by a 10 MeV 0.1–0.2 mA electron beam and a 0.2 mm thick tungsten target with a copper heat remover. Under these conditions, a dose rate of 40 Gy/s was obtained, but not without compromising the SSD, which reached only 17 cm. The group of Bazalova-Carter is commissioning the ARIEL electron linac at TRIUMF (Vancouver, BC, Canada) to accelerate electrons with energy up to 30 MeV. ARIEL produces a quasicontinuous beam with a power of 10 kW with a maximum PRF of 10 kHz. The minimum PRF is 10 Hz, and the expected average dose rate for a 10 MeV electron beam is greater than 600 Gy/s. This group also recently reported on the development of a bremsstrahlung target for megavoltage (MV) x-ray irradiations with UHDR at TRIUMF (Esplen *et al.*, 2022) and a tantalum target with a thickness of 1 mm was actively cooled by water through an aluminum flange to remove heat. They simulated with MC code a dose rate of 130 Gy/s at 7.5 cm and 40 Gy/s dose delivery at 4.5 cm in depth.

Sampayan *et al.* (2021) described the linear induction accelerator that was developed at Lawrence Livermore National Laboratory for high instantaneous and high average dose rate. Although the accessibility of this technology is limited and the gradient must be improved, it provides a deep penetrating beam with high dose rate capability that can be used as a starting point for further development of conformal FLASH with photons.

The most mature technology to produce an xFLASH beam to date was attributed to Gao *et al.* (2022), who used the superconducting linac at the Chengdu terahertz free electron laser (CTFEL). Experimental dosimetric validation was performed with Gafchromic films (EBT3) and validation of the FLASH effect was demonstrated using *in vivo* models of breast cancer as well as lung and gut normal tissue sparing; see Sec. III.B. This superconducting linac, called PARTER, delivers a 6–8 MeV >40 kW electron beam with ∼5 ps micropulses with an adjustable average current of up to 10 mA and an energy spread of less than 0.2% (root mean square measured at a beam energy of 8.2 MeV). The beam can be directed onto a rotating tungsten target to produce high-energy x rays. The beam structure consists of electron micropulses with a 5 ps duration, a 20 A peak current, and a period of 18.5 ns (54 MHz repetition rate). With a beam size of 10 mm, the dose rate can reach ∼750 Gy/s at depths of 0.5 cm, 7 MV, and 7 cm SSD. MC calculations predicted dose rates greater than 50 Gy/s at depths of up to 15 cm.

The biological relevance of these MV xFLASH beams is that they use the same type of radiation as found in the most prevalent type of clinical treatment systems. Unlike clinical linear accelerators that already operate near their maximum electron beam current to produce MV x-ray dose rates hundreds of times lower than required to achieve FLASH biological effects, the TRIUMF and CTFEL beamlines are massive facilities designed to produce much higher beam current. However, such technologies do not readily translate to the clinical environment because the size and power requirements are not compatible with standard clinical vaults and are not amenable to mounting on gantries to deliver beams from multiple directions, as required for the production of conformal dose distributions.

At the Stanford School of Medicine and SLAC National Accelerator Laboratory, the pluridirectional high-energy agile scanning electronic radiotherapy (PHASER) program consists of the development of a new class of electron linear accelerator capable of producing the required beam currents in a compact form factor with much greater efficiency, and therefore much lower consumption of rf power that can be produced by novel compact rf power sources. Rate-limiting mechanical motion is eliminated by having an array of 16 beamlines to provide a full complement of treatment beam angles for highly conformal RT; Fig. 7.

Intensity-modulated beams from each of the beamlines are produced by a novel electronic scanning pencil-beam high-speed intensity-modulated x-ray source (SPHINX) in place of conventional mechanical multileaf collimators (Whelan *et al.*, 2022); see Fig. 8. The philosophy adopted to achieve the required increase in current is, to begin, to use a highly efficient linac that operates at a ∼1 kHz pulse repetition rate, with a longer pulse length of around 5 μs and a much higher beam loading than typical linacs. This by itself will achieve only about a 30-fold increase in current.The project proposes the use of 16 linacs of this type to achieve the remaining order of magnitude increase in the total delivered average current.

The rf frequency of the linac for the PHASER project has been kept high within the *X* band (8–12 GHz) to keep the linac compact and reduce its peak power consumption. This is necessary for 16 linacs to fit within a typical RT room; see

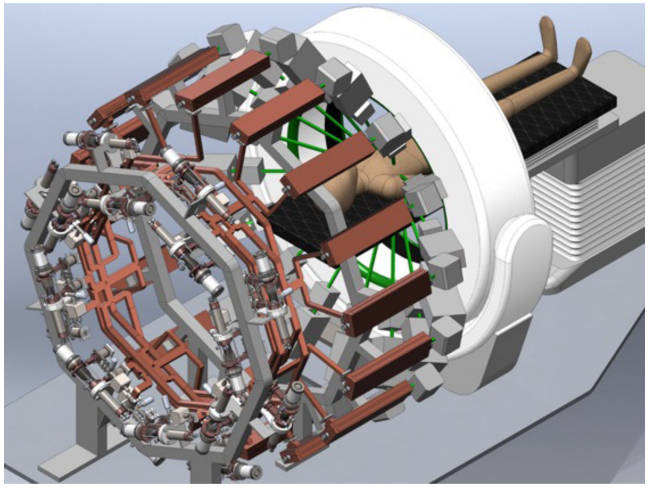

FIG. 7. Conceptual rendering of the integrated PHASER system. The power of 16 klystrinos is combined through the RAPiD network and distributed to an array of 16 stationary DRAGON linacs. The noncoplanar beamlines arranged in a conical geometry share a common isocenter with a full ring multidetector CT scanner. Each beamline includes a SPHINX system comprising scanning magnets, an extended bremsstrahlung target, and a collimator array to produce all-electronic intensity-modulated x-ray beams. From Maxim, Tantawi, and Loo, 2019.

Fig. 7. At a higher frequency, the power consumption on the linac walls is reduced and is typically inversely proportional to the square root of the frequency. However, for PHASER the power density on the linac walls is increased because the surface area is reduced inversely by the square of the frequency. The SLAC/Stanford team sought a paradigm shift in the design of the linac to reduce the wall power consumption and allow for simplified rf sources and reasonable mechanical cooling for the linac. The new class of linac that materialized due to this effort is the so-called distributed rf-coupling architecture with a genetically optimized cell design (DRAGON) linac (Tantawi *et al.*, 2020), a new linac topology that allows each accelerator cell to be fed independently using a periodic feeding network. This adds another degree of freedom to the design; the coupling between cells can have a wide acceptable range and can even minimize it to negligible values. The added flexibility in the geometry optimization of the accelerator cells is then used to attain the highest possible shunt impedance for a set of cells. The linac structure (see Fig. 9) depicts where the manifolds feeding each cell are revealed in the cross-sectional view. The linac is also divided into different sections corresponding to the different speeds of the electrons as they get accelerated from about 50 keV (the gun potential) to a final energy of more than 10 MeV.

The rf system also needs to supply the power to the beam, and for the PHASER system the peak current is about 0.3 A, with a final energy of about 10 MeV for the electrons. This translates to about 3 MW of peak beam power; the accelerator walls consume about 0.8 MW for a total of 3.8 MW needed from the source. Given that the system also uses 16 linacs, it is cost and size prohibitive to use 16 roughly 4 MW klystron systems to power the PHASER linac. The PHASER rf system is still composed of 16 klystrons, but these are "miniklystrons" or "klystrinos" that operate at a much smaller voltage and produce less power: ∼350 kW each (Jensen, Neilson, and Tantawi, 2015). Because of the low voltage, the klystrinos and their prospective modulators occupy much less volume than conventional klystron modulators that must operate at a higher voltage, which necessitates the use of oil tanks and special electronics for producing the high voltage pulses required to drive them. The PHASER system then utilizes the developed art of ultrahigh-power rf manipulation (Tantawi *et al.*, 2005) to combine the output of 16 klystrinos to produce the needed rf peak power. This is done through a network of waveguides in a special geometry (cross potent superhybrid) (Nantista and Tantawi, 2000) with 16 inputs and 16 outputs (U.S. Patent No. 9640851) that allows the combined power of all inputs (the klystrinos) to be directed to any given output (each individual linac), one at a time in rapid succession, through adjustment of the phases of the inputs. Indeed, these small klystrons have to operate at a repetition rate that is 16 times higher than the repetition rate of the individual linacs ∼16 kHz; i.e., the Stanford team has transformed the problem from a bulky high-peak-power klystron to small klystrons that have a reasonable peak power but have to operate at a high duty factor, a formidable engineering problem for the designers of such a device.

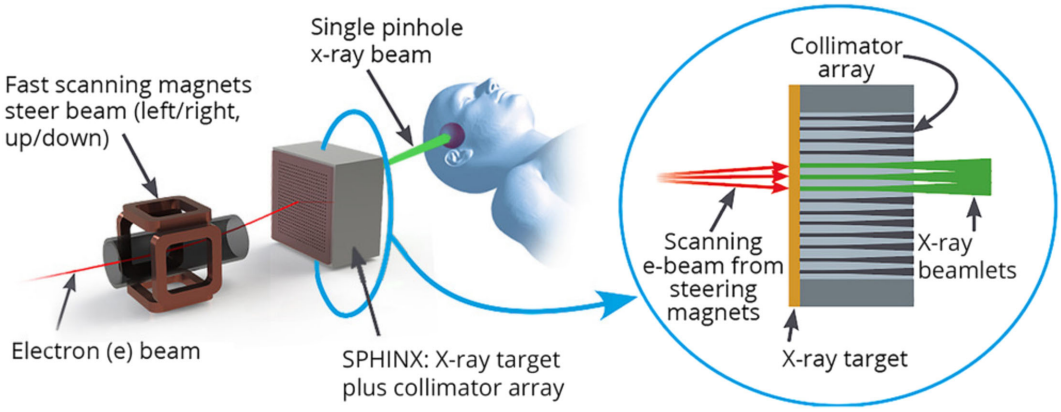

FIG. 8. The SPHINX electronic intensity modulation comprises rapid scanning of the source electron beam from a high-current linear accelerator onto an extended bremsstrahlung target matched to a collimator array to produce scanning x-ray beamlets with a highly modulated intensity pattern. From Whelan *et al.*, 2022.

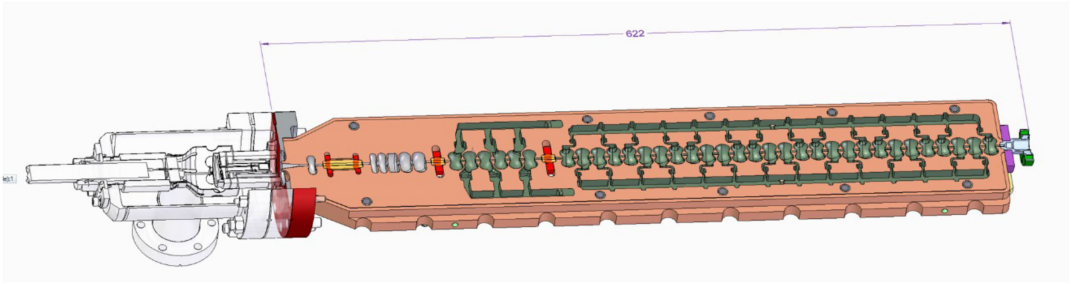

FIG. 9. Cross-sectional view of the 11.4 GHz accelerator structure proposed as the heart of the future PHASER concept machine.

C. Hadron FLASH beams

Proton therapy demands large, complicated facilities with substantial infrastructure that are rare worldwide; nonetheless, extending such operations to the FLASH regime has been possible with nontrivial yet relatively incremental developments. However, comparing these developments to the initial infrastructure of such a modality makes the proton modality a candidate for realizing near future FLASH facilities with several limitations, as later discussed. In present-day hadron therapy machines, the protons and ions are accelerated in either a cyclotron or a synchrotron. The main advantage of a cyclotron is that it is cheaper and more compact. However, it runs at fixed energy because tuning for different energies takes too long for it to be practical during treatment time. In synchrotrons, the energy can be varied. For the majority of synchrotrons, although one can tune for the optimal beam energy for the treatment in question, it takes too much time to change energy during the treatment, and the synchrotron beam energy is essentially fixed during a particular treatment. To treat tumors of different sizes and different depths, and to allow for beam delivery coming from different directions, the hadron beam needs to be adjustable in energy. This adjustment needs to reduce the energy so that the Bragg peak for energy deposition corresponds to the depth of the tumor in the body, and it needs to fine-tune this energy to allow for treatment at different depths due to the size of the tumor along the beam direction. Typically this is done by putting material in the beam. An energy degrader is placed before the gantry to adjust for the depth of the tumor. The beam coming out of the degrader is then collimated and transported along the gantry. An energy ranger placed in the treatment head is used for the energy fine-tuning for the longitudinal size of the tumor. In addition, some proton therapy systems put material in the beam to increase the treatment field size.

Radiotherapy with protons has advantages compared to electrons and photons due to more favorable dosimetry afforded by the Bragg peak. The existence of the Bragg peak allows for conformal treatments with a small number of beams while achieving smaller collateral damage to nearby organs at risk compared to x-ray therapy. In the clinical setting, proton beams are usually accelerated using synchrotrons or cyclotrons to energies of up to 250 MeV, and they can be produced as either pulsed or quasicontinuous. In principle, any cyclotron- and synchrotron-based proton accelerator system should be able to produce mean dose rates of 40 Gy/s or more with millimeter beam sizes that will require implementation of pencil-beam scanning to treat large targets. Several experimental studies have reproduced the FLASH effect with multiple pFLASH irradiation systems, as reviewed by Diffenderfer *et al.* (2022). They were able to irradiate small targets with their existing clinical proton machines with minor or no modifications (Diffenderfer *et al.*, 2020). However, one of the main difficulties with pFLASH will be to maintain ultrahigh dose rates across an extended volume to generate the spread-out Bragg peak (SOBP). Therefore, most preclinical studies were performed in the plateau region of the Bragg curve using a single, monoenergetic beam (Diffenderfer *et al.*, 2022). In any case and as already mentioned, proton beam therapy (PBT) is the most mature technology for the transfer of FLASH in the clinic. This modality offers UHDR and can treat deep-seated tumors with high conformality under a limited set of parameters. Several high-energy clinical PBT facilities have been modified to generate FLASH dose rates and isochronous cyclotrons such as the Varian ProBeam and the IBA Proteus Plus that produce a quasicontinuous dc beam current have successfully demonstrated the FLASH effect in multiple biological studies; see Sec. III.C (Diffenderfer *et al.*, 2020; Cunningham *et al.*, 2021; M. M. Kim *et al.*, 2021; Velalopoulou *et al.*, 2021; Singers Sørensen *et al.*, 2022; Sørensen *et al.*, 2022).

The ProBeam system uses an isochronous cyclotron with a frequency of 72 MHz that accelerates protons to energies up to 250 MeV. Typically proton beams utilize a 3 mm scanned pencil beam with varying energies to "paint" the tumor layer by layer, thus creating the SOBP. The average dose rate to a 2×2 cm^2 area in the plateau region can reach 240 Gy/s, which is sufficiently high to trigger the FLASH effect. The proton beam is typically delivered in quasicontinuous mode; however, it can also be delivered with a pulse width of 4 μs and a repetition rate of up to 2 kHz. This system was used to evaluate the skin toxicity in mice following FLASH and conventional radiation (Cunningham *et al.*, 2021; Singers Sørensen *et al.*, 2022; Sørensen *et al.*, 2022), and more recently to conduct the first clinical trial. The Feasibility Study of FLASH Radiotherapy for the Bone Metastases (FAST-01) trial[2] was performed at the Cincinnati Children's/UC Health Proton Therapy Center and completed accrual after ten patients (Daugherty *et al.*, 2023; Mascia *et al.*, 2023). A second study (FAST-02) is ongoing; see Sec. V. The primary end point of FAST-01 was to evaluate the clinical workflow

[2]See https://clinicaltrials.gov/ct2/show/NCT04592887.

feasibility of delivering a single dose of 8 Gy in a broad beam given an ultrahigh dose rate. Here no unforeseen toxicities were observed that were also not expected at 8 Gy given the low total dose and short-term follow-up (Daugherty *et al.*, 2023; Mascia *et al.*, 2023). Apart from this trial, published studies on pencil-beam scanning (PBS) pFLASH are increasing (Cunningham *et al.*, 2021; M. M. Kim *et al.*, 2021; Singers Sørensen *et al.*, 2022; Sørensen *et al.*, 2022), and more work is necessary to substantiate whether the FLASH effect can be obtained under clinical settings that resemble human disease. To answer that question, a study with cat patients bearing oral squamous cell carcinoma (SCC) seeks to accrue up to 20 patients (principal investigator: Professor C. Rohrer-Bley, Zurich Veterinary School; Dr. S. Psoroulas, PSI; and Professor M-.C. Vozenin, Hospital of Geneva) that will be treated with fractionated proton irradiation in transmission using 3×11 Gy conventional and FLASH dose rate side by side. This regimen was chosen for the following reasons: (1) 3×10 Gy was shown to produce the FLASH effect (Montay-Gruel *et al.*, 2021) and (2) the relative biological effectiveness (RBE) of 3×11 Gy is close enough to the 10×4.8 Gy fractionation scheme reported in the literature (when an α/β ratio of 10, which is the ratio currently applied to head and neck tumors, is considered) (Poirier *et al.*, 2013; Marconato *et al.*, 2020). If launched successfully, this protocol should be highly informative and relevant for facilitating further human studies with protons since (1) oral SCC in cats models human disease, (2) oral SCC in both cats and humans exhibits poor therapeutic outcomes, and (3) the selected hypofractionation regimen is highly translatable.

The Proteus proton therapy system (Ion Beam Applications S.A, Louvain-La-Neuve, Belgium) accelerates protons to energies of up to 230 MeV. The proton beams are accelerated using an isochronous cyclotron that effectively delivers a continuous beam. Diffenderfer *et al.* (2020), M. M. Kim *et al.* (2021), and Velalopoulou *et al.* (2021) used this system to deliver an ultrahigh dose rate, double scattered, and collimated 230 MeV proton beam with a mean dose rate of 78.9 Gy/s to mice.

Other proton sources are also under development (such as the synchrotron beam from Hitachi, Proton, and Optivus) that are characterized by beam spill times on the order of seconds using slow cycle extraction techniques, while subsecond spill times could in theory be adapted to produce UHDR using fast cycle techniques. More recently clinical implementations of synchrocyclotrons produced by the Mevion s250 and IBA Proteus One have provided the advantage of producing a pulsed beam structure with macropulse widths in microseconds and repetition rates of a few hundred to 1000 Hz. This pulsed structure is closer to the structure of the electron FLASH beams and may prove useful in evaluating whether or how this pulsed structure could replicate or improve on prior eFLASH or pFLASH biological outcomes.

The implementation of FLASH PBT still has technical limitations since the beam currents provided from accelerators need to be delivered efficiently to the patient. Most FLASH planning and experimental studies use so-called transmission beams, i.e., beams of very high energy (usually 230 or 250 MeV) that shoot through the patient; high energies can be transported more efficiently to the treatment rooms, thus maximizing dose rates, but result in larger dose baths with respect to standard proton therapy plans. Note that for the latter this effect may well be compensated for by the FLASH-sparing effect. Another complication comes from treating extensive volumes (more than few millimeters in diameter), which require spreading the beam using either scattering or PBS (Zou *et al.*, 2021). Both techniques result in reduced dose rates when the dose is spread across the tumor. Scattering enlarges the beam size to cover the tumor volume, thus decreasing the dose rate considerably if volumes larger than a few millimeters are irradiated. In PBS, the pencil beams are moved sequentially through the tumor volume with magnetic scanning; therefore, PBS delivers ultrahigh dose rates in each individual (small) spot, but the time taken to scan all spots over a large volume is extended, thereby dropping mean dose rates and increasing treatment durations. Estimation of the FLASH effect with PBS is ongoing with simulation and experimental studies (Folkerts *et al.*, 2020; van Marlen *et al.*, 2020; Krieger *et al.*, 2022). In addition, the dose rate dependence of the FLASH effect with protons may differ from observations with electrons (Kacem *et al.*, 2022) and will require detailed investigations. This highlights the challenge of defining the correct beam parameters for triggering the FLASH effect in proton beams.

However, other designs have already been explored to avoid the issue of putting material in the beam, which can be problematic for two major reasons. First, it increases beam emittance, thereby making the beams transversely larger and making the beamline elements on the gantry larger and the gantry itself more massive. Second, the beam collimation after the degrader reduces the beam flux and creates neutrons, some of which make it to the treatment site and add to the dose delivered. A current effort at SLAC National Accelerator Laboratory aims to address all these issues by introducing a relatively compact rf energy modulator followed by an rf deflector (Lu *et al.*, 2021). For example, a 70 MeV linac specially designed to accommodate protons with variable β (the ratio of the particle velocity to the speed of light) and modulate their energy (accelerate or decelerate) combined with an initial 150 MeV hadron beam will give an energy range of 80–220 MeV. This linac can also be followed by an rf deflector to provide transverse deflection of the beam position and angle. The small angle and position induced by the deflector are then magnified using a series of compact permanent quadrupole magnets to cover a larger field. The fundamental problem addressed in this research effort is the design of linac structures that generate sufficient accelerating gradients for the low and variable β (for example, ~0.507 for 150 MeV proton beam energy) hadrons used for therapy. SLAC developed a new generation of high-efficiency accelerator structures that are capable of much higher gradients than traditional structures (Simakov, Dolgashev, and Tantawi, 2018). In addition, the individual accelerator cells in the structure are not coupled and can be independently phased. The combination of higher gradients and efficiencies and independent rf cell phasing allows for a specially designed linac to modulate the treatment beam energy without the need for any physical beam spoiling. A similar philosophy can be applied to the deflector structure. Combined, the rf energy modulator and deflector can rapidly scan proton Bragg peaks

in all three dimensions without the degradation of spot size or penumbra induced by conventional physical modulators.

In addition to protons, heavy ions might provide advantages for advancing research in the field of FLASH. Recently the Durante group demonstrated an occurrence of the FLASH effect with the SIS18 synchrotron of the GSI Helmholtz Center in Darmstadt, Germany). The device has been upgraded to produce $>10^{11}$ ions/spill, which makes the irradiation of rodents at a dose rate above >100 Gy/s possible with a single spill of a duration ≤ 200 ms (Tinganelli *et al.*, 2022a). Using a hind limb osteosarcoma model irradiated with a dose of 18 Gy, tumor control and substantial sparing of the muscle tissue was shown, as was a possible reduction of the metastatic potential (Tinganelli *et al.*, 2022b).

D. Very-high-energy electron FLASH beams

Another way to overcome the low efficiency of the bremsstrahlung converter used with photon RT is to use high-energy electron beams. This demands that the electron beam energy exceed 100 MeV to minimize the scattering within the treated tissues. As the energy increases, the depth-dose characteristics of very-high-energy electrons (VHEEs) in the energy range of 100–250 MeV becomes more favorable than MV energy photons, with a shallower dose falloff with depth and decreased lateral scatter and penumbra (DesRosiers *et al.*, 2000, 2008; Papiez, DesRosiers, and Moskvin, 2002). VHEE beams also have the advantage of a more uniform dose at boundaries between tissues of varying density compared to photon beams. Compared to protons that are much heavier, rapid electromagnetic scanning is easier. Researchers from Indiana University originally studied the dosimetric advantages of VHEEs through simulations, and subsequent work has further demonstrated the improvements in radiation treatment plans achievable with VHEEs compared to MV photons (DesRosiers *et al.*, 2000; Palma *et al.*, 2016; Schueler, Eriksson *et al.*, 2017). In addition, as with lower energy electrons, the dose efficiency of direct treatment with electrons is much higher than with photon treatment. The dose per unit charge, and correspondingly the dose per pulse of the electron beam, is much higher for electrons than for photons, which may be advantageous in the context of achieving a FLASH effect. A challenge, however, is the size and power demands of the facilities required to accelerate electrons to an order of magnitude higher energy than is typically used in clinical technologies. To date such energies have been produced for preclinical research using large accelerator research facilities. However, generating 100 MeV electrons in the same footprint as a typical medical linac requires the linacs to operate with 10 times higher gradients. Since the peak rf power required to establish the linac gradient is proportional to the square of the gradient, rf sources needed to drive a VHEE linac require 100 times more peak power than a typical rf source for a medical linac. Furthermore, for a footprint about 1 m in length, the linac has to operate at a gradient of 100 MV/m; this indeed is at the edge of state of the art. A technological paradigm shift is again needed to make this modality viable for a practical RT modality. Such developments toward compactness are ongoing in many places around the world. Studies have been performed using normal conducting (NC) and superconducting rf linacs and laser plasma accelerator facilities provide a large panel of parameters for investigations and clinical applications.

NC rf *X*-band linacs including CLEAR at CERN[3] and the Argonne Wakefield Accelerator (AWA) at Argonne National Laboratory[4] are available. CLEAR is based on Compact Linear Collider technology and has an energy range of 50–250 MeV, a bunch charge ranging from 0.01 to 0.4 nC, transverse normalized emittance of 3/30 μm for 0.05/0.5 nC, a relative energy spread $<0.2\%$, a bunch length of 200–1200 μm, a repetition rate of 1–5 Hz, and a number of bunches 1–150 with 1.5 GHz of microbunch spacing. This technology was chosen in a collaboration between Centre Hospitalier Universitaire Vaudois (CHUV) and CERN to develop a clinical VHEE-FLASH device for treating human patients with deep-seated tumors.[5] The biological investigations are ongoing. AWA has a lower range of energy from 6 to 63 MeV, a bunch charge from 0.1 to 100 nC, a transverse normalized emittance of 0.5/240 μm, a bunch length of 0.1–3 mm, and a repetition rate of 0.5–10 Hz.

NC rf *S*-band linacs are also available, including Compact Linear Accelerator for Research and Applications (CLARA) at Daresbury[6] and Accelerator Research Experiment at SINBAD (ARES) at DESY (Hamburg, Germany).[7] CLARA was developed in two phases, with the first phase providing a 40 MeV, 10 Hz, 100 pC *e* beam and the second phase providing a source at energies up to 250 MeV. Several studies with plasmid and cell irradiation, dosimetry, and treatment planning are ongoing. ARES has an advanced, polarizable *X*-band transverse deflecting structure installed for beam characterization and a dedicated experimental area fully equipped for beam diagnostics. Note that this is one of the few installations where *in vivo* experiments with rodents and larger animals will be possible.

Superconducting rf linacs are available in Germany with PITZ-DESY and ELBE-HZDR and in Canada with ARIEL-TRIUMF. In Dresden, Germany, Electron Linac for Beams with High Brilliance and Low Emittance (ELBE) is capable of delivering pulsed electron beams with energies of up to 40 MeV using 5 ps micropulses with charges up to 70 pC at quasicontinuous beam currents of up to ∼1 mA. The micropulse dose per pulse is 60 mGy, and the quasicontinuous beam can be further modulated by superimposing a macropulse structure with 0.1–40 ms macropulse widths or using a finite number (<4096) of micropulses in a single-pulse mode. The high dose rate of 109–1010 Gy/s makes this system an ideal platform for radiobiological studies, especially when short-lived and early radiochemical processes are being studied. In the context of potential clinical applications, simulations have shown that opposing electron beams with energy as low as 40 MeV can produce treatment plans comparable to conventional photon beams when a part of the body with limited thickness is treated and high dose

[3]See https://clear.web.cern.ch.
[4]See https://www.anl.gov/awa.
[5]See https://cerncourier.com/a/adapting-clic-tech-for-flash-therapy.
[6]See https://www.astec.stfc.ac.uk/Pages/CLARA.aspx.
[7]See https://ares.desy.de.

conformity is not required (Breitkreutz *et al.*, 2020). Normal tissue sparing with FLASH has been shown at ELBE using zebrafish embryos (Pawelke *et al.*, 2021). In Vancouver, ARIEL-TRIUMF allows for investigations into the effects of temporal parameters, including PRF, pulse width, beam current, and pulse sequence over a broad range.

Laser plasma acceleration (LPA) technology can also be applied to VHEEs, and several later-discussed groups have expressed interest in developing FLASH research programs. Many places around the world are becoming interested in this technology and have developed dosimetry and radiobiology programs as first steps before clinical applications such as DRACO-ELBE[8] and Intense Laser Irradiation Laboratory (ILIL) at INO[9] with PW laser sources. DRACO has an energy of 50–400 MeV electrons by LPA (laser driven) with up to a 500 pC bunch charge, a 10 fs pulse length, a 5 mrad divergence, and a 1 Hz repetition rate. ILIL is also in the VHEE energy range, with a charge per bunch between 100 and 200 pC in the selected spectral range with a current repetition rate in the hertz scale. It is being upgraded to 100 Hz in the near future. Laboratoire d'Optique Appliquée at ENSTA[10] is a laser driven wakefield plasma electron accelerator delivering an electron beam with a maximum energy in the range of 100–150 MeV, with a maximum charge in the range of 10 pC to a few nC, depending on the injection mechanism and the saturation of the accelerating structure. A new beamline dedicated to medical applications is also being constructed.

Novel linear accelerator technologies promise to generate VHEE beams in a more compact structure using less rf power (Maxim, Keall, and Cai, 2019). Designing a linac that is capable of accelerating electrons to energies of ∼100 MeV within a meter is well within the known state of the art. However, the typical amount of rf power needed for such a linac to achieve this high gradient requires ∼150–200 MW of peak rf power at the *X* band. The sources that can generate this type of power typically occupy the space of several treatment rooms. Furthermore, the cost of such a source would be prohibitive; a VHEE device would not be competitive with other RT modalities. There is an effort at the SLAC National Accelerator Laboratory to design a system that requires only 5–8 MW of rf power at 11.4 GHz to generate a 100 MeV beam, as compared with the 150–200 MW required for typical linacs. This would make the VHEE modality a viable one (Fig. 10). This is being accomplished by, first, designing a novel linac with an extremely high shunt impedance that reduces the amount of power required to establish a gradient of 100 MV/m. This 135° phase-advance linac represents another evolution of the distributed coupling linac topology, a novel, recently invented topology that was just described as designing a novel linac. Second, the linac will operate at ∼77 K. At this temperature, both the tolerance to high gradient and the shunt impedance are boosted dramatically; the already extremely high shunt impedance is multiplied by a factor of 2.7. At this stage the linac requires only 20 MW to operate at a gradient of 100 MV/m. Finally, the team working on this modality is developing a novel pulse compressor that will feed the standing-wave linac. The result is to reduce the required power from the source to only about 5 MW. The pulse compressor needs to be able to feed the cold linac; hence, the output pulse length of the pulse compressor needs to be on the order of the long filling time of the cold structure. A straightforward way to achieve that is to cool the pulse compressor as well. However, the team has been working to create a new cavity geometry that would allow that to happen at room temperature based on recent developments of compact high-efficiency rf pulse compressors (Franzi *et al.*, 2016).

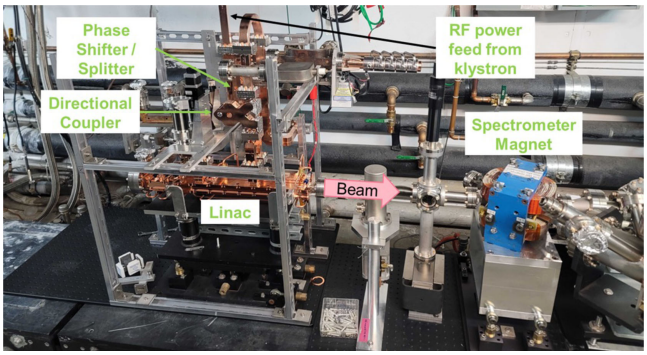

FIG. 10. Test setup at SLAC for evaluating the new distributed coupling accelerator structure proposed for the PHASER concept. Note that the input power is distributed from the input waveguide into the different sections of the linac through a complicated waveguide network to control the power and phase in each section.

E. Conclusion

Despite major differences in the macrostructure and microstructure of the beams (see Fig. 11) impacting the dose deposition within tissue, the FLASH effect has been found in preclinical mouse models using electron, x-ray, proton, and carbon ion FLASH beams. This finding suggests that the most important physical parameter is probably the overall time of exposure, at least when small volumes of tissue are irradiated. It also suggests that the definition of a common imprint defined by profiles analyzing genomics, proteomics, metabolomics, metagenomics, phenomics, and transcriptomics (i.e., omics) will likely identify the molecular determinants of the FLASH effect.

III. CONCEPTUALIZATION OF THE "FLASH EFFECT": *IN VIVO* MODELS

A. The *in vivo* FLASH effect: Electron beams

In the early 1970s–1980s electron irradiators capable of delivering sufficiently high dose rates of electrons ($>10^5$ Gy/s) uncovered some surprising findings involving the induction of hypoxia and the reduction of skin reactions and rat tail necrosis (Hornsey and Bewley, 1971; Field and Bewley, 1974; Inada *et al.*, 1980; Hendry *et al.*, 1982). Contrary to more traditional views of the dose rate effects that prevailed in the literature at that time, the finding that dose

[8]See https://www.hzdr.de.
[9]See https://ilil.ino.cnr.it.
[10]See https://loa.ensta-paristech.fr.

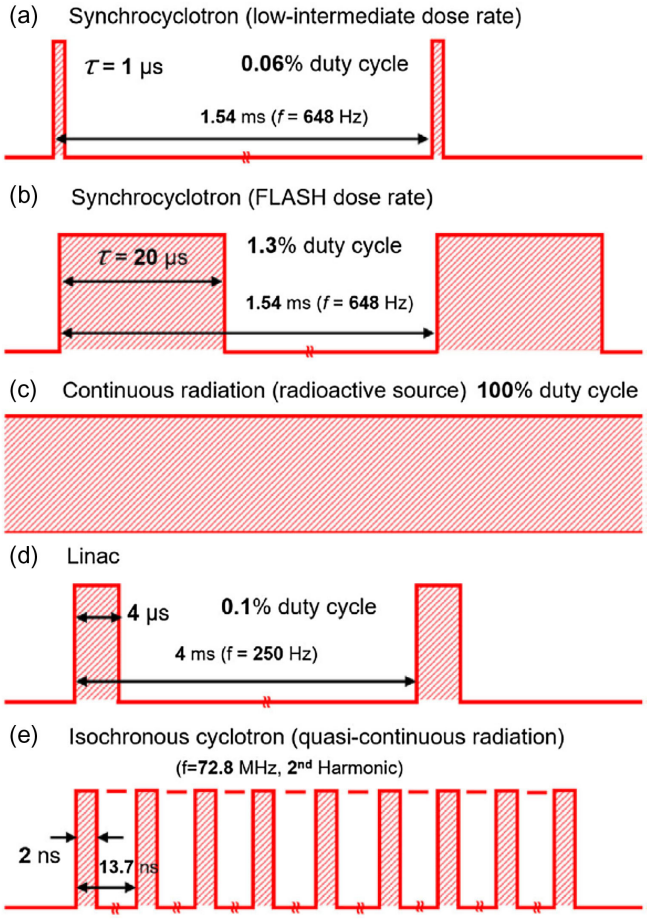

FIG. 11. Temporal structure of various beams used to investigate the FLASH effect in experimental animal models. From Romano *et al.*, 2022.

rates in excess of an ill-defined threshold could result in less rather than more normal tissue toxicity defied conventional radiobiological explanations and was in part the genesis of the oxygen depletion hypothesis (which is further discussed later). Note that no similar studies were conducted on tumors at the time, as it was presumed that hypoxia induced by a high dose rate would protect tumors as well, thus rendering clinical translation of high dose rate RT a moot strategy. Regardless of the underlying assumptions, the field of high dose rate RT entered a period of dormancy lasting for over three decades, until a renaissance paper in 2014 ushered in the modern era of FLASH (Favaudon *et al.*, 2014). With that paper, the concept that dose rate modulation might be used as an adjustable parameter for therapeutic gain attracted the attention of several key scientists in the field who were determined to investigate the basis of what would soon be known as the FLASH effect.

Although it was not generally appreciated at the time, there was the forthcoming recognition that the definition of the "FLASH effect" was ultimately dependent on a rigorous *in vivo* validation. For many investigators, this fundamental tenet imposed significant practical constraints, as experts across multidisciplinary fields juggling a myriad of adjustable beam parameters and different radiation modalities and biological end points would ultimately need to converge and define a common set of physical parameters necessary and sufficient for triggering biological outcomes. Notwithstanding interexperimental and intraexperimental variations between FLASH enabled systems, confirmation of the FLASH effect would still be reliant on a defined set of normal tissue assays capable of validating (or not validating) the capability of dose rate modulation to spare normal tissue toxicities while being equally proficient at killing tumors.

Favaudon *et al.* (2014) were the first to use the term "FLASH" (not an acronym) to distinguish ultrahigh dose rate radiation beam delivery from more conventional dose rate modalities (~0.03 Gy/s) used clinically. Notably Favaudon *et al.* (2014) were also the first to critically evaluate the effects of FLASH irradiation on both normal tissue and tumor outcomes. Using a system originally built to investigate pulse radiolysis, the Kinetron linac was designed to deliver 4.5 MeV electrons in large doses at a conventional dose rate as well as at an ultrahigh dose rate using short pulses as described in Sec. II, Table I displays mean dose rates in excess of 40 Gy/s. Cohorts of mice were exposed to conventional dose rates (CONV, ≤0.03 Gy/s) from the Kinetron, CONV dose rate photon (200 kV photon), and γ ray (^{137}Cs) and compared to mice exposed to FLASH (>40 Gy/s mean dose rate). Mice subjected to an isodose of 17 Gy were followed over 36 weeks, and those subjected to CONV developed classical pathogenic patterns of lung fibrosis involving activation of the TGFβ cascade, pulmonary lesions, collagen deposition, and significant immune cell infiltration as soon as eight weeks, with inflammation and fibrosis progressing over the course of follow-up. In contrast, mice subjected to the same isodose of FLASH developed no histological signs of pulmonary fibrosis and were devoid of TGFβ/SMAD4 cascade activation. Over this same dose range (≤20 Gy), FLASH mice did not develop cutaneous lesions that were severe within the CONV irradiation field. Early (≤24 h) histological evidence also suggested that a marked proapoptotic response observed after CONV was dampened significantly in the bronchi epithelial and smooth muscle cells after FLASH. Dose escalation studies did reveal, however, certain thresholds for the benefits of FLASH in sparing late (≥30 weeks) lung toxicities, as mice exposed to doses in excess of 23 Gy did develop late complications.

In parallel to the aforementioned normal tissue assessments, Favaudon *et al.* (2014) also evaluated the response of human tumor xenografts and syngeneic orthotopic lung tumors to dose rate modulation. Human breast cancer (HBCx-12A) and human head and neck carcinoma (Hep-2) xenografts exposed to various doses of CONV or FLASH (15–25 Gy) exhibited similar tumor growth delay, while the FLASH-irradiated cohort showed no signs of skin damage in the irradiation field. For mice harboring orthotopic TC-1 luciferase and lung tumors, isodoses of 15 Gy CONV and FLASH were also equally effective at forestalling tumor growth, while higher doses of FLASH (28 Gy) were largely curative in the absence of overt fibrotic complications. The findings of Favaudon *et al.* (2014) have been emphasized as they set the preamble for defining several key considerations for the field to move forward, namely, (1) defining that normal tissue response was dose rate dependent, (2) revealing that tumor kill was dose rate independent, (3) establishing dose-limiting toxicities for FLASH, (4) pointing to possible mechanisms of the

TABLE I. Characteristics of currently available electron devices.

	Kinetron (CGR-MeV/ PMB-Alcen)	Oriatron eRT6 (PMB-Alcen)	Oxford linac	Modified Varian (Stanford)	Modified Elekta	Mobetron (IntraOp)	FLASH-knife (PMB-Alcen)	SIT (Sordina)	FLEX (RadiaBeam)	PITZ
Available beam energy (MeV)	4.5	5	6	17	8 and 10	6 and 9	6–10	5–12	9	22
Maximum average dose rate (Gy/s)	2500	1000	1500	750	≥300	>700 at 6 MeV, >800 at 9 MeV	Up to 350 Gy/s at 30 mm depth	1500	7500	10 000
Maximum dose per pulse (Gy)	6.3	12	5	3	1.9	>8 at 6 MeV, >9 at 9 MeV	⋯	18.2	>25	1000
Max. beam size for at least 1.5 Gy/pulse (cm)	5	20.5 (FWHM)	5 (FWHM)	5	2 (5% flatness)	6 at 90%	⋯	1.3 (FWHM)	6	15
Max. beam size at max. dose rate (cm)	0.012	0.5	⋯	5	2 (5% flatness)	4 at 90%	⋯	0.5 (FWHM)	6 (FWHM)	2
Short-term stability (%)	⋯	<1	⋯	<2	1 to 4	0.8	⋯	⋯	±2%	<1%
Long-term stability	⋯	4.1%	⋯	∼4%	⋯	1.8 at 6 MeV, 2.3 at 9 MeV	⋯	⋯	±2%	<1%
Commissioning reference(s)	Lansonneur *et al.* (2019)	Petersson *et al.* (2017), Jaccard *et al.* (2018), and Jorge *et al.* (2019)	⋯	Schueler, Trovati *et al.* (2017)	Lempart *et al.* (2019)	Moeckli *et al.* (2021)	⋯	Di Martino *et al.* (2020)	Kutsaev *et al.* (2021)	Stephan *et al.* (2022)
FLASH effect validated	Favaudon *et al.* (2014), Vozenin *et al.* (2019), and Fouillade *et al.* (2020)	Montay-Gruel *et al.* (2017, 2019, 2020, 2021), Vozenin *et al.* (2019), Alaghband *et al.* (2020), Allen *et al.* (2020), Limoli *et al.* (2020), Chabi *et al.* (2021), Kacem *et al.* (2022), and Rohrer Bley *et al.* (2022)	Ruan *et al.* (2021)	Simmons *et al.* (2019), Levy *et al.* (2020), Y.-E. Kim *et al.* (2021), and Eggold *et al.* (2022)	No	Valdes Zayas *et al.* (2023)	No	No	No	No
Dosimetrically intercompared	Dismantled in 2020	Gonçalves Jorge *et al.* (2022)	No	Gonçalves Jorge *et al.* (2022)	No	No	No	No	No	No
Biologically intercompared	Dismantled in 2020	Yes	No	Yes	No	No	No	No	No	No

FLASH effect that may involve a dampening of inflammatory, immune, and apoptotic cascades in normal tissues that is relatively independent of the tumor microenvironment, and (5) providing initial guidance for the minimum mean dose rate (≥40 Gy/s) required to achieve the *in vivo* FLASH effect. It is noteworthy that the two main observations of Favaudon *et al.* that defined the *in vivo* FLASH effect (points 1 and 2) have stood the test of time, while the other points have required considerable refinement as our understanding of FLASH has evolved (this is especially salient for point 5).

As the stage was set for further studies evaluating the potential merits of dose rate modulation, a duplication of the Kinetron was ordered and installed at CHUV, an Oriatron 5.5 MeV (eRT6; PMB-Alcen) electron linac; see Fig. 12. The CHUV team (Drs. Vozenin and Bailat) dedicated significant time to operating the beam and defining and refining the requisite dosimetry and beam parameters able to reproduce the results obtained earlier with the Kinetron (Jaccard *et al.*, 2017, 2018; Petersson *et al.*, 2017; Jorge *et al.*, 2019). The versatility of this experimental and dedicated FLASH linac provided the capabilities to vary pulse repetition frequency (hertz), pulse width, source-to-surface distance, and field size, which is useful in prescribing large doses over short treatment durations at a convenient working distance for *in vivo* studies. Also important for the field at this time were the needs to (1) establish the potential benefits of FLASH with various beams and groups, (2) validate the FLASH effect at different organ sites and with different model systems, and (3) understand the mechanisms underlying the unexpected FLASH effect. The scientific contributions published at this time defined two major categories: FLASH beam validation and furthering our understanding of the mechanisms of the FLASH effect.

The CHUV team launched a series of studies focused on the brain, with a focus on neurocognitive sparing as the functional outcome. In another landmark paper, Montay-Gruel *et al.* (2017) performed a comprehensive dose rate escalation study

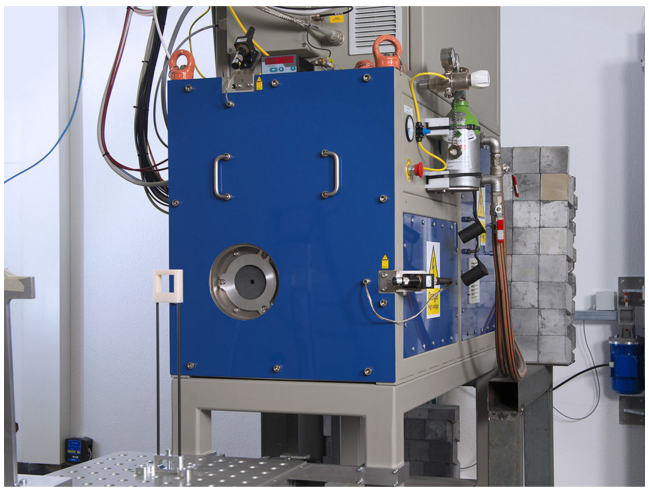

FIG. 12. The Oriatron/eRT6 (PMB-Alcen) is currently considered the reference for demonstrating and investigating the FLASH effect, as more than 15 peer-reviewed publications produced with the Oriatron eRT6 have reproduced the FLASH effect in many organs and animal models.

to assess some of the critical beam requirements to achieve memory sparing using an established learning and memory paradigm called the novel object recognition (NOR) test; see Fig. 5. With this test, which returned a recognition ratio proportional to intact learning and memory, they were able to carefully adjust the number of pulses to vary the dose rate over a range of 0.1 to 500 Gy/s during the delivery of a whole-brain isodose of 10 Gy, keeping the repetition frequency (100 Hz) and pulse width (1.8 μs) constant (except at the lowest dose rate). Data revealed a more accurate dose rate threshold, where robust sparing of learning and memory was achieved at dose rates ≥60 Gy/s, an effect that was coincident with sparing of neural progenitor cell survival in the hippocampal dentate gyrus. Using a different system, Schueler, Trovati *et al.* (2017) later pioneered the conversion of a clinac (Varian) into a FLASH irradiator, albeit with a significantly different time structure. In efforts led by Drs. Loo and Maxim, they were able to remove the flattening filter and minimize the source-to-surface distance of their target volumes, able to deliver 16 or 20 MeV electrons at FLASH dose rates of 300 or 200 Gy/s, respectively, delivered over subsecond intervals (0.1–0.16 s). Differences between this system and that of the Oriatron related to a lower average dose per pulse (1.75 Gy), a slightly lower average intrapulse dose rate (8.75×10^5 Gy/s) requiring a train of pulses (∼18) depending on dose rate modality. Dosimetry confirmed the delivery of a 30 Gy isodose to the whole brain at FLASH or CONV dose rates, and data corroborated many prior findings, in that FLASH preserved recognition memory on the novel object location and NOR tasks, preserved spine density in apical hippocampal dendrites, and was able to attenuate certain markers of neuroinflammation (IL-6 and IL-1β) (Simmons *et al.*, 2019). Noteworthy here was the confirmation that a high single dose of FLASH was still able to reduce normal tissue toxicities in the irradiated brain compared to CONV.

Armed with this new knowledge the group in Lausanne teamed up with the group at University of California, Irvine (UCI) headed by Dr. Limoli to embark on an extensive series of follow-up studies that has since laid the foundation for much of what we currently know about the central nervous system (CNS) response to FLASH. The Lausanne-UCI team significantly expanded on prior work, beginning with an extensive series of functional and molecular studies aimed at elucidating the biological basis of the FLASH effect at the normal tissue level. Using a comprehensive behavioral platform, mice exposed to a single 10 Gy dose of CONV or FLASH irradiation were evaluated for neurocognitive outcomes over six months using three distinct exploration tasks measuring hippocampal and cortical learning and memory, social interaction, anxietylike and depressionlike behavior, and lastly extinction memory (Montay-Gruel *et al.*, 2019). In each instance, control and FLASH cohorts were statistically indistinguishable, while CONV cohorts exhibited significant impairments on each of the tasks. Compared to the CONV cohorts, the beneficial behavioral outcomes found with FLASH were associated with a significant attenuation of astrogliosis, microgliosis, and a preservation of dendritic architecture and spine density, which suggested that at least a certain fraction of the beneficial effects of FLASH

irradiation could be attributed to reductions in neuroinflammation and maintenance of an intact host neuronal structure. The FLASH benefit was also found to be dose dependent, as the sparing effect was lost when a dose of 14 Gy was used; a first DMF of 1.4 was identified for single dose whole-brain irradiation in mice. Cell-free, cell, and zebrafish models were used to corroborate the benefits of FLASH through reductions in reactive oxygen species (hydrogen peroxide) and the preservation of fish morphology. Also interesting was a mouse study implementing carbogen breathing, with the aim of increasing oxygen tension in the brain to evaluate the role of this potent radiosensitizer on the FLASH effect; see Fig. 13 (Montay-Gruel *et al.*, 2019). Note that while normoxic cohorts corroborated all prior findings, carbogen breathing was found to abolish the beneficial FLASH effect on learning and memory, a finding recently replicated with pFLASH (Iturri *et al.*, 2023). This is notable because at the time it provided the most compelling experimental evidence supporting the oxygen depletion hypothesis, a tenet that posits FLASH capable of eliciting a transient, volume-dependent oxygen depletion, resulting in radioprotection. That carbogen breathing increased oxygen levels supported this idea, as the single 10 Gy dose was considered insufficient to deplete the excess oxygen and resultant reactive species to provide normal tissue protection. The oxygen depletion hypothesis has been a topic of intense scrutiny, modeling, and numerous reviews, and further discussed in Sec. IV.

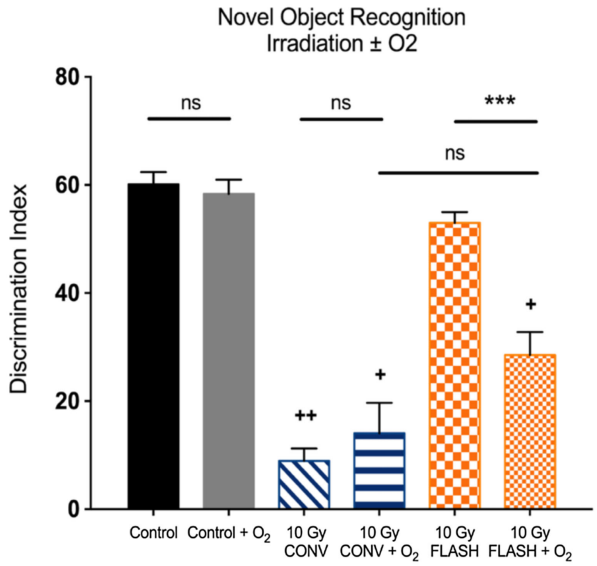

FIG. 13. The carbogen experiment: demonstration of the importance of oxygen in the FLASH effect. Prior to and during irradiation mice were subjected to normal (normoxia) carbogen breathing (O_2 groups). Two months following irradiation, mice were tested on the novel object recognition task for an assessment of neurocognition. Regardless of changes in pO_2, unirradiated mice performed well [high discrimination index (DI)] and eCONV mice exhibited significant performance decrements (low DI). Mice subjected to eFLASH under normoxia exhibited memory sparing, while mice given eFLASH under elevated pO_2 did not. While these data were the first *in vivo* evidence pointing to the importance of oxygen in the FLASH effect, they do not substantiate the oxygen depletion hypothesis; see the text for more details.

Follow-up studies from this same group have addressed several different perspectives related to the response of the CNS to FLASH. Alaghband *et al.* (2020) used an approach similar to that taken by Montay-Gruel *et al.* to evaluate the response of the highly radiosensitive juvenile mouse brain to FLASH. Here two- to three-week-old mice were given a single isodose (8 Gy) of CONV or FLASH irradiation using the 6 MeV Oriatron unit in Lausanne. Mice subjected to a similar comprehensive behavioral battery two to four months after irradiation exhibited the same neurocognitive benefits as found in adult animals, where significant decrements found after CONV were conspicuously absent in FLASH-irradiated juvenile cohorts. These finding were noteworthy since at the time it was uncertain what the single-fraction tolerance dose of the juvenile mouse brain was, but data confirmed again that FLASH provided persistent and long-term beneficial outcomes in the irradiated CNS. Corroborating data were equally compelling, demonstrating that FLASH of juvenile cohorts preserved the neurogenic niche, with significantly higher levels of immature (DCX+) and mature (Brdu + /NeuN+) neurons, minimized neuroinflammation, and preserved increased plasma levels of growth hormone. These studies prompted additional investigation aimed at evaluating the impact of FLASH on the blood brain barrier and the complementary system. In the former case, higher single doses of FLASH (10–25 Gy) were followed over acute (one week) and later times (one month) and found to ameliorate vascular dilation and endothelial nitric oxide synthase expression colocalized with vessels, along with disruptions to the integrity of a tight junction monitored by occludin and claudin-5 expression (Allen *et al.*, 2020). From a more general perspective, analysis of inflammatory markers in the brain pointed to a global suppression of chronic inflammation after FLASH compared to CONV. A deeper probe of astrogliosis (a cell-type-specific form of neuroinflammation) revealed that FLASH suppressed glial fibrillary acidic protein and TLR-4 compared to CONV but had little impact on expression levels of complement Clq and C3 (innate immunity markers) which were elevated regardless of dose rate, pointing to the complexities of the neuroimmune axis in the irradiated brain (Montay-Gruel *et al.*, 2020). For each of the aforementioned studies, an instantaneous dose rate of 10^7 Gy/s (1.8 μs) of 5.5 MeV electrons delivered in one to two pulses was used for FLASH.

The FLASH effect has been evaluated most thoroughly in the irradiated brain, where the functional neurocognitive benefits have translated to sparing of inflammation, neurogenesis, and the preservation of neuronal and vascular morphology. Nonetheless, one clear gap in the field that persisted was how the tumor bearing brain would respond to FLASH and how it would respond to more clinically relevant irradiation regimens involving dose fractionation. Many of those questions were resolved by another major paper demonstrating the benefits of different hypofractionation protocols delivered to well characterized murine orthotopic glioblastoma model. We recognize that preclinical studies designed to evaluate late toxicities in tumor bearing animals must obtain functional outcomes in the face of aggressive tumor growth, a

fact that necessitates shorter and more practical normal tissue assessments; see Fig. 14. Montay-Gruel *et al.* (2021) subjected nude mice engrafted with murine H454 glioblastoma (GBM) cells to select isodoses of FLASH or CONV to evaluate how different fractionation protocols impacted tumor growth, survival, and cognition. In each instance, tumor growth delay was found to be insensitive to dose rate modulation, where increasing the total dose increased tumor growth delay with concomitant improvements in survival.

Cognitive assessments using the validated NOR task in the presence of tumor again confirmed the benefits of a single 10 Gy dose of FLASH on learning and memory but were lost at the higher single dose of 14 Gy. This observation highlights an important point in that tissue-specific dose thresholds exist for FLASH, and that higher doses and fractions can still elicit dose-limiting toxicities that must be evaluated and considered as the FLASH field moves toward clinical translation. When the 14 Gy single dose was split into equal 7 Gy fractions, neurocognitive sparing was again achieved. When an isodose of 30 Gy was delivered in three fractions of 10 Gy, marked H454 tumor growth delay and improved survival coincided with significant neurocognitive sparing. Montay-Gruel *et al.* (2021) demonstrated for the first time in tumor bearing mice that the FLASH effect could be achieved under a hypofractionated regimen and was associated with marked improvements in tumor control. Although tumor growth delay has mainly been used to date, tumor cure was also achieved under the same dosing paradigm with U87 orthotopic tumors (Montay-Gruel *et al.*, 2021), and the isoefficacy of FLASH and CONV to induce long-term complete response was also recently confirmed in an orthotopic model of NS1 rat glioblastoma by Liljedahl *et al.* (2022) and by Almeida *et al.* (2024) in an orthotopic model of GL261 mouse glioblastoma.

As data from the FLASH-irradiated brain accumulated, the first negative results were published with a transformed clinac (Varian) and a dose rate of 35 Gy/s (Venkatesulu *et al.*, 2019). Venkatesulu *et al.* (2019) investigated acute responding organs including cardiac and splenic models of lymphopenia and the intestine. Severe lymphodepletion was found to be induced by eFLASH versus eCONV, and no crypt protection was reported alongside high lethality after whole-abdomen exposure to 16 Gy eFLASH versus eCONV. The reasons for these contrasting results remain uncertain but likely center around the low dose rate, technological issues, and/or the acute model. Furthermore, initially Venkatesulu *et al.* (2019) did not fully characterize the beam and physical parameters, as the dose per pulse, number of pulses, and overall time of

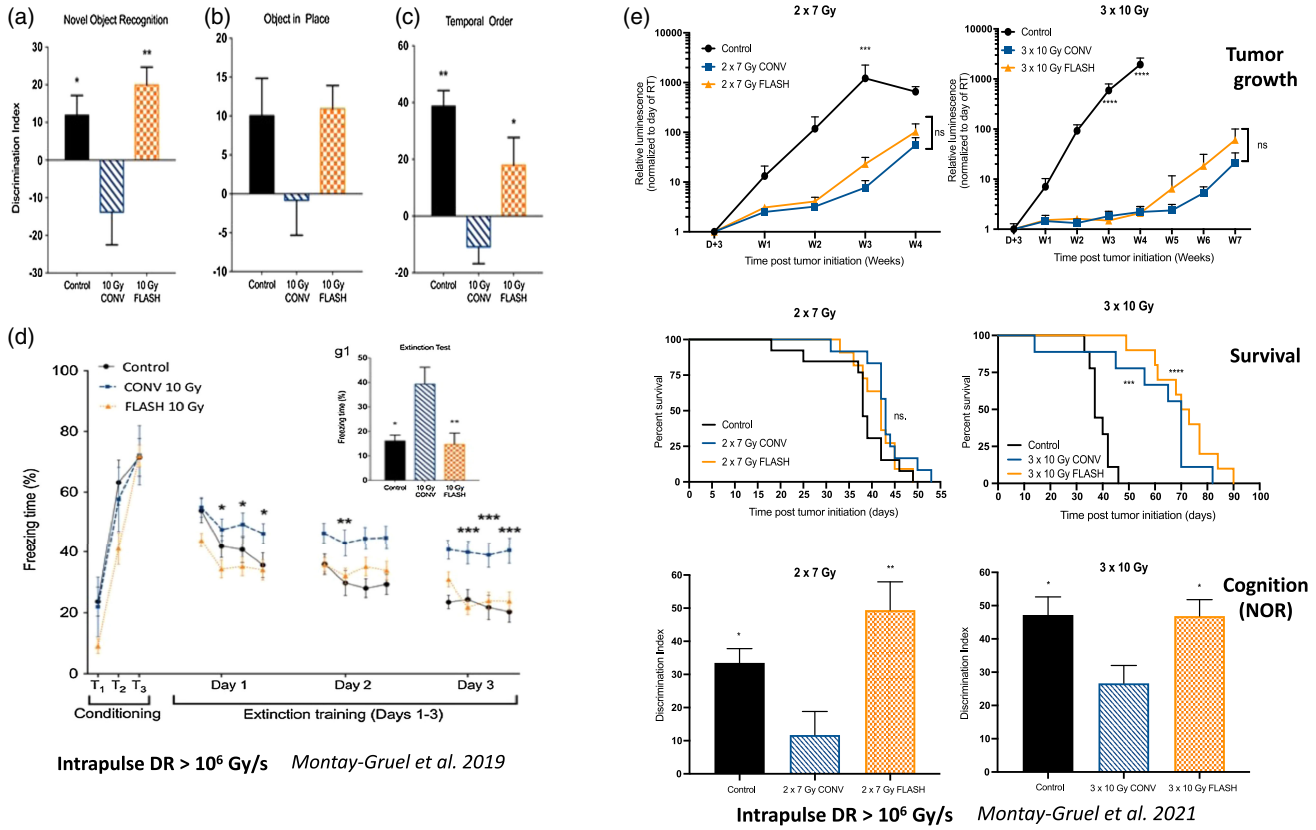

FIG. 14. eFLASH spares adverse neurological outcomes in tumor-free and tumor bearing mice. (a)–(d) In tumor-free mice, a single 10 Gy dose of eFLASH spares cognition over a six-month postirradiation time. (a)–(c) Open field exploration tasks that rely on a rodent's innate curiosity regarding novelty routinely show that eCONV elicits marked reductions in the discrimination index that are not observed in controls or eFLASH cohorts. Similarly, using a fear extinction task, eCONV results in marked long-term impairments in extinction memory, as shown by (d) an elevated freezing behavior, decrements not found in control or eFLASH cohorts. (e) In mice bearing orthotopic GBM tumors, fractionated irradiation (2×7 or 3×10 Gy) slows tumor growth and exhibits similar benefits (3×10 Gy) on survival. However, only those cohorts subjected to eFLASH exhibit memory sparing.

exposure were not defined, but a corrigendum was later published (Venkatesulu *et al.*, 2020) reporting a pulse rate of 180 Hz, a pulse length of 4 μs, and 20 MeV electrons leading to a dose rate of 32.6 and 38.8 Gy/s for the 2×2 and 4×4 cm^2 fields, respectively, that seemed too low to produce the FLASH effect.

At the time, further work investigating the impact of eFLASH on acutely responding, stem cell rich tissues had not been investigated. Shortly thereafter, Levy *et al.* (2020) applied whole-abdomen irradiation to mice using 16 MeV electrons at lethal (16 Gy) and sublethal (14 Gy) doses using FLASH (mean dose rate 216 Gy/s) or CONV (mean dose rate 0.08 Gy/s). They reproduced the FLASH effect in the gut conversely to what was reported by Venkatsesulu *et al.* The main difference between the two studies was the dose rate: 35 versus 216 Gy/s. In the Stanford experiments, while 16 Gy CONV triggered rapid lethality by the acute gastrointestinal syndrome, FLASH did not, instead preserving the number of regenerating crypts that promoted normal gut histology 12 weeks postirradiation (post-IR) with a DMF of 1.14. At sublethal doses FLASH preserved intestinal integrity, which was measured by sparing of the epithelial barrier, faster recovery of normal stool formation, and increased numbers of regenerating crypts. Bromodeoxyuridine (BrdU) labeling confirmed that FLASH spared crypt base columnar cells, a finding that was corroborated in part by early ($\leq$24 h) reductions in apoptosis and DNA damage in the same populations of crypt cells. This study also evaluated the safety and efficacy of FLASH and CONV in a preclinical model of ovarian cancer metastasis. Mice harboring diffuse ID8 ovarian metastases throughout the peritoneal cavity were given 14 Gy abdominal irradiation and followed for selected toxicities and outcomes. In tumor bearing mice, FLASH was still found to preserve intestinal function and was as efficacious as CONV in controlling metastatic tumor burden. These noteworthy findings demonstrated that, in a radiosensitive organ like the gut, the FLASH effect could still preserve normal intestinal function in tumor-free or tumor bearing mice while maintaining equal potency in reducing metastatic ovarian tumor nodules compared to CONV. These results also suggest that a higher dose rate (>200 Gy/s) seems to be required in the gut, whereas 40 Gy/s was sufficient in the lung and 60 Gy/s was sufficient in the brain.

In a follow-up study by Eggold *et al.* (2022), abdominopelvic irradiation was used to investigate the immunomodulatory properties of 16 MeV eFLASH (mean dose rate 210 Gy/s, 2 Gy/pulse, and repetition rate 90 Hz) versus eCONV (mean dose rate 0.126 Gy/s) in preclinical ovarian cancer models. Mice harboring intraperitoneal ID8 murine cell-derived ovarian tumors and given a sublethal isodose of 14 Gy eFLASH showed a sparing of intestinal crypts and similar efficacy in the treatment peritoneal tumors compared to eCONV, results that were consistent with prior findings. Following the same dose, early (96 h) and late (17-day) changes in the ovarian tumor microenvironment were evaluated and each irradiation modality was found to induce a similar early drop in intratumoral regulatory T cells and a latter rise in cytolytic CD8+T cells. Early intratumoral infiltration of T cells, however, was more evident in FLASH versus CONV arms. In combination with anti-PD-1 treatment, FLASH and CONV were found to maintain increased intratumoral CD8+T cell infiltration and reduce immunosuppressive monocyte populations. Overall, these data suggest that immune checkpoint inhibition could slow tumor progression in the αPD-1 resistant ID8 and sensitive UPK10 ovarian cancer models when combined with FLASH without compromising efficacy or increasing toxicities compared to monotherapy alone and CONV.

As the capability to convert clinacs to FLASH irradiators was gaining traction, investigations addressing the necessary beam parameters required to optimize the FLASH effect also started. To investigate how changes in the temporal structure of the beam might differentially impact normal tissue sparing, Ruan *et al.* (2021) systematically varied the number of pulses or spacing between successive pulses to deliver isodoses of 6 MeV FLASH or CONV electrons. They worked in 95% oxygen with differently aged mice given sublethal (11.2–12.5 Gy) whole-abdomen irradiation that exhibited intestinal sparing at mean FLASH dose rates $\geq$280 Gy/s. While the magnitude of sparing was relatively small compared to prior reports (DMF = 1.1), probably due to the hyperoxia, the benefits of FLASH diminished as the pulse number and overall treatment time increased. FLASH was also found to alter the gut microbiome to a lesser extent than CONV, which provided some clues to the preservation of intestinal function reported elsewhere. Notable here was the effort made at extending prior work with electrons in defining critical beam parameters, where current datasets collected from various eFLASH studies indicate that electron beams able to provide the highest dose per pulse using a minimum of pulses delivered over the shortest duration (high repetition frequency) are the most likely to provide a robust *in vivo* FLASH effect.

Studies dedicated to further investigating the biological aspects of the lung were conducted with the Kinetron FLASH linac at the Institut Curie. New data corroborated several prior findings and shed new light on the mechanisms of FLASH. Fouillade *et al.* (2020) found that following a bilateral thorax exposure to 17 Gy FLASH reduced early (one week post-IR) proliferation measured by 5-ethynyl-2 deoxyuridine (EdU) uptake, minimized early (one week) and more persistent (three month) DNA repair foci (53 bp-1) and attenuates levels of radiation-induced senescent cells (β-gal) compared to an isodose of CONV. Radiation-induced fibrosis that was again found to be minimized after FLASH was not in a mouse background having shortened telomeres ($Terc^{-/-}$), thus pointing to a link between telomere shortening and senescence that may have genetically suppressed the FLASH effect. RNA sequencing (RNAseq) analysis of lung homogenates did uncover a reduction in certain gene expression (Tgfβ, Cebpb) that supported other findings that FLASH can attenuate profibrotic and inflammatory cascades in the irradiated lung. *In vitro* studies (discussed later in this section) corroborated several *in vivo* findings in terms of reduced DNA repair foci and survival of bronchial epithelial cells. In a separate study on Lewis lung carcinoma subcutaneous tumors from Stanford and Seoul National University (Y.-E. Kim *et al.*, 2021), the effects of a 15 Gy isodose of CONV or FLASH

(16 MeV electrons delivered from their converted clinac) was investigated on the tumor and microenvironment. FLASH was not found to cause early vascular constriction or significant changes in hypoxia. At similar early time points (6 h post-IR) FLASH was not found to elicit the marked activation of myosin light chain (p-MLC) in endothelial and tumor cells found after CONV and was reactive oxygen species (ROS) independent, since FLASH was found to potentiate ROS levels in tumors compared to CONV. DNA repair foci were significantly higher in tumors irradiated at CONV versus FLASH. Inhibition of the MLC through the administration of the ML-7 prior to CONV irradiation was observed to phenocopy certain FLASH-induced changes in the tumor microenvironment, suggesting that while overt tumor cell kill may be insensitive to dose rate modulation, the impact on the tumor microenvironment that contains normal cells from the host is dose rate sensitive.

In efforts to address the impact of FLASH on the skin, Soto *et al.* (2020) performed the first dose-response study for skin toxicity in mice comparing FLASH and CONV dose rates using their converted clinac. They were able to deliver 16 MeV electrons at a mean dose rate of 180 Gy/s, delivered at a pulse repetition rate of 90 Hz, with an instantaneous dose rate of 4.5×10^5 Gy/s (5 μs pulse width) at a total dose of 2 Gy/pulse. Following hemithoracic irradiation over a range of doses (10–40 Gy), single high doses of FLASH (30 and 40 Gy) significantly lowered the incidence and severity of skin ulcerations at an eight-week follow-up compared to CONV. Survival was also improved following FLASH due to fewer mice reaching skin euthanasia toxicity criteria. These studies corroborate additional datasets collected from larger vertebrate models (minipig, cat, and dog) and from the first human patient treated with FLASH (each discussed later in this review) and point to the capability of FLASH to spare skin toxicity in multiple species.

B. The *in vivo* FLASH effect: Photon beams

Technical requirements for generating ultrahigh dose rate photon (x-ray) FLASH systems are not readily available, as typical beam currents require intensities in the range of several milliamperes, as opposed to microamperes, and require optimized electron guns and conversion targets, as discussed in Sec. II. As such, specialized facilities or *de novo* instrumentation are required to investigate xFLASH, which has limited the number of *in vivo* studies to date using high dose rate x rays. The first such study, conducted at ESRF in Grenoble in collaboration with the CHUV, took advantage of its capability to produce ultrahigh dose rates of x rays that through specialized sources could deliver highly coherent and nondivergent x rays at a mean energy of 102 keV using a well-controlled animal model of whole-brain irradiation. With the ability to spatially fractionate this source into 50 μm parallel microbeams, a dose rate of 12 000 Gy/s was obtained, and by rapidly moving the target region (brain) through this slice an average dose rate of 37 Gy/s could be achieved for the delivery of 10 Gy whole-brain irradiation over 0.27 s using the same geometry that was used with the Oriatron eRT6. Using this system, cohorts of mice exposed to xFLASH or CONV were evaluated on the well characterized NOR task, where memory sparing was found after 10 Gy doses at two and six months post exposure (Montay-Gruel *et al.*, 2018). At the two-month time point, the number of proliferating BrdU-positive cells in the hippocampal subgranular zone were spared and reactive gliosis was reduced in the FLASH cohort compared to CONV. While the technical requirements associated with delivering synchrotron-derived x rays preclude rapid clinical translation, this proof-of-principle study did demonstrate that the FLASH effect was not unique to electron beams and pointed to a more general applicability of dose rate modulation for therapeutic gain among different radiation modalities.

However, the positive results obtained at ESRF with 37 Gy/s on the brain were not reproduced at the Australian Synchrotron with 37 and 41 Gy/s after whole-thorax and whole-abdomen irradiation (Smyth *et al.*, 2018). Here again several explanations may account for these discrepancies. At ESRF investigations were performed on a small volume (17 mm diameter) and late-responding tissue (brain), whereas at the Australian Synchrotron investigations were performed on large volumes ($> 30 \times 20$ mm^2) as well as on two acute responding organs (gut and hematopoietic) and one late-responding organ (lung). These results suggest that higher dose rates are needed to produce the FLASH effect in acute responding organs and/or larger volumes and argue that direct transposition of parameters obtained in one condition (dose rate, volume, and organ) to another condition is not possible, a supposition that was confirmed in later experiments performed on large animals; see Sec. V.

Studies conducted at a superconducting linac facility in China were able to deliver 6–8 MeV x rays at a mean dose rate around 1000 Gy/s (Gao *et al.*, 2022). FLASH and CONV (0.01 Gy/s) dose rates were used to compare the impact of near or matched isodoses on tumor control and survival following whole-thoracic or whole-abdomen irradiation. Data revealed that subcutaneous human EMT6 breast cancer tumors in Balb/C mice were responsive to both FLASH (18 Gy) and CONV (15 Gy) with no significant differences in survival and a DMF of 1.2. For thoracic irradiation (30 Gy, FLASH or 24 Gy, CONV) survival was significantly higher, and evidence of alveolar fibrosis was reduced for FLASH with a DMF of 1.25. For abdominal FLASH (15 Gy) or CONV (12 Gy) lethality occurred over shorter times but the FLASH cohort showed signs of reduced inflammation, possibly due to collagen remodeling and a DMF of 1.25. For isodoses of 30 Gy thoracic or 12 Gy abdominal, FLASH cohorts exhibited superior survival, particularly in the latter case. While additional quantification of normal tissue toxicities will be required, data corroborated xFLASH to be efficacious at controlling tumor growth and equally effective if not superior in prolonging survival for selected partial body exposures compared to CONV.

C. The *in vivo* FLASH effect: Proton beams

While the field of eFLASH was progressing rapidly, major limitations for clinical applications became obvious (see Secs. II and V) and those engaged in the use of protons for therapeutic gain were determined to evaluate whether and how dose rate modulation of high-energy proton beams might

elicit similar benefits in terms of normal tissue sparing and isoefficient tumor growth delay. As discussed, the delivery of protons differs substantially from that of electrons or x rays due both to the temporal structure of the beam, which is semicontinuous, and to the pattern of proton deposition in the matter, with a plateau phase followed by a maximal deposition of energy in the Bragg peak. Range shifters (ridge filters) have been developed to maximize the Bragg peak deposition to cover the entire target (tumor) volume with the SOBP. Proton beams also intrinsically operate at UHDR when the beam is focused, suggesting that scanning would be needed to treat human tumors. The first reports on the pFLASH effect were performed in the plateau region, using what is often referred to as shoot through mode or transmission mode, as controlling dose and enhancing the dose rate were easier in this region (Diffenderfer *et al.*, 2020). However, given the interest of combining the deposition of the Bragg peak (SOBP) in the tumor with normal tissue sparing in the plateau at UHDR, the various groups working with pFLASH developed this aspect. Other important research developed with proton FLASH is related to the maintenance of the FLASH effect when the beam is scanned. These investigations are highly complex as they involve both temporal and spatial modulations, which might impact dosimetric and biological responses in different ways (Griffin *et al.*, 2020; Prezado, 2021). However, these investigations are of the utmost importance to move the FLASH field to the clinic.

While the first report with transmission pFLASH at 100 Gy/s by Beyreuther *et al.* (2019) on zebrafish embryos was negative (as discussed later in the review), Karsch *et al.* (2022) were able to observe the sparing effect of FLASH with a proton when they enhanced the dose rate to 300 Gy/s, and positive mice data were published soon thereafter by several groups, thus supporting the idea that a single dose rate suffices for all purposes and all targets. Zhang *et al.* (2020) reported on the development of an experimental proton beam from the Harvard cyclotron facility running at 300 nA using a double-scattering system able to deliver 226 MeV protons to a target at the entry plateau region while maintaining mean dose rates in excess of 100 Gy/s. With this system able to deliver ~3 ns bunches (pulses) spaced 9.4 ns (rf of 106 MHz) apart, they evaluated the dose response of partial abdominal (1.2×1.6 cm^2) irradiation in mice. Mice received total FLASH doses of 13–22 Gy in 180 ms at an average dose rate of 120 Gy/s and were compared against CONV proton dose rates between 1.9 and 4.5 Gy/ min over the same dose range. At higher lethal doses (19–22 Gy) no benefits in survival or weight were observed between the dose rates, whereas at 16 Gy FLASH improved mice survival (100% versus 40%) and prevented weight loss (nine-day follow-up) compared to an isodose of CONV and a DMF of 1.23 was found. Late intestinal injury was more difficult to follow given the limited number of mice surviving but did hint at signs of reduced intestinal toxicity after FLASH compared to CONV.

Simultaneously Diffenderfer *et al.* (2022) adopted a similar approach using their IBA proton system to deliver proton beams at 230 MeV using a double-scattering system and collimation apparatus able to deliver a mean dose rate of 78 Gy/s over similar operating currents (300 nA), cyclotron rf (106 MHz) in 2 ns beam pulses, and dosimetric validation. Acute (3.5 days) normal tissue toxicity in the gut after whole-abdomen irradiation (15 Gy) was evaluated along with tumor growth delay after a subcutaneous injection of cells derived from the KPC autochthonous PanCa model to generate flank tumors given doses of 12 or 18 Gy. All pFLASH end points were evaluated in the plateau region and compared against a CONV proton dose rate of 0.9 Gy/s. Incorporation of EdU was used to quantify intestinal crypt cells and Masson's trichrome staining to quantify tissue thickness and fibrosis. pFLASH showed marked sparing of regenerating crypts a few days after exposure to 15 Gy, while fibrotic onset was reduced eight weeks after exposure to 18 Gy when compared to CONV. Note that mice harboring pancreatic flank tumors showed no dose rate dependence in tumor growth control after either 12 or 18 Gy single dose exposures, demonstrating for the first time the isoefficiency of pFLASH with conventional dose rate delivery using proton beams (pCONV). These results corroborated the past work with eFLASH beams despite major temporal differences in the structure of the beam and suggested that a mean dose rate of 70 Gy/s was sufficient to produce the FLASH effect.

Diffenderfer *et al.* (2022) extended their research using the same experimental proton beam (230 MeV). Mice were again irradiated in the plateau region using pFLASH (69–124 Gy/s) and compared with pCONV (0.39–0.65 Gy/s), where studies focused on normal tissue responses of skin and mesenchymal tissues of the muscle and bone (Velalopoulou *et al.*, 2021). In this model, higher doses are needed and exposures over 30–45 Gy showed that pFLASH provided protection against mortality and severe morbidity compared to pCONV and limited severe skin reactions requiring euthanasia. As the latter complication dictated the most severe toxicities following high-dose proton exposure, follow-up RNAseq studies uncovered that, compared to pFLASH, apoptotic and keratinocyte differentiation were upregulated in pCONV, whereas pathways involved in tissue and vascular repair were more highly upregulated after pFLASH. Additional analyses provided further insights into the epithelial sparing of pFLASH, which was shown to preserve populations of skin stem cells ($Lgr6^+$) and reduce the extent of epidermal necrosis and hair follicle atrophy. Radiation-induced inflammatory reactions evaluated on the hind limb suggested that myeloid cell infiltration was reduced three weeks after pFLASH compared to pCONV. The inflammatory benefits were modest yet significant and were associated with less hyperplasia in the FLASH versus CONV group at 30 Gy but were not realized after a higher isodose of 45 Gy, pointing to certain skin dose thresholds for the pFLASH effect. At this higher dose, the severity of lymphedema, which represents a significant clinical complication, was significantly reduced by pFLASH, although lymphedema incidence was less responsive to proton dose rate modulation. For mesenchymal tissues, pFLASH reduced muscle atrophy and preserved myofibril anatomy one month after exposure. Similarly, indications of bone remodeling were minimized after pFLASH, although whether this was due to changes in the ratio of bone forming osteoblasts versus bone resorbing osteoclasts at this early postirradiation time was uncertain. As with epithelial tissues, pathways involved with differentiation

and activation of bone remodeling were upregulated by pCONV as compared to pFLASH, suggesting lower burdens of normal tissue damage after FLASH and a reduced need to activate inflammatory-mediated tissue recovery. In support of the latter, early immunofluorescent-based (18 days post-IR) and enzyme-linked immunosorbent assay– (ELISA-) based (5 days post-IR) quantification of TGFβ1 in murine and canine skin was performed. A lower level of this fibrogenic growth factor was found in pFLASH-irradiated cohorts. While the relevance of these findings obtained at an early time point in the development of delayed fibrosis is low, they supported an early and protective impact of pFLASH on the wound healing response. Finally, this study also evaluated the response of two murine models of sarcoma to dose rate modulation of pFLASH. In a subcutaneous (KP) flank model or in an orthotopic intramuscular fibrosarcoma model, tumor responses were indistinguishable between dose rates, substantiating significant past data from other FLASH modalities that support tumor kill being dose rate independent.

The next step for proton investigations was to assess the capability of maintaining the FLASH effect when large, deep-seated tumors are treated with state-of-the-art PBS techniques. The scanning procedure involved the delivery of doses in small volumes (spots) scanned over the entire target volume. In a first of its kind study Cunningham *et al.* (2021), working at the University of Cincinnati, used a clinical cyclotron (Varian ProBeam) and a pencil-beam scanning nozzle to deliver 250 MeV protons in the plateau region at pCONV (1 Gy/s) or pFLASH (57 115 Gy/s) dose rates. Their approach was to cover the irradiation field with approximately thirty 4 mm spots as rapidly as possible to reach a uniform absorbed dose of 35 or 15 Gy. They evaluated skin toxicity (hind limb) and tumor control. Compared to pCONV, skin toxicity and leg contracture ($\leq$12 weeks) and TGFβ-1 levels in the plasma and skin ($\leq$96 h) were decreased significantly in pFLASH cohorts at each of the high dose rates. Differences between select circulating cytokines were less responsive to dose rate modulation apart from Cxcl-1, G-CSF, and GM-CSF. Importantly, immune hot (MOC1) and cold (MOC2) murine squamous cell carcinomas grown in the hind limb were equally responsive to proton irradiation, regardless of the dose rate, which corroborated all previous studies with different beam modalities that tumor kill is dose rate independent and suggested that the tumor microenvironment does not contribute to the pFLASH response.

The last aspect of pFLASH related to the Bragg peak, which was recently validated in two papers. Evans *et al.* (2022) used a synchrocyclotron proton therapy system equipped with a ridge filter to distribute uniform doses over the SOBP (80% entrance to distal) from 10 to 19 Gy down to a depth of 2.5 cm across an 11 mm^2 field size to the abdomen of mice at pFLASH (100 Gy/s) or pCONV (0.1 Gy/s) dose rates. Over a 21-day follow-up, cohorts subjected to pFLASH had higher LD50 values and an improved survival rate (10%–20%) compared to pCONV. These findings provided some of the first indications that normal tissue sparing could be achieved with the SOBP using pulsed synchrocyclotron proton beams.

In a more detailed study, Y.-E. Kim *et al.* (2021) compared the effects of whole-abdomen 230 MeV proton irradiation (15 Gy) in mice. They evaluated how intestinal sparing and tumor control might be differentially affected by pFLASH or pCONV at the entrance region or SOBP, with the latter modulated over a 2.5 cm width using 3D-printed ridge filters. With this setup, entrance region dose rates of 107 and 0.83 Gy/s and SOBP dose rates of 108 and 0.82 Gy/s were achieved for pFLASH and pCONV, respectively. Early time point studies (3.5 days after RT) confirmed their earlier work with the plateau and found that both plateau and SOBP pFLASH preserved the number of EdU+ jejunum crypt cells and regenerated intestinal crypts compared to pCONV. Flank tumors derived from syngeneic mouse pancreatic tumor cells and exposed to a single 18 Gy isodose of pFLASH or pCONV showed no difference in tumor growth, regardless of whether the absorbed dose was in the entrance or the SOBP region. Note that while mice survived entrance region dose rate modulation, lethality observed in pCONV SOBP cohorts was significantly spared when tumors were irradiated with pFLASH at the SOBP region. Thus, Y.-E. Kim *et al.* (2021) further established that normal tissue sparing and isoefficient tumor growth delay could be achieved with the plateau and the SOBP; however, the study was not designed to define dose modifying factors between pCONV and pFLASH or between the plateau and the SOBP.

The dose modifying factor was addressed later by the Aarhus group, who performed a state-of-the-art dose-response curve in mice. In a first study Singers Sørensen *et al.* (2022) used right hind limb irradiation of mice from the CDF1 strain and a single fraction of proton PBS in the entrance plateau at 244 MeV, 0.33–0.63 Gy/s CONV and 250 MeV, 71–89 Gy/s FLASH. They found that a 44%–58% higher dose was required to give the same acute biological response to normal tissue with FLASH than with CONV. In a second study using the same irradiation setup and a C3H mouse bearing a subcutaneous mammary carcinoma, they found a similar TCD_{50} (dose for 50% tumor control) for CONV and FLASH, whereas the DMF for late fibrosis was 1.14 (Sørensen *et al.*, 2022).

As a last point of discussion, we return to the initial negative results reported by Beyreuther *et al.* at 100 Gy/s that were later reversed into positive results when they increased the dose rate up to 300 Gy/s using a clinical proton beam (Karsch *et al.*, 2022) and decreased oxygen tension as well as a 10^9 Gy/s dose rate within the pulse and a 10^5 Gy/s mean dose rate using the research electron accelerator ELBE (Pawelke *et al.*, 2021). The zebrafish (ZF) embryo is a relatively new model in the field of radiation biology. It has several distinct advantages including the fact that it is a fully integrated *in vivo* model, ethics approval is not required at early stages, and it is a short-term model with a rapid biological response (five days). Zebrafish embryos also have other interesting characteristics, such as a rapid shift in their radiation resistance profile according to developmental status (DL100 ranging from 15 to 50 Gy within the first 24 h of their development) (Traver *et al.*, 2004). Therefore, to investigate the impact of clinically relevant doses (in the range of 10 Gy), working at 4–4.30 hours post fertilization is required. In a recent study, the CHUV group showed that ZF embryos appear to be more sensitive to the nature of the beam and/or

dose rate variation than mice are. ZF embryos were less sensitive to proton beams than to electron and photon beams at conventional dose rates. Their development was preserved to the same extent after exposure to pCONV and pFLASH, as opposed to exposure to eFLASH (Kacem *et al.*, 2022). These results are consistent with Beyreuther's initial results showing no FLASH effect between 0.1 and 1260 Gy/s with proton beams but not with the later results showing the FLASH effect above 300 Gy/s. Results from the CHUV group also showed that the apparent lack of the FLASH effect was related not to enhanced damage but to a preservation of ZF development after proton irradiation at either dose rate. In their follow-up studies, Montay-Gruel *et al.* (2019) and Vozenin, Hendry, and Limoli (2019) suggested that hypoxia was required in ZF embryos to trigger the FLASH-sparing effect in response to UHDR, a factor that was not found to be required in our previous experiments with 5.5 MeV eFLASH beams. In summary, these studies showed that the FLASH effect is a complex process likely involving multiple mechanisms and that the normal tissue sparing triggered by pFLASH beams (>70 Gy/s). As consistently reported by many groups working with various murine models (gut, skin, and brain), the studies also showed that the FLASH effect may not be universal.

1. Summary of the *in vivo* findings

The normal tissue sparing effect of FLASH has been reported for a normal brain, lung, and gut when FLASH is delivered with electrons and protons. Data indicate that FLASH can spare (minimize) apoptosis and prevent senescence (see Fig. 15); it also spares progenitor and stem cells (see Fig. 16) as well as vascular integrity (see Fig. 17). Observations also point to a net reduction of inflammatory responses (see Fig. 18) in the relative absence of structural damage and functional outcomes. In tumors, FLASH and CONV are isoefficient.

D. The *in vitro* FLASH studies: Cell survival, DNA damage, and DNA repair

In the field of radiobiology applied to oncology, many *in vivo* models have been developed to investigate normal tissue damage and recovery. These models are time and labor intensive, especially for late-responding tissue (lung, brain, and bone) that are largely devoid of a rich stem cell population and necessitate a focus on functional outcomes that can take several months to manifest (for example, cognitive dysfunction, lung fibrosis, and osteradionecrosis). Even stem cell rich early responding tissues (bone marrow, gut, and oral mucosa)

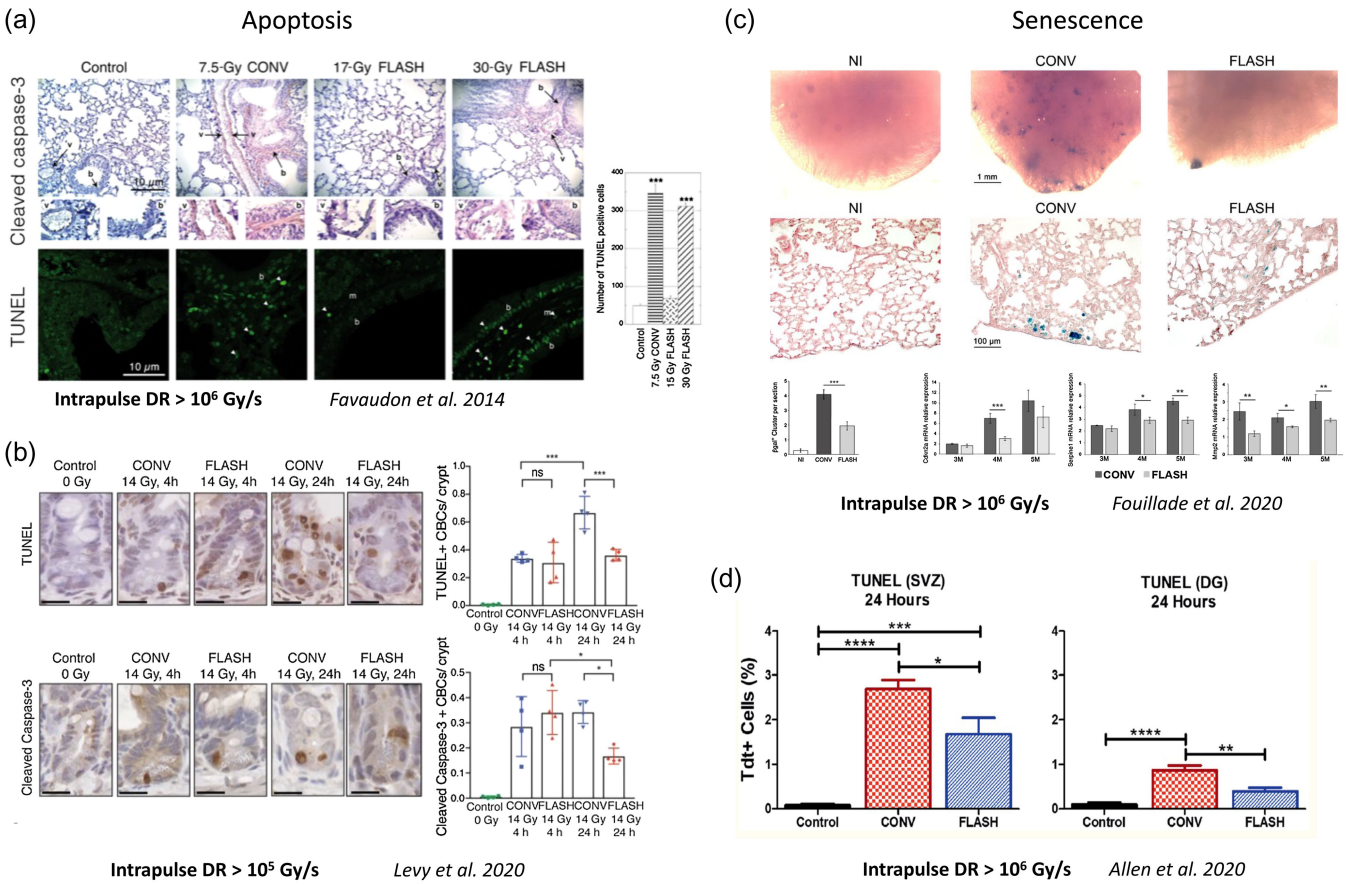

FIG. 15. eFLASH spares apoptosis and senescence *in vivo*. (a)–(c) In the lung, eFLASH reduces the yield of apoptotic markers (cleaved caspase-3, TUNEL positive cells) and markers of senescence (beta-galactosidase, messenger ribonucleic acid expression of specific genes) compared to eCONV. (d) Similar apoptotic markers used in the intestinal epithelium or the neurogenic regions of the brain (SVZ, subventricular zone; DG, dentate gyrus) reveal the capability of eFLASH to minimize apoptosis in multiple tissues compared to eCONV. From Favaudon *et al.*, 2014, Allen *et al.*, 2020, Fouillade *et al.*, 2020, and Levy *et al.*, 2020.

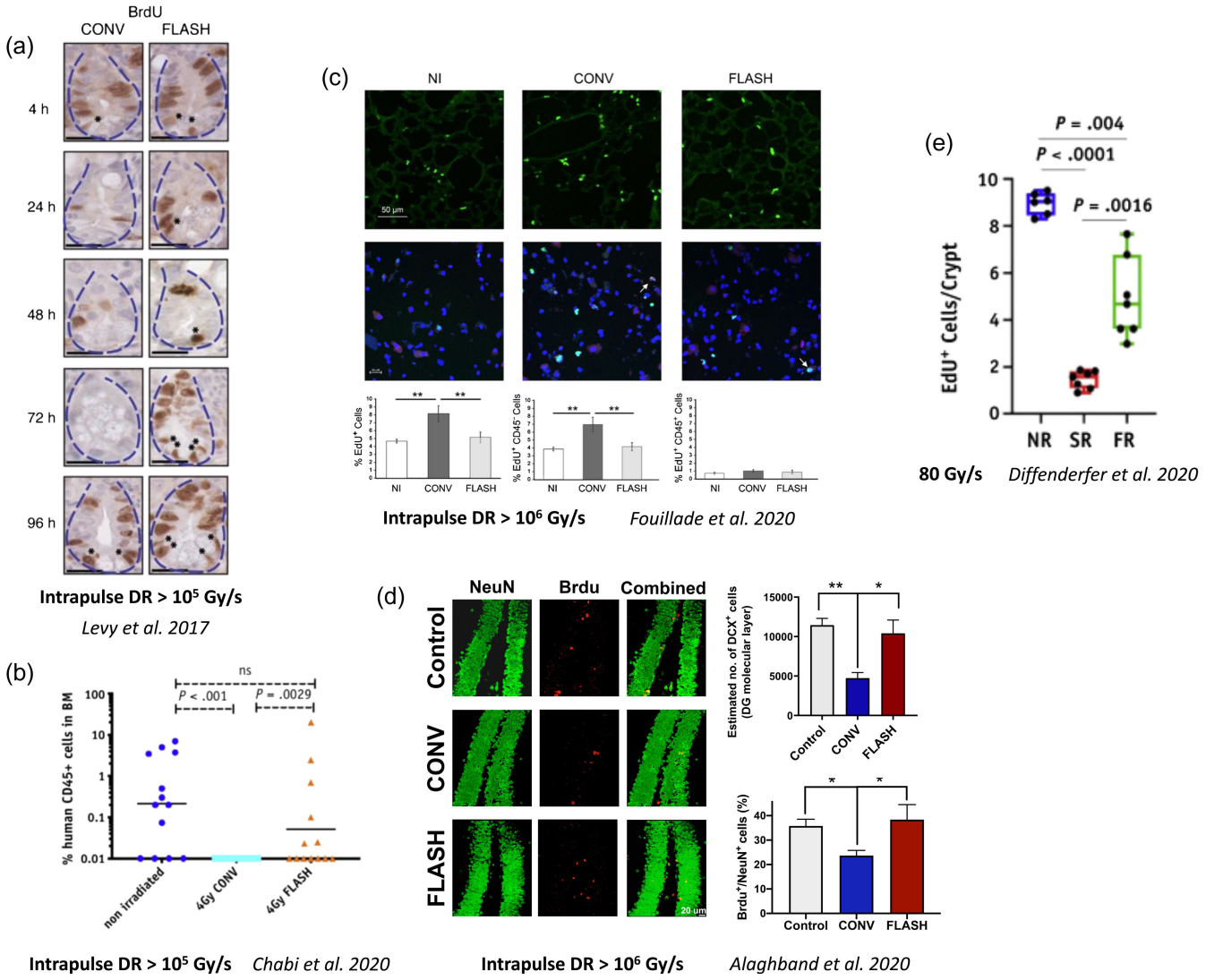

FIG. 16. eFLASH and pFLASH spare stem and progenitor cells *in vivo*. In (a) the gut, (b) bone marrow, (c) lung, and (d) brain, eFLASH does not deplete the level of stem or progenitor cells to the same extent as eCONV. (a) Higher levels of intestinal crypt cells labeled with BrdU (b) increased yields of CD45 positive cells in the bone marrow and (c) preserved EdU positive cells in the lung, and (d) higher yields of immature neurons (DCX, doublecortin positive) and neurogenesis ($BrdU^+/NeuN^+$) in the brain highlight the capability of eFLASH to preserve these highly proliferative cell populations across multiple tissue types. (e) For the case of pFLASH, corroborating data reported for the gut found the yields of EdU-positive intestinal crypt cells to be spared compared to pCONV. NI, no irradiation; NR, no radiation; SR, standard proton radiation; FR, FLASH proton radiation. From Alaghband *et al.*, 2020, Diffenderfer *et al.*, 2020, Fouillade *et al.*, 2020, Levy *et al.*, 2020, and Chabi *et al.*, 2021.

require specialized expertise to evaluate the consequences of acute and chronic radiation injury. As such, *in vitro* assays of cell survival, cell death mechanisms, cell cycle progression, and DNA damage and repair have been preferred models able to provide more rapid, cheaper, and more convenient assessments of cellular responses to irradiation that are more easily manipulated for mechanistic insight. To date simple 2D *in vitro* models have not been able to demonstrate the FLASH effect. Several possible reasons are detailed later in the review; however, intensive efforts are ongoing in the field to validate 3D models, organoids, organs-on-chips, and *ex vivo* slice models for investigation of the FLASH effect, as those models would ease mechanistic studies and decrease animal experimentation.

The link among cell survival, the production of radiolytic DNA lesions, and their repair has a long history in radiobiology. Clonogenic survival following irradiation is most tightly linked with the production and repair of DNA double-strand breaks following nonhomologous end joining and homologous recombination repair mechanisms. Cell lines exhibiting the highest radiosensitivity typically possess mutations in DNA repair genes or upstream regulators of the DNA damage response that compromise their ability to restore genetic fidelity or properly arrest cell cycle progression prior to DNA synthesis or chromosome segregation, thereby exacerbating the effects of unrepaired genetic lesions. In fact, the superposition of DNA repair during low dose rate exposure (∼cGy/h) explains why cell survival increases at low dose rates, as genetic lesions leading to elevated mutational

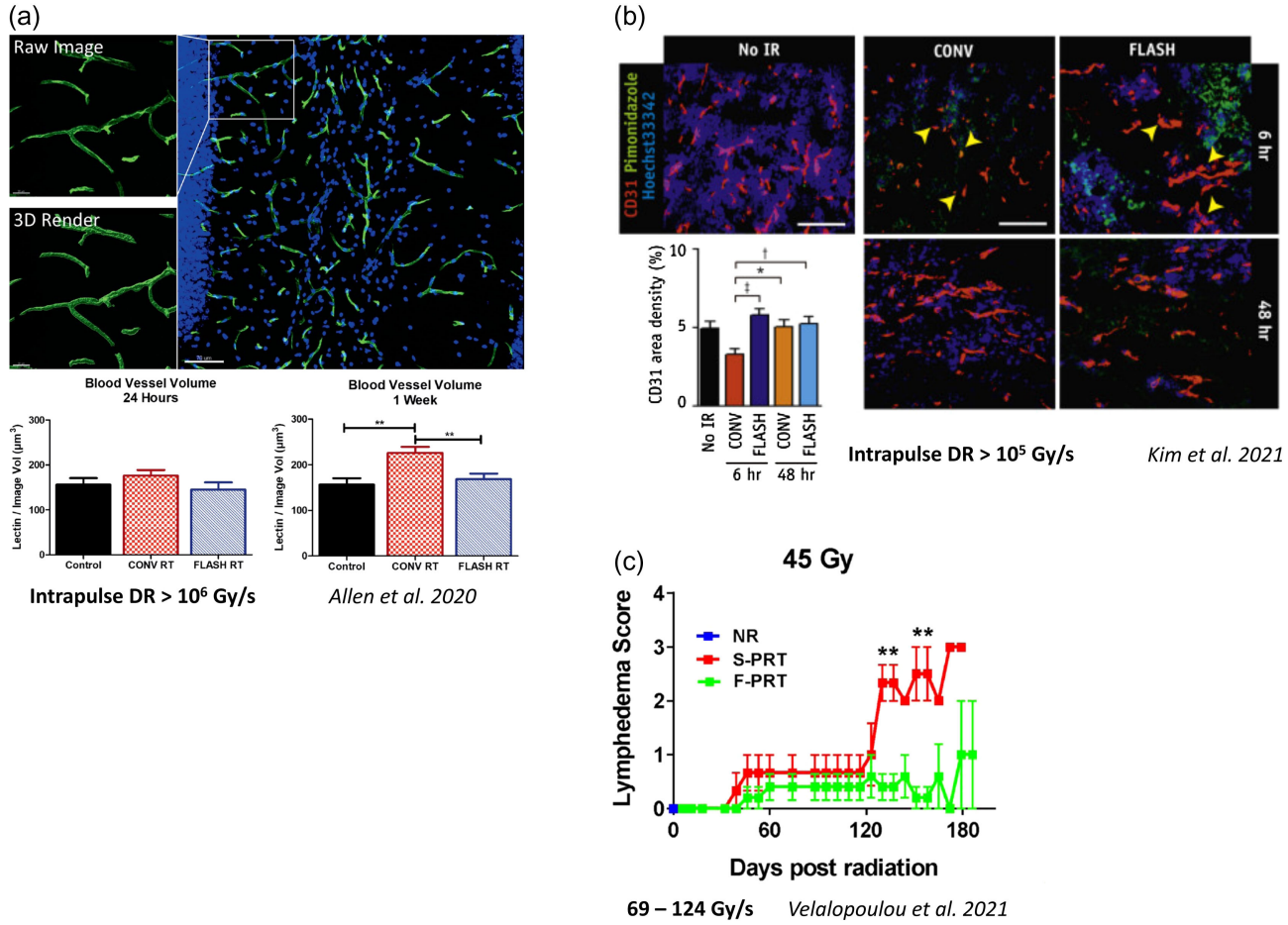

FIG. 17. eFLASH and pFLASH spare the vascular system. (a) In the normal brain eFLASH spares vessel dilation observed after eCONV, and (b) in a Lewis lung carcinoma model eFLASH does not elicit vascular collapse and preserves vessel density compared to eCONV. (c) In the peripheral vasculature of the leg, pFLASH was found to significantly reduce the severity of lymphedema months after exposure when compared to pCONV. From Allen *et al.*, 2020, Y.-E. Kim *et al.*, 2021, and Velalopoulou *et al.*, 2021.

loads and chromosome aberrations are repaired and decrease compared to CONV dose rates used clinically. Following this logic, FLASH exposure should enhance the yield of unrepaired DNA lesions and be more toxic, which is not the case. Work from the Curie Institute by Fouillade *et al.* (2020) was able to uncover a relatively small sparing (decrease) in the yields of 53BP1 foci after eFLASH measured just 30 min after irradiation and only in normal human lung fibroblasts (MRC5 and IMR90); no changes were detected in γ-H2AX foci or any repair foci in lung cancer cells (A549). In similar studies but using 4.5 MeV protons delivered at CONV (0.05 Gy/s) or FLASH dose rates (100–1000 Gy/s), Buonanno, Grilj, and Brenner (2019) investigated early and late biological responses in normal human skin cells (IMR90). Dose rate modulation of protons again had little effect on survival or DNA repair foci (γ-H2AX) formation at 30 min post-IR, except at the highest applied doses (>10 Gy), although modest sparing of senescent cells (b-gal$^+$) and TGFβ levels were found one month after pFLASH compared to pCONV. Work from the same group found no dose-rate-dependent variation between the survival fractions of two human (A549 and HAP1) and one murine (TSA) cancer cell lines irradiated at dose rates of 0.1, 10, and 100 Gy/s up to 10 Gy (Grilj *et al.*, 2020) and, notably, suggested preservation of mitochondrial fitness after FLASH (Guo *et al.*, 2022). Investigations of γH2AX residual foci was also performed *in vivo* in the gut versus ID8 ovarian tumor cells by the Stanford group (Levy *et al.*, 2020). They measured a lower number of γH2AX foci in the gut after 14 Gy eFLASH versus 14 Gy eCONV at an acute time point (4 h), whereas the number of foci was similar in ID8 tumor cells exposed to 14 Gy eFLASH versus 14 Gy eCONV. However, the number of residual foci that are relevant for triggering functional outcomes remained essentially the same in the gut and tumor after eFLASH versus eCONV.

Consistently, relatively small changes in clonogenic survival noted after *in vitro* (Montay-Gruel *et al.*, 2019; Adrian *et al.*, 2020, 2021; Schueler *et al.*, 2022) are reported after exposure of cancer cell lines to eFLASH beams. Notably in clonogenic assays both normal cells and cancer cells are radioprotected at UHDR. *In vitro* work with accelerator and laser driven proton beams has also failed to provide any conceptual advances on the FLASH effect. Earlier work comparing pulsed and continuous 20 MeV proton beams able to deliver 3 Gy in < 1 ns and 100 ms, respectively, failed to uncover significant differences in RBE (Auer *et al.*, 2011).

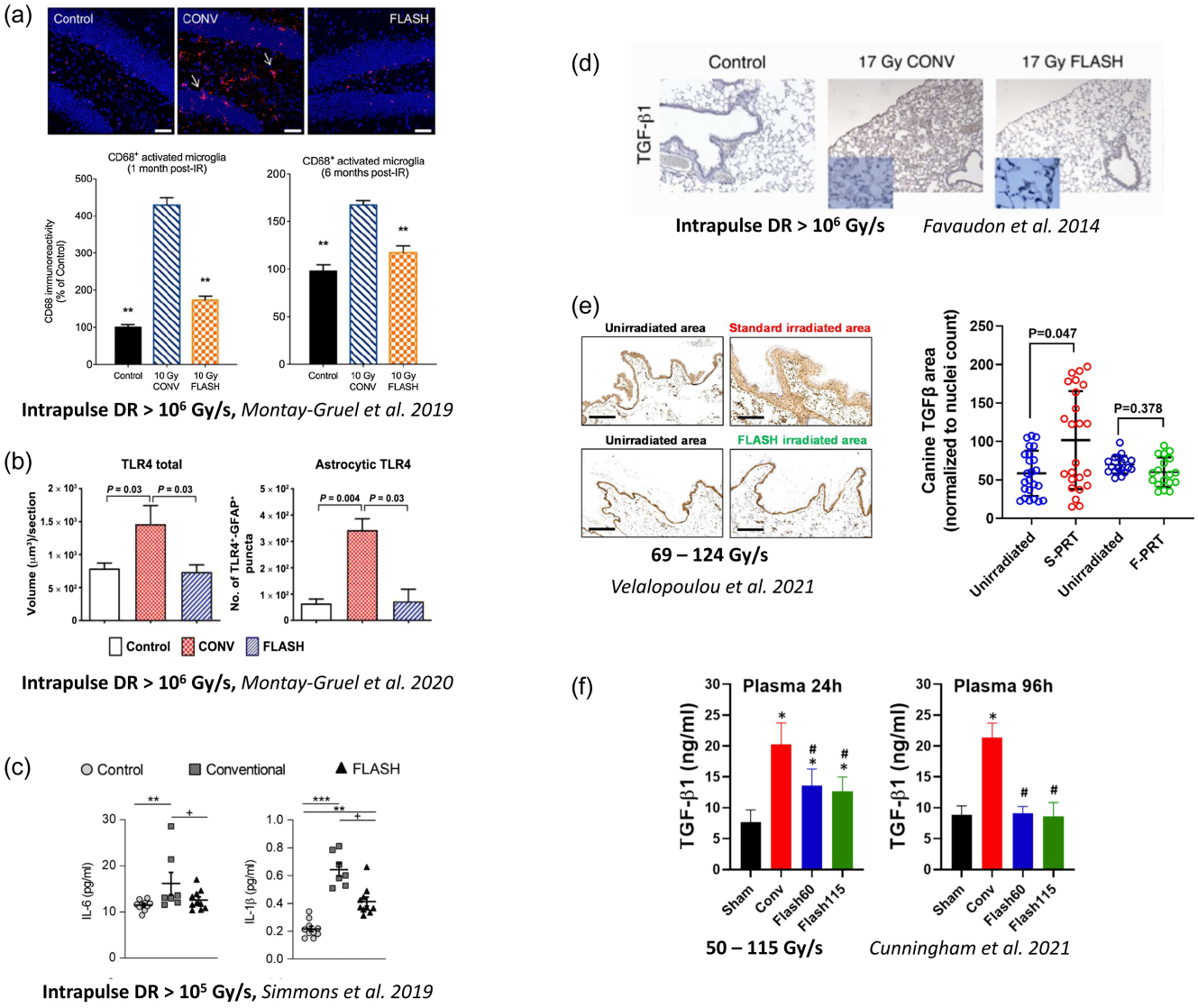

FIG. 18. eFLASH and pFLASH spare inflammatory responses. In the brain, eFLASH significantly reduced the levels of (a) microgliosis, (b) TLR4, and (c) IL-1β expression weeks to months after exposure compared to eCONV. (d) Similarly, in the lung eFLASH was found to minimize TGF-β1 levels compared to eCONV. (e) In the skin of canines exposed to hind limb pFLASH, TGF-β1 levels were also found to be lower when compared to pCONV treated cohorts. (f) In mice subjected to hind limb pFLASH, plasma levels of TGF-β1 were reduced significantly compared to animals given pCONV. These examples illustrate the marked capability of different FLASH modalities to dampen inflammatory processes across distinct normal tissue types. No irradiation, (a)–(d) control, (e) unirradiated, (f) sham; S-PRT, standard proton radiation therapy; F-PRT, FLASH proton radiation therapy; DR, dose rate. From Favaudon *et al.*, 2014, Montay-Gruel *et al.*, 2019, 2020, Simmons *et al.*, 2019, Cunningham *et al.*, 2021, and Velalopoulou *et al.*, 2021.

Similar studies from the same group failed to uncover significant differences in the RBE for the levels of γ-H2AX foci between pulsed and continuous proton beams (Zlobinskaya *et al.*, 2012). Early efforts developing laser driven proton beams were able to deliver mean energies between 1 and 5 MeV that could traverse cells at an instantaneous dose rate of 10^9 Gy/s and a dose up to 5 Gy (Fiorini *et al.*, 2011). More recent studies using laser driven proton beams ($\leq$10 MeV) able to deliver similar instantaneous dose rates found little difference between the RBE of 53BP1 repair kinetics in human skin cells (Hanton *et al.*, 2019) or γ-H2AX foci formation and cell kill in glioma cells (Bayart *et al.*, 2019) compared to standard 225 kVp x rays.

It becomes increasingly evident why traditional radiobiological tenets were challenged by findings that normal tissue toxicities were ameliorated significantly at ultrahigh FLASH dose rates. Extending this logic further and given the opposing trends in adverse normal tissue outcomes found after FLASH versus CONV dose rates, one could argue that unrepaired and lethal lesions in the DNA (i.e., double-strand break) are not the critical target responsible for mediating the FLASH effect. Therefore, clonogenic survival assay is simply not the relevant or right *in vitro* assay to investigate the FLASH effect.

In vitro models are used to rationalize a role for oxygen (as further discussed later) in the FLASH effect. In a clonogenic assay an enhanced survival of cancer cells was found at lower

oxygen tension, but again these changes were small and found only at a high dose (18 Gy) (Adrian *et al.*, 2020). Oxygen has long been recognized as a potent radiosensitizer, with long-standing views that have spawned several models hypothesizing that a rapid depletion of oxygen during a pulse of eFLASH can elicit a transient, volume-dependent radioprotection (Spitz *et al.*, 2019; Petersson *et al.*, 2020). The idea that overall oxygen depletion constitutes a credible mechanism for explaining the biological effects of FLASH has recently come into question, based in part on data obtained *ex vivo* with solid optical sensors (TROXSP5) subjected to photon and particle FLASH beams (Jansen *et al.*, 2021) and based on the first *in vivo* measurement of real-time oxygen depletion during FLASH using a phosphorescence quenching method and water soluble probe (Oxyphor) (Cao *et al.*, 2021; El Khatib *et al.*, 2022). The aforementioned studies independently concluded that radiobiologic relevant hypoxia caused by FLASH-mediated oxygen depletion was unlikely to occur in most normal tissue. This, coupled with significant past work in cell-free and *in vivo* models finding that a dose of ~100 Gy is required to reduce oxygen levels by 3%, cast doubt on the validity of the oxygen depletion hypothesis as a tenable explanation of the FLASH effect.

The field of cancer biology has long recognized the various limitations of 2D-culture models, which in recent years has prompted significant efforts at developing more advanced 3D spheroid, organoid, and organ-on-a-chip models in hopes of more accurately representing the *in vivo* microenvironment. To date only one such study implementing these *in vitro* alternatives, where multicellular spheroids were again used to probe the nuances of oxygen depletion after eFLASH, has been published (Khan *et al.*, 2021). Using spheroids as a more natural system for investigating the impact of hypoxic regions at the spheroid core due to limited oxygen diffusion, Khan *et al.* found a transient expansion of the hypoxic core after eFLASH (90 Gy/s) that was attributed to increased survival (threefold), effects that were not observed after eCONV (0.075 Gy/s) or in normoxic 2D monolayer cultures. The observed dose modifying factor of 1.3 was consistent with *in vivo* results and after doses >10 Gy. These data suggest that more investigations are needed.

1. Summary of the *in vitro* findings

Collectively, *in vitro* studies have shed little light on the FLASH effect, as they have focused largely on surrogate end points (clonogenic survival and DNA damage and repair) that are likely to play little to no role in impacting the *in vivo* FLASH effect [recently reviewed by Limoli and Vozenin (2023)]. They have provided useful models, however, for investigating the oxygen depletion hypothesis and have provided distractions for a field grappling with whether and how to rationalize DNA damage and repair levels that are indistinguishable at postirradiation time >8 h after dose rate modulation of eFLASH and pFLASH beams. Moreover, the fact that the most significant *in vitro* changes observed after FLASH are found at doses far exceeding those required to observe *in vivo* normal tissue sparing in multiple normal tissue beds points to the relative futility in extracting useful mechanistic data regarding the FLASH effect from *in vitro* approaches. There are opposing opinions to the potential validity of *in vitro* approaches for dissecting the FLASH effect (Adrian *et al.*, 2022), but the preponderance of evidence to date argues against the utility of *in vitro* measurements to yield consequential readouts relevant to the mechanistic basis of the *in vivo* FLASH effect.

IV. MECHANISTIC BASIS OF THE FLASH EFFECT: FROM PHYSICAL INTERACTIONS TO BIOLOGICAL OUTCOMES

At the mechanistic level, the FLASH effect might be interpreted based on traditional radiochemical and radiobiological concepts governed by the free radical chemistry initiated during the primary interactions between radiation and matter. The early activation cascades have been well characterized and are summarized in Fig. 19. After the interaction of ionizing radiation with matter, the initial reactions depend largely upon water radiolysis, which has traditionally not been considered to vary with dose rate. This has led to the long-standing (and accurate) tenet that radiation chemistry is linear with dose. However, the impact of FLASH dose rates on water radiolysis has never been systematically studied and compared side by side with conventional dose rate irradiation. Whether the significant difference in the duration of irradiation between FLASH and CONV could differentially affect early physicochemical and/or subsequent radiochemical reactions may be relevant for understanding the primary event(s) involved in the initiation of the FLASH effect.

A. Water radiolysis upon FLASH irradiation

As shown Fig. 19, the cascade is initiated by ionization and excitation processes during the physical step when energetic species (photons and particles) interact with water within

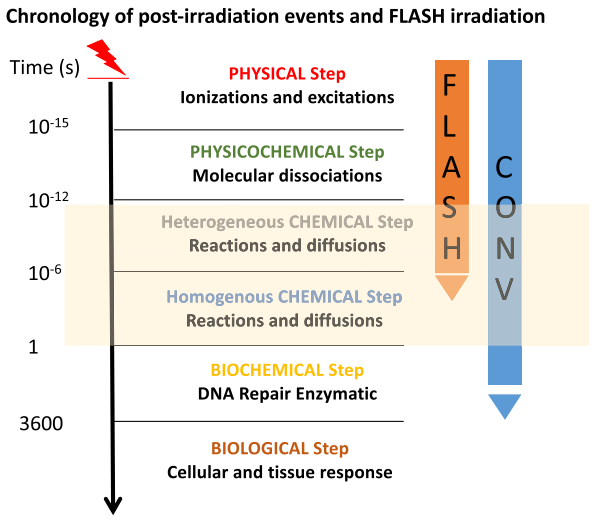

FIG. 19. Chronology of physical, physicochemical, chemical, biochemical, and biological events occurring after irradiation in biological tissue. The difference between FLASH and RT delivered at CONV is the duration of the exposure to the ionizing radiation during the chemical step of the cascade (yellow area). The chemical steps are highly dependant upon dioxygen concentration within tissues.

femtoseconds. Highly unstable ionized and excited molecules transfer energy to the closest molecules and the physicochemical step that is continuous between 10^{-15} and 10^{-12} s. Water molecules can then return to their fundamental state without dissociation by heat loss or dissipate energy by electron emission, leading to activation of the free radical cascade. Typically for low linear energy transfer irradiation, this cascade involves the production of hydrogen, hydroxyl radicals ($HO^{\bullet}$), singlet oxygen [$O^{\bullet}(^1D)$], and triplet oxygen (O^3P), as well as aqueous electrons that will react further with water to produce molecular hydrogen (H_2), hydroxyl radicals ($HO^{\bullet}$), or hydrogen peroxide (H_2O_2). These chemical species are distributed nonhomogeneously in randomly produced regions of high radical density that are commonly referred to as spurs (Baldacchino *et al.*, 2019). The nonhomogeneous chemical stage starts between 10^{-12} and 10^{-6} s. Radical species then diffuse and react together at different rates to form new radical species, rapidly becoming homogeneously distributed within a given volume. Between 10^{-7} and 10^{-6} s, molecular yields of free radicals can be computed to yield G^0 values or "primary yields." Primary free radical yields have been measured via pulsed radiolysis and scavenging methods (Hiroki, Pimblott, and LaVerne, 2002; Wasselin-Trupin *et al.*, 2002). They correspond to the yields of free radical formation at the start of the homogeneous stage and are expressed in $\mathrm{mol\,J^{-1}}$ or in mol/100 eV. Certain free radicals ($HO^{\bullet}$) are highly reactive molecules able to react with any organic molecules within one atomic distance, leading to covalent changes in the critical functional biomolecules of tissues including DNA, lipids, and proteins (Hall and Giaccia, 2012; Joiner and van der Kogel, 2018). The aqueous electron (e^-_{aq}) is less reactive but can interact with metal ions (Fe^{+3}) to reduce them (Fe^{+2}) or combine with molecular oxygen to form superoxide ($O_2^{\bullet -}$) that serves to initiate signaling cascades through the formation of H_2O_2. Furthermore, O_2 can react with nitric oxide (NO) to form the highly reactive peroxynitrite anion ($ONOO^-$). While the direct effects of ionizing radiation lead to the formation of organic radicals ($R^{\bullet}$) on critical biomolecules and are classically thought to account for 30% of the net damage from ionizing radiation, indirect effects contribute to the remaining 70% of radiolytic damage, as derived from water radiolysis. The resultant generation of hydroxyl radicals ($HO^{\bullet}$) that react rapidly ($t_{1/2} \approx 10^{-9}\ \mathrm{s^{-1}}$) through hydrogen atom abstraction and addition reactions generate a variety of organic radicals that result in the accumulation of oxidative damage to critical organic biomolecules. As mentioned, radiation chemistry is stochastic and linear with dose but leads to a plethora of nonlinear biological responses. To further evaluate whether and how fundamental radiation chemistry might vary at UHDR, the CHUV group in collaboration with PSI and CERN implemented FLASH-validated (eRT6 and Gantry 1-PSI) and unvalidated (VHEE-CLEAR) beams able to operate at UHDR to systematically study the possible radiochemical basis of the FLASH effect. Ongoing evaluations of the primary yield and production of H_2O_2 after the recombination and diffusion steps in water irradiated with UHDR and CONV show similar G^0 and G values of H_2O_2 (Kacem *et al.*, 2022). These recent results support the relative dose rate independence of early physicochemical events and suggest that minor differences in radiochemical yields of reactive species at the time of irradiation cannot account for the FLASH effect. If these first observations are corroborated, they should provide helpful insight in determining future priorities for research topics in the field of FLASH. Furthermore, these results suggest that conventional Monte Carlo codes (used in treatment planning systems) could also be used for FLASH irradiation but also suggest that more resources and focus should be allocated to investigate downstream biochemical and biological processes that ultimately drive the FLASH effect. As a caveat, radiochemical changes measured in water cannot recapitulate the complexities of biological systems. Cellular constituents interact within the normal tissue and tumor microenvironment, and such interactions may not be the same at UHDR, where subsequent biochemical and biological responses may be modulated and may contribute to the FLASH effect.

B. The relevance of oxygen tension upon FLASH

Among the many microenvironmental factors, oxygen (O_2) has long been recognized as a potent radiosensitizer. Much past work has defined both tumor and normal tissue oxygen levels and the doses required to deplete oxygen at a target site (Epp, Weiss, and Santomasso, 1968; Epp *et al.*, 1972; Ling *et al.*, 1978; Michaels *et al.*, 1978). Logically the role of oxygen tension as a possible mediator of the FLASH effect has attracted considerable attention, with both proponents and opponents of the idea that oxygen depletion may represent a plausible mechanism (Favaudon, Labarbe, and Limoli, 2022). The most compelling experimental evidence in favor of oxygen's contribution to the sparing effect of FLASH was derived from neurocognitive measurements of cranially irradiated rodents. In those studies, the cognitive benefits of FLASH irradiation were reversed when rodents were given carbogen or pure oxygen to breathe before and during irradiation, leading to a doubling of oxygen levels in the brain (Montay-Gruel *et al.*, 2019; Iturri *et al.*, 2023). At the time the hypothesis was that higher oxygen tension in the brain was compensating for FLASH-induced radioprotective hypoxia, where the total dose of 10 Gy was then insufficient to reduce oxygen levels required for neurocognitive sparing. However, sensitive real-time measurements of oxygen tension *in silico*, *in vitro*, and *in vivo* have now provided convincing evidence that the radiolytic hypoxia induced by FLASH was insufficient to provide any biological benefit (Boscolo *et al.*, 2021; Cao *et al.*, 2021; Jansen *et al.*, 2021). Current experimental evidence shows that, while oxygen plays a role in dictating the response to FLASH, radiation-induced oxygen depletion cannot account for the *in vivo* FLASH effect at therapeutic doses.

C. Redox metabolism: A possible rheostat in controlling the cellular response to FLASH?

Free radical reactions with O_2, as well as oxidative metabolism involving the formation of ROS and reactive nitrogen species (RNS) such as superoxide ($O_2^{\bullet -}$) and hydrogen peroxide (H_2O_2), organic hydroperoxides (ROOH), nitric

oxide (NO), and peroxynitrite ($ONOO^-$), as well as redox-active metal ions such as labile iron, can contribute significantly to the acute and delayed effects of ionizing radiation (Spitz *et al.*, 2004; Dayal *et al.*, 2008, 2009). It is also evident that cancer cells possess altered steady-state levels of ROS and RNS and redox-active metals as compared to normal cell irradiation (Aykin-Burns *et al.*, 2009; Schoenfeld *et al.*, 2017); see Fig. 20. Such differences can have a significant impact on the therapeutic responses to agents able to disrupt redox metabolism such as irradiation (Aykin-Burns *et al.*, 2009; Schoenfeld *et al.*, 2017; Alexander *et al.*, 2018; Zhu *et al.*, 2018). Supplementation with antioxidants such as superoxide dismutase, amifostine, and α-tocopherol is known to protect normal tissue from radiation injury and to attenuate radiation-induced fibrosis (Delanian and Lefaix, 2007; Greenberger and Epperly, 2007; Yarnold and Brotons, 2010; Montay-Gruel, Boivin, and Vozenin, 2016). More recently the differential oxidative metabolic response between normal and tumor tissue to redox-active agents has been harnessed in preclinical and clinical trials to improve responses to therapy by selectively exacerbating oxidative stress and DNA damage in cancer versus normal tissues (Schoenfeld *et al.*, 2017; Alexander *et al.*, 2018; Zhu *et al.*, 2018). In this context, investigating the possible relationships between the FLASH effect and the redox metabolism seems logical, and it is interesting to speculate that differences in the redox biology and oxygen metabolism between cancer and normal tissues may be contributory (if not causal) to the differential FLASH effect (Favaudon, Labarbe, and Limoli, 2022); see Fig. 20.

The formation and processing of FLASH-induced oxidative damage to organic molecules in actively respiring cancer versus normal tissues is currently being evaluated. The timescale of events may be important here, as cells can counteract acute oxidative stress by metabolic reprogramming, whereas the response to chronic oxidative stress may require exploitation of genetic reprogramming. Acute oxidative stress is associated with nicotinamide adenine dinucleotide phosphate (NADPH) depletion that alleviates the negative feedback regulation exerted by NADPH on glucose-6-phosphate dehydrogenase (G6PD), enabling G6PD to rapidly produce and compensate for NADPH depletion. NADPH will enhance glutathione reductase 1 and thioredoxin redox cycling, leading to the stimulation of glutathione- and thioredoxin-based antioxidant systems to restore cellular redox equilibrium and scavenge H_2O_2 and ROOH. Simultaneously, exposure of cells to free radicals induces the activation of glyceraldehyde 3-phosphate dehydrogenase (GAPDH) and pyruvate kinase M2 (PKM2), which block glycolysis and increase glucose catabolism via the pentose phosphate pathway, thereby increasing NADPH production by G6PD. The effects of ROS on GAPDH, PKM2, and G6PD activities are likely coordinated with oxidation of Fe-S clusters and protein subunits of complexes I, III, and IV of the mitochondrial electron transport chain that contain Fe-S clusters. This could potentially decrease O_2 consumption and ROS production (van der Reest *et al.*, 2018). Regulation of pathways involved in repair (ATM), proliferation (PI3K), and survival (NF-kB) are also activated to optimize cell recovery, as reviewed by Hayes, Dinkova-Kostova, and Tew (2020). Adaptation to chronic oxidative stress is a longer-term process regulated at the transcriptional level. The hypoxia-inducible factor 1α (HIF-1α) is one of the transcription factors involved that is stabilized under hypoxic conditions by the oxidation of Cys-326 in the prolyl hydroxlase domain 2. This can then activate the switch from oxydative phosphorylation to glycolysis (Lee *et al.*, 2016); see Fig. 21.

An accumulation of endogenous reactive electrophiles, a depletion of glutathione or thioredoxin, and an upregulation of antioxidant genes (Patterson *et al.*, 2013) also occur via another important transcription factor called nuclear factor erythroid 2-related factor 2 (NRF-2) (Hayes and Dinkova-Kostova, 2014; Yamamoto, Kensler, and Motohashi, 2018). NRF-2 binds to the antioxidant response element present in the promoter of genes coding for antioxidant proteins and enzymes involved in iron or metal metabolism, intermediate metabolism, glutathione synthesis or metabolism, and lipid peroxidation or ferroptosis (Hayes, Dinkova-Kostova, and Tew, 2020); see Figs. 20 and 21. The transcription factors HIF-1α and NRF-2 have both been described as potent regulators of radiation sensitivity.

D. Lipids: Major targets of FLASH?

While classical radiobiology studied after CONV has largely focused on DNA damage and repair, some recent results show that DNA damage is equivalent after FLASH and CONV (Barghouth *et al.*, 2023), suggesting that this fundamental radioresponsive pathway is perhaps not a major determinant of the FLASH effect. Emerging evidence points to a possible role for lipids in the response to FLASH, as reviewed by Favaudon, Labarbe, and Limoli (2022). Recent studies by Froidevaux *et al.* (2023) used cell-free linoleic acid micelles and phosphatidylcholine liposomes as cell membrane surrogates to probe lipid peroxidation yields after FLASH and CONV. Yields of malondialdehyde (MDA) increased linearly with doses of CONV but were conspicuously absent after FLASH. These findings, showing a major differential dose-rate-dependent response in lipid peroxidation, point to lipids as a potentially critical target in mediating the FLASH effect. While caution is warranted before translating these findings directly to living cell membranes, the role of lipid damage and lipid peroxidation that occurs on highly sensitive phospholipids containing polyunsaturated fatty acids (PUFAs) warrants further investigation, for several reasons. First, ROS (hydroxyl and hydroperoxyl radicals) mediate nonenzymatic lipid peroxidation in PUFAs, whereas enzymatic lipid peroxidation is catalyzed primarily by several enzymes such as cyclooxygenases, lipoxygenases, and, to a lesser extent, phospholipase A. Lipid hydroperoxides undergo further oxidative fragmentation reactions forming unsaturated α,β-aldehydes, including 4-hydroxynonenal and MDA. Both adducts represent traditional surrogates for measuring lipid peroxidation in biological systems. Second, lipid peroxidation disrupts lipid asymmetry, which reduces the hydrophobicity of the interior lipid membrane, causes depolarization and the loss of membrane integrity. Lipid peroxidation of select phospholipids of the plasma and organelle membranes (such as the mitochondria) may also trigger altered cell signaling, cell dysfunction, and/or cell death. Third, oxidation of phospholipids leads to

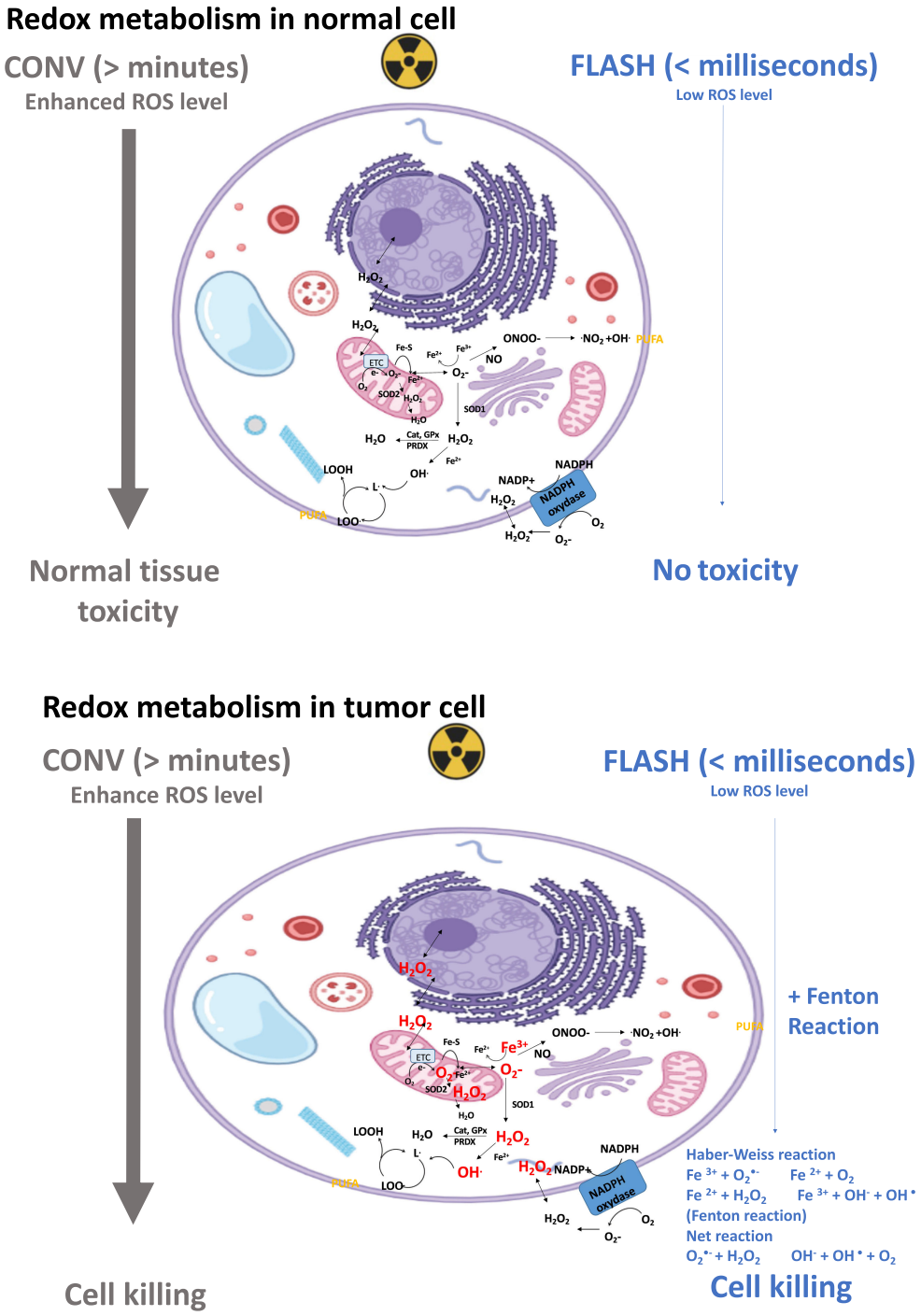

FIG. 20. Redox metabolism and ROS in normal and tumor cells. In normal cells various types of ROS are produced in the mitochondria at the membrane level and traffic in and out to the extracellular. They are potent intracellular signaling molecules able to modify cell fate. In the mitochondria, the electron transport chain (ETC) produces superoxide ($O_2^{\bullet -}$), which interacts with iron-sulfur (Fe-S) clusters to release iron (Fe_2^+) and reduces ferric iron (Fe_3^+) to ferrous iron (Fe_2^+). Superoxide dismutases (SOD1 and SOD2) convert $O_2^{\bullet -}$ to hydrogen peroxide (H_2O_2) which is less reactive but able to diffuse in the intercellular space and target proteins and DNA. H_2O_2 is itself scavenged by catalase (Cat), glutathione peroxidase (GPX), and peroxiredoxins (PRDX). $O_2^{\bullet -}$ is also produced by the NADPH oxidase and can produces peroxynitrite ($ONOO^-$) with nitric oxide (NO). Another reactive radical is the hydroxyl radical ($OH^{\bullet}$) that is formed from the reaction of H_2O_2 with Fe_2^+ and the decomposition of $ONOO^-$. This initiates the lipid peroxidation cascade. The high level of ROS produced by CONV irradiation induces a pro-oxidant redox imbalance that triggers acute cell death and a pathological wound healing process leading to fibrosis, whereas after FLASH ROS production is low and the redox metabolism is only mildly impaired, thus maintaining tissue homeostasis. In tumor cells, the redox balance is altered at base line and high level $O_2^{\bullet -}$ and H_2O_2 are found. In addition, cancer cells present an altered redox-active iron metabolism and an enhanced tolerance of the pro-oxidant status. FLASH does not enhance the ROS level but might affect the redox balance via reaction with labile iron and amplification of the Fenton reaction, while CONV would enhance the pro-oxidant status in a more global manner. The two irradiation modalities lead to similar cell death. Adapted from Harris and DeNicola, 2020, and Schoenfeld *et al.*, 2017.

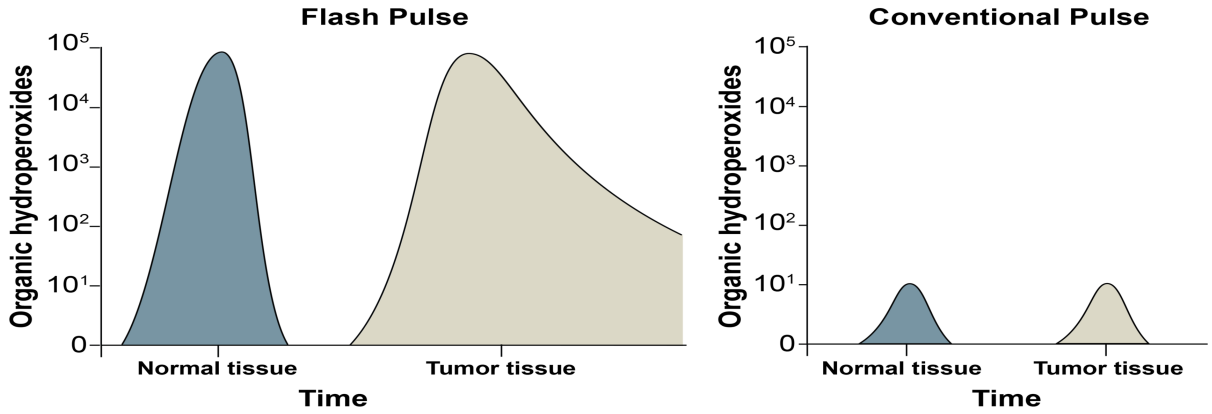

FIG. 21. A proposed mechanism for the differential decay of organic hydroperoxide levels in FLASH vs conventional radiation damage to biological material. A schematic representation showing that a given pulse of eFLASH produces ~4 orders of magnitude more organic hydroperoxides (ROOH) than a pulse of eCONV. While the initial yields of these radiolytic species will be dose dependent, their decay will differ between normal and tumor tissues. Factors prolonging the half-life of ROOH in tumor tissue may be due to elevated levels of labile iron (Fe^{2+}), higher levels of the resultant Fenton chemistry, and an inability to detoxify ROOH rapidly compared to normal tissue. The result is a relative protection of normal tissue compared to tumors resulting in a widening of the therapeutic index.

thinning and increased curvature of the exterior and interior cellular membrane structure that might promote rupture (Agmon *et al.*, 2018) and/or autophagy. Fourth, lipid peroxidation is predominant in PUFAs that depend on the acyl-CoA synthetase long chain family member 4 (ACSL4) for incorporation into cellular phospholipids (Doll *et al.*, 2017). Lipid peroxidation also depends on the activation of the GPX4 system, which will reduce lipid hydroperoxides to more benign alcohol groups, and on the activation of the cystine transporter SLC7A11. This molecular transport system moves cystine into the cell, where it serves as a necessary precursor of glutathione synthesis required for the formation of the GPX4 system (Stockwell *et al.*, 2017; Wiernicki *et al.*, 2020). Last, functional activation of ACSL4 and suppression of GPX4 and/or SLC7A11 can lead to robust lipid peroxidation, which may result in a form of cell death referred to as ferroptosis. Ferroptosis is a cell death mechanism that involves labile iron (Fe^{2+}) in the propagation of the lipid peroxidation reactions (Lang *et al.*, 2019).

In summary, the lack of direct increases in lipid peroxidation on linoleic acid in FLASH compared to CONV-irradiated lipid samples in cancer versus normal cells could be highly significant to biological effects (Spitz *et al.*, 2019; Favaudon, Labarbe, and Limoli, 2022; Froidevaux *et al.*, 2023). However, the implication of these findings for normal tissue versus tumor responses remains uncertain, as iron metabolism has been shown to be different between cancer versus normal tissues and to contribute to radiosensitization by pharmacological ascorbate (Schoenfeld *et al.*, 2017). One potential resolution of this paradox is that the normal tissue or cell response to FLASH could be lipid peroxidation or ferroptosis dependent, whereas FLASH-induced tumor kill could be ferroptosis independent, a process converse to that described after CONV. Ferroptosis agonists are described to be potent radiosensitizers after exposure to CONV in tumors, whereas ferroptosis antagonists limit RT efficacy in tumor models (Lang *et al.*, 2019). Recent studies have consistently revealed that SLC7A11 overexpression is able to promote tumor growth partly through the suppression of ferroptosis (Lei *et al.*, 2021), while cystine depletion is able to induce ferroptosis in pancreatic tumors in mice (Badgley *et al.*, 2020). On the other hand, normal cells could be insensitive to lower levels of lipid peroxidation induced by FLASH, whereas tumor cells could remain highly sensitive to the same low levels of lipid peroxidation. Reasons for this might include altered redox-active iron metabolism, increased labile iron pools (Schoenfeld *et al.*, 2017), a reduced ability to detoxify organic hydroperoxides (Spitz *et al.*, 2019), and metabolic acidosis generated by a glycolytic shift and high level of lactate production (Hayes, Dinkova-Kostova, and Tew, 2020). Further, increased labile iron pools in tumors compared to normal tissues can enhance Fenton chemistry to specifically potentiate tumoricidal effects of irradiation. Elevations in free iron concentration and low pH are hallmarks of a high lipid peroxidation yields, and the iron and pH dependency could make cancer cells more vulnerable to iron-catalyzed ferroptosis following irradiation.

V. TOWARD CLINICAL APPLICATION

In the field of oncology, the timeline from new treatment discovery to clinical application can be lengthy (five to 20 years) as well as costly. For drug development, decades are needed from preclinical development and testing of a new anticancer drug to regulatory approval. In addition, ultimately only about 10% of drugs identified at the preclinical level make it to human testing, which leads to the perception that drug discovery and development are highly uncertain. In this context, the relevance of preclinical models that are essentially based on rodents has and continues to be debated and underscores the need to develop better models that recapitulate human conditions. For example, inclusion or larger vertebrate models is acknowledged to shorten the timeline between preclinical and clinical trials and ultimately to improve the success rate in human clinical trial participants. In the field of radiation oncology, the story is somewhat different since past

treatment improvements such as proton therapy, image-guided RT, and stereotactic RT were essentially based on advancements in technology. Surprisingly, subsequent implementation has jumped directly to large-scale clinical applications without any preclinical or clinical trial investigation and/or validation.

Similarly, clinical studies on FLASH have already started. Primary end points of the current clinical reports and trials focus mostly on workflow feasibility (Bourhis *et al.*, 2019; Mascia *et al.*, 2023) and investigate acute and subacute toxicity such as pain relief and skin erythema in patients treated in a palliative setting. The reference doses, i.e., 8 Gy on bone metastasis and 15 Gy on the skin, are known to be nontoxic when delivered at conventional dose rates and, correspondingly, no difference in the skin toxicity profile has been reported between FLASH and CONV dose rates (Gaide *et al.*, 2022; Mascia *et al.*, 2023). These suboptimal approaches are safe but, because they were almost guaranteed not to fail, may prove misleading in the end and unlikely to reveal the true potential of FLASH.

While the precise FLASH beam requirements (see Sec. II) to produce the FLASH effect are still under investigation, the direct transposition of mice findings to human patients is not straightforward and has many limitations. Specifically, (1) mice studies have been performed mostly with single high doses of irradiation (>10 Gy), both for practicality and due to the radiation response profile inherent to rodent tissues; (2) the intrinsic small size of the rodents limits the volume of irradiation to 1 cm^3, whereas larger volumes and fractionated dose regimens will be required to treat human cancer patients; (3) the genetic homogeneity in rodent models does not account for the heterogeneous population of cancer patients presenting with various tumors and normal tissue radiation sensitivity profiles; and (4) studies in mice using whole-brain and whole-abdomen irradiation protocols, as well as studies performed in zebrafish embryos using total embryo irradiation with electron beams, have found that the optimal normal tissue sparing effect was obtained using a single electron pulse (over microsecond timescales) (Montay-Gruel *et al.*, 2017, 2018; Vozenin, Hendry, and Limoli, 2019; Ruan *et al.*, 2021; Kacem, Almeida *et al.*, 2022), whereas normal tissue sparing was reported with proton-FLASH experiments performed in the millisecond range. These observations suggest that the temporal structure of the beam is critical for normal tissue sparing, but whether the same temporal requirements will apply when dose and volume are increased remains unknown. Ongoing studies in pigs, where the field size of the skin that was irradiated was systematically varied, strongly suggests that volume effects will be a confounding factor and that optimization of the beam parameters will be required to effectively treat and manage larger target volumes.

With the limited availability of FLASH enabled devices such an optimization is typically not possible. For instance, for irradiating large fields with the eRT6/Oriatron, the beam parameters require modifications to achieve a relatively flat field and high dose. In the small field experiment (2.6 cm), a dose of 31 Gy FLASH was delivered in ten pulses of 1.8 μs, 100 Hz, and 90 ms, whereas in the large field experiment the same dose was delivered in 20 pulses of 1.8 μs, 100 Hz, and 190 ms. Notably the overall duration of irradiation was doubled (Rohrer Bley *et al.*, 2022). In summary, these results indicate that further technological developments are necessary to perform systematic investigations to characterize the optimal beam parameters required to reveal the full potential of FLASH in various clinical scenarios. More biological studies and more technological developments are needed to safely move FLASH to the clinic (Buchsbaum *et al.*, 2021), and a road map was recently proposed (Taylor *et al.*, 2022); see Fig. 22.

We also suggest that experiments with large animals such as pigs, as well as clinical trials with domestic animal patients (cats and dogs), could accelerate the implementation of new RT approaches such as FLASH, thereby saving time and minimizing adverse outcomes in human clinical trials.

A. Pig models for investigating FLASH

Pig models share significant similarities with humans in terms of size, anatomy, pathophysiology, metabolism, genetics, and epigenetics. Pigs have been extensively used in the field of radiopathology (Hopewell and van den Aardweg, 1988; Lefaix and Daburon, 1998) for both radiation protection and therapeutic studies. Recently a pig tumor model has also been developed. The commercially available Oncopig cancer model harbors mutations in a key tumor suppressor and oncogenes TP53R167H and KRASG12D that recapitulate transcriptional hallmarks of human disease and exhibit clinically relevant histological and genotypic tumor phenotypes, as reviewed by Schachtschneider *et al.* (2017). This model, which is now used for drug testing, has never been used in the context of radiation studies. The exposure of pig skin to high doses of ionizing radiation (>25–100 Gy) leads to acute radiation injury and cutaneous fibrogenesis. The severe initial reaction progresses through erythema to skin necrosis and scab formation. For lower doses and/or smaller volumes, a spontaneous resolution of the lesion after skin contraction into a scar is usually observed over a couple of months (Lefaix and Daburon, 1998). Early onset symptomology observed on the skin is limited, however, and yields little in-depth information regarding pathology, as cutaneous and muscular radionecrosis can develop at later stages. These complex reactions generally start with early microvascular lesions, leading to epithelial ulceration and evolve into deeper vascular lesions alongside delayed muscular and connective tissue alterations. In one of our earlier studies, we performed a dose escalation trial to compare the impact of high doses of CONV to FLASH on the skin of a single minipig (Vozenin *et al.*, 2019). In this first set of experiments, spot sizes of 2.6 cm diameter were exposed to a single shot of irradiation at doses of between 22 and 34 Gy delivered in ten pulses of 1.8 μs, 100 Hz, and 100 ms. Aside from depilation, no other signs of acute toxicity were observed. However, nine months postirradiation, the spots exposed to CONV developed dramatic fibronecrosis, whereas the spots exposed to FLASH displayed no signs of pathology. At the macroscopic level, the skin had a normal appearance, and microscopic evaluation revealed preserved epidermis, dermis, vasculature, and hair follicles. The follow-up of these lesions has now reached five years, and morphologic alterations of the skin in the FLASH-irradiated zones remains minimal, with only hyperkeratosis and depilation, whereas the

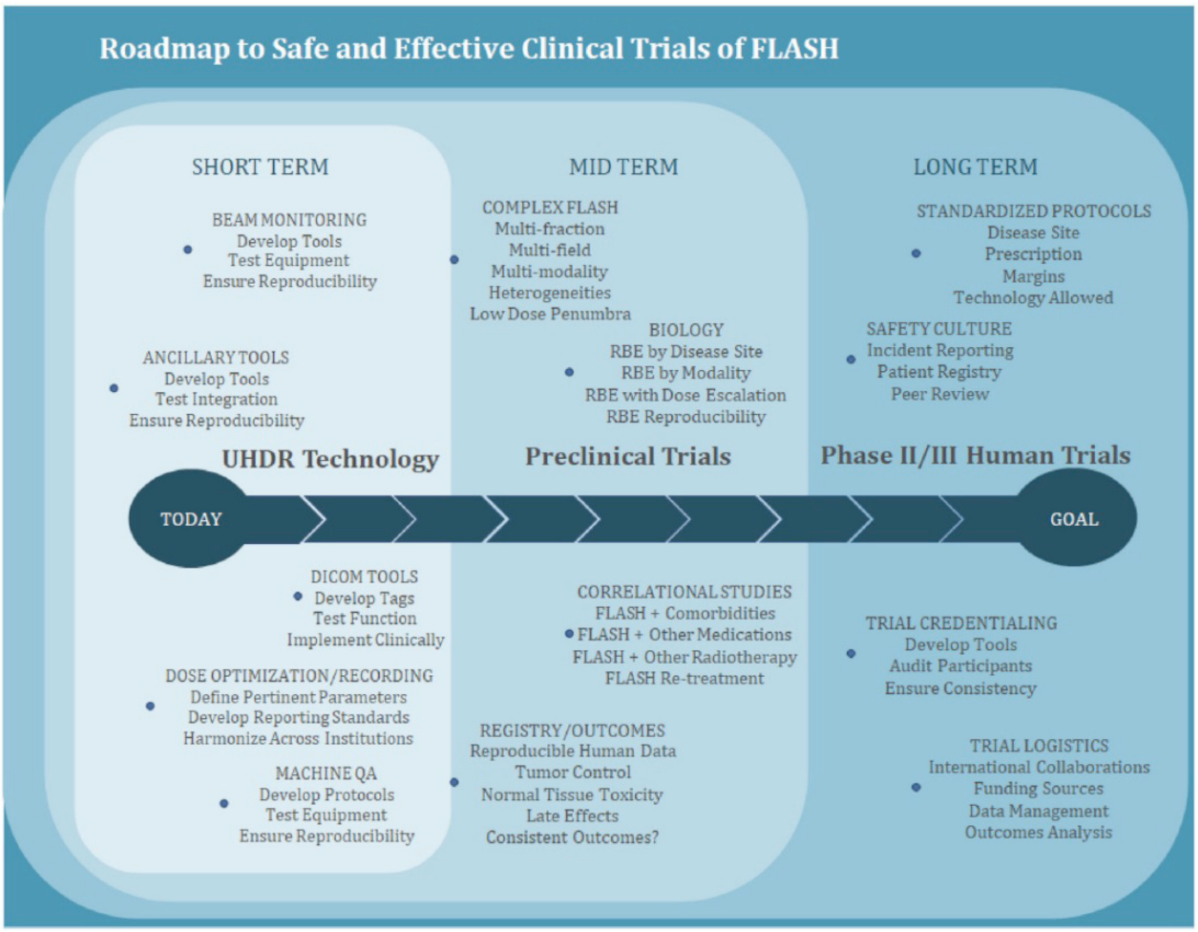

FIG. 22. How does one move toward clinical applications? This road map was proposed by Taylor *et al.* (2022).

CONV-irradiated zones still show severe skin contraction and deep fibrosis; see Fig. 23.

The investigations on the skin of the same minipig continued in order to comply with ethics regulations and to reduce as much as possible the number of animals needed for experimentation. The primary objective was to investigate the impact of large radiation fields to assess whether the beam requirements applicable in mice and small volumes could directly transfer to the larger fields required to treat human tumors (Rohrer Bley *et al.*, 2022). Our results showed that even with FLASH, as with CONV, increasing the volume increased the toxicity. However, in our previous experiments with the spot (2.6 cm diameter × 1.6 cm depth) given a single dose of 31 Gy at 280 Gy/s, 100 Hz, and 1.8 μs, neither acute nor long-term damage was induced. However, when the field size was increased by $3.5 \times 4.5 \times 1.6$ cm^3 and $8 \times 8 \times 1.6$ cm^3, and under similar FLASH parameters (150 Gy/s, 100 Hz, and 1.8 μs) severe necrosis on the pig's skin was induced (Rohrer Bley *et al.*, 2022). We could not directly compare FLASH versus CONV as our prior data documenting severe ulcerations and fibronecrosis with a spot size of 2.6 cm precluded ethical approval of these larger field treatments at conventional dose rates. Therefore, we can only speculate that, if 31 Gy had been delivered via these larger field sizes using CONV, the fibronecrosis would have occurred much earlier, been more severe, and/or would not have resolved over time or even extended outside the target volume. This assertion is, however, supported by previous studies performed on pig skin irradiated with conventional dose rates (Lefaix and Daburon, 1998; Hopewell and Trott, 2000), where the field size was shown to influence the dose required to induce acute skin reactions. For late skin reactions, however, this held true only for smaller fields (<10 mm), whereas with larger field sizes the median effective dose was independent of the area exposed. For anatomical or structural radiation damage, the field size is empirically defined and inherent to the species and tissue, depending on the structural organization of functional subunits composing that tissue; others have proposed that no scaling factor can be related to animal size (Hopewell and Trott, 2000).

For the aforementioned adverse outcomes, the severity of the lesion was significant and was related to its size ($8 \times 8 \times 1.6$ cm^3). It caused fever and pain to the pig that was therapeutically managed by antibiotics and painkillers, as the lesion remained essentially superficial and spontaneously resolved after skin contraction. Eventually it resulted in a stable fibrotic scar after 12 months; see Fig. 24.

Lesion progression observed after 31 Gy FLASH was similar to that described earlier by Lefaix and Daburon (1998) after 74 Gy CONV, with telangiectasia (dilated blood vessels) appearing at four months postirradiation in the center of the field, followed by epidermis ulceration and skin

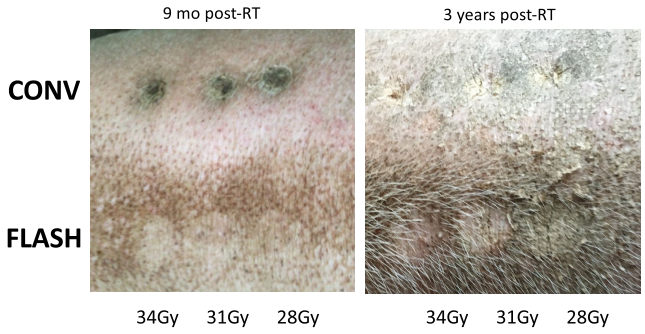

FIG. 23. Side-by-side comparison of CONV and FLASH on the skin of a minipig. In 2016, a study with a single minipig was launched to compare CONV and FLASH responses side by side. The study was approved by the Swiss Ethics Committee for Animal Experimentation under numbers VD3145 and 3482 and performed within institutional guidelines. One female Göttingen, Germany, minipig (43 kg) entered the study and was housed at the animal research facilities of the University of Lausanne. Irradiation took place under general anesthesia. The irradiation was performed on the back of the pig using a graphite applicator whose thickness was sufficient to stop electrons with a 26 mm diameter circular aperture in direct contact with the skin. The prescribed doses 28 to 34 Gy to the skin surface were delivered CONV at ≈5 Gy/min (on one side of the back) and FLASH (on the other side of the back) in ten pulses of 90 ms and 280 Gy/s. Nine months postirradiation (36 weeks), macroscopic visualization showed severe fibronecrotic lesions in CONV (upper side) and the quasinormal macroscopic morphology with preserved hair follicles in FLASH (lower side) (Vozenin *et al.*, 2019). Long-term follow-up was performed and is still ongoing. After three years, the skin alteration in the FLASH-irradiated zones was still minimal, with a slight hyperkeratosis and depilation, whereas the spots irradiated at conventional dose rates showed severe but stable contraction of the skin and deep fibrosis. From Schüller *et al.*, 2020.

necrosis over the entire field of irradiation at six months postirradiation. Given the dose modifying shift in normal tissue tolerance enabled by FLASH, the pathogenic process triggered by FLASH and CONV on normal tissue seem similar. The similarity (or dissimilarity) of dose-rate-dependent pathogenesis can be investigated further at the tissue, cell, and molecular levels using isoeffect measurements instead of isodose experiments. In addition to our investigations in Switzerland, other groups in the U.S. are conducting large-scale experiments with pigs and FLASH. Teams at Dartmouth College and MD Anderson Cancer Center are conducting dose escalation studies using UHDR versus CONV and a modified electron clinac (Rahman *et al.*, 2021) and the Mobetron using skin toxicity as the biological outcome; another team at Emory University uses proton beams and investigates the impact of dose escalation with proton FLASH vs proton CONV using spinal cord toxicity as the outcome. Results of these investigations have not yet been published but should provide additional data useful in assessing dose-limiting toxicities related to FLASH using larger vertebrate models. We emphasize that large vertebrate models require rigorous ethics reviews, are expensive, and require teams with specific training, including veterinarians, as well as specific infrastructures to manage all related treatment and follow-up animal husbandry.

The implementations of FLASH in domestic cats and dogs with cancer constitute suitable models for performing therapeutic studies as the treatment options for animal patients can be limited, whereas there are large numbers of candidate patients. In these instances, RT remains relatively affordable for dog and cat patients bearing various tumors, as reviewed by Nolan, Kent, and Boss (2019). Dogs and cats provide a unique opportunity to study the impact of FLASH in spontaneously developing tumors that represent a genetically heterogeneous population of patients. In cats and dogs, cancers occur naturally but may be enhanced by human-associated factors such as processed food and smoking. Currently around 45% of ten-year-old dogs die of cancer, which is comparable to humans (60% of patients are diagnosed with cancer after age 65). In dogs, osteosarcoma in large breeds (Gardner, Fenger, and London, 2016) display genomic, epigenetic, and metabolic characteristics similar to those found in humans. These relatively rare tumors enable longitudinal studies, facilitating investigations on the interaction between long-term modification of the tumor microenvironment versus the response to treatment. In cats as in humans, oral squamous cell carcinoma represents an increasing problem with poor prognosis and an observed six-month progression-free survival of less than 10%. While RT increases survival up to about 45%, acute and late toxicity are substantial and include xerostomia, odynodysphagia, and bone necrosis. Full-course definitive-intent protocols delivered to either dogs or cats require general anesthesia and therefore tend to be hypofractionated, resembling some accelerated protocols that are currently used to treat human patients. Since dogs are more radiosensitive than cats, around 20 daily fractions of 2–4 Gy are used to treat dogs, whereas twice daily (bis in die) fractionation schemes can be used in cats at 4 Gy per fraction following a classical treatment regimen from Monday through Friday. In the past, intranasal canine tumors were used to support the early development of helical tomotherapy (Forrest *et al.*, 2004). A similar approach is now used in FLASH as an intermediate step in the scale-up between rodents and humans. The use of pet patients is relevant for assessing safety and establishing clinical workflows that can be applied more directly to human patients. In addition, unlike trials with human patients, pet patient accrual in select trials will be far less competitive and costs can be mitigated by academic grants. The latter point is highly relevant, as cost stands as a significant limitation and pet owners typically limit expenses to between 1500 and 4000 euros/treatment; the fact that FLASH can be delivered using hypofractionated regimens naturally lowers the out-of-pocket financial burden (fewer veterinarian visits), which can hasten its adoption and the implementation in routine veterinary practice.

Four clinical trials with domestic animals have been published to date, as well as one mechanistic short-term study using dog samples. The short-term study confirmed in dogs with osteosarcoma (Velalopoulou *et al.*, 2021) prior results obtained in mice and showed that pFLASH did not induce the fibrogenic cytokine TGF-β1, whereas pCONV did. To compare outcomes between pFLASH vs pCONV, dogs were given a single dose from 8 to 12 Gy, and five days post RT, the hind limbs of the dogs were amputated as part of the standard of care (SoC) procedure and analyzed for TGF-β1

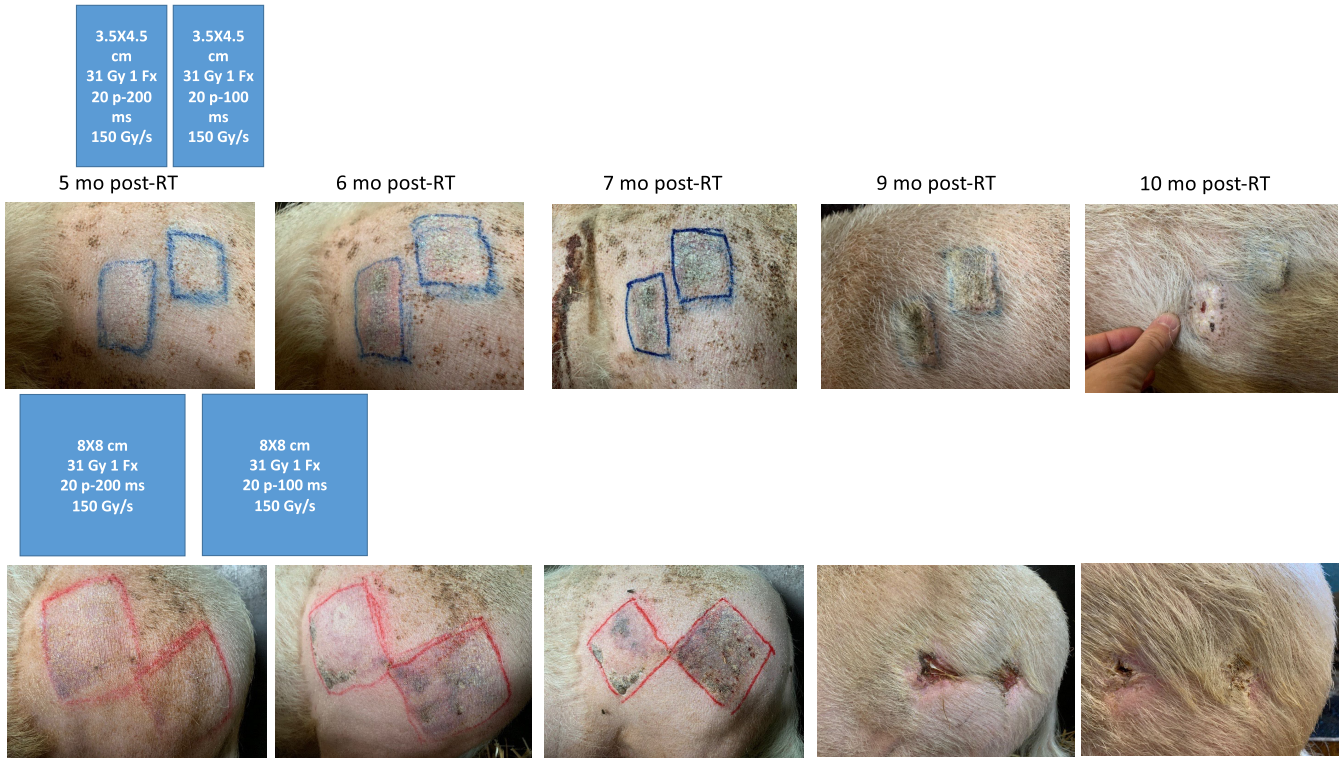

FIG. 24. The impact of volume on the sparing effect of FLASH. To investigate whether the beam requirements known to produce the FLASH effect in small volumes (as with mice) could be directly transferred to larger fields of irradiation for the same dose levels, a minipig model of skin toxicity was used in a volume escalation study. Regardless of the volume of skin irradiated, no acute toxicity was seen by macroscopic evaluation and subacute toxicity was limited to depilation. However, late skin toxicity was found to occur in a volume-dependent manner. When irradiating a 2.6 cm diameter spot with a single dose of 31 Gy FLASH (ten pulses of 1.8 μs, 100 Hz, and 90 ms) induced minimal long-term damage that mainly involved depilation $>$ 12 months postirradiation and up to five years postirradiation. In the same volumetric configuration, 31 Gy delivered at conventional dose rates resulted in the development of a severe fibronecrosis at nine months post-irradiation and the evolution toward persistent fibrocontracture (Vozenin *et al.*, 2019; Schüller *et al.*, 2020). When the size of the field increased, late cutaneous toxicity occurred. From left to right, the macroscopic evolution of skin lesions is shown at various times post FLASH treatment when 3.5×4.5 cm^2 (shoulder) and 8×8 cm^2 (leg) fields were irradiated. Blue schemes present a summary of the physical parameters used to irradiate the two adjacent areas. With the smaller field (3.5×4.5 cm^2), the late skin lesions evolved from erythema and ulceration to permanent hyperkeratosis and skin contracture at six, seven, and eight months postirradiation. Moreover, the larger 8×8 cm^2 field induced a severe skin reaction with telangiectasia at five months postirradiation evolving into progressive epithelial ulceration over the entire field of irradiation at six months and necrotic scabs between seven and nine months postirradiation. Antibiotics, painkillers, and anti-inflammatory agents were administered during the ulcerative period, and ultimately the lesion healed 11 months postirradiation. Note that the resolution occurred by a classical wound contraction process and reepithelialization growing from the margins. In-field radiation-induced skin contracture remained stable. From Rohrer Bley *et al.*, 2022.

expression. Velalopoulou *et al.* (2021) suggested that similar molecular mechanisms occur across species. Follow-up studies led by K. Cengel at the University of Pennsylvania are using the same osteosarcoma model in dogs in a clinical trial. In another clinical trial by Konradsson *et al.* (2021), dogs with various solid tumors were used to investigate FLASH outcomes. FLASH treatments were found to be feasible with a modified clinac able to produce UHDR and single dose treatments ranging from 15 to 35 Gy. In 11 dogs from the 13 included in this trial, tumor response was partial, complete, or stable, but a subsequent long-term study by Børresen *et al.* (2023) reported severe late toxicities in this cohort of animals.

The issue of long-term toxicity is critical and is a central focus of our ongoing investigations. We conducted the first phase I dose escalation clinical trial with cats suffering from locally advanced SCC of the nasal planum. Follow-up was set at one year and a single dose of 30 Gy was found to be safe and effective. Next, we performed a phase III clinical trial with the tumor-control rate at one year as the primary end point and toxicity as a secondary end point with an overall follow-up reaching three years. Cat cancer patients were randomized between two groups: The first group used single dose FLASH at 30 Gy [89% isodose line (IDL)] using the eRT6/Oriatron, delivered in 20 ms using three pulses and providing an instantaneous dose rate of 6.3×10^6 Gy/s and a mean dose rate of 1500 Gy/s. The other group received SoC with CONV at 48 Gy delivered in ten fractions following an accelerated fractionation protocol (90% IDL) using a 6 MeV clinical linear accelerator and a dose rate of 600 monitor units per minute (Melzer *et al.*, 2006; Gasymova *et al.*, 2017). Despite

good cosmetic and tumor-control outcomes, three cats developed osteoradionecrosis at 9–15 months post-FLASH. Given this high-grade toxicity, the trial was interrupted, prompting several hypotheses to rationalize the toxicity profile. First, whereas dose fractionation protocols have been optimized to protect normal tissues, the design used in the study of Gasymova *et al.* (2017) encapsulated several high-risk factors known to precipitate normal tissue complications, including single, high-dose (>30 Gy) irradiation. The target volume was small (2.6 cm), while the dose rate was ultrahigh (1500 Gy/s) and was delivered in a single fraction (30 Gy with hot spots up to 42 Gy). As compared to the absence of late effects in the SoC arm (10×4.8 Gy), the adverse outcomes in the FLASH arm can at first approximation be attributed to the significant imbalance between the biological equivalent dose (BED) of the two arms of the study. We emphasize, however, that the FLASH protocol was based on our previous dose escalation study and not on BED calculations, which are not likely to be predictive on single high-dose treatments (much less with FLASH). In human patients treated for carcinoma of the tonsil, field size is not relevant for mucosal breakdown but is a significant factor for mandibular (bone) complications. The estimated α/β ratio for bone is 0.85 Gy (−0.48, 2.4 Gy) as summarized by Hong *et al.* (1995), thus rendering dose per fraction an important factor. This value also falls at the lower end of estimated α/β ratios when compared to other late-responding normal tissues. While bone possesses the radiobiologic characteristics of late-responding normal tissues exhibiting heightened sensitivity to increased dose per fraction (Withers *et al.*, 1995), other factors such as oral hygiene, dental status, or post-radiation trauma such as tooth extraction could further exacerbate normal tissue sequelae. Second, the SoC protocol was administered using a vertical beam and a bolus, whereas the administration of the 30 Gy FLASH protocol was frontal and performed without a bolus. Given the dose depth profile of the electron beam provided by the eRT6/Oriatron (Jorge *et al.*, 2019), hot spots (125% of the dose) occurred at the maxilla level, as shown by our retrospective dosimetric reconstruction. However, while this electron pattern of dose deposition occurred in all seven FLASH-treated cats, only three of them developed severe complications, which points to the sparing capabilities of FLASH despite the high single dose protocol used. In retrospect, a lateral angle (cat position in lateral decubitus) could have been implemented to optimize the conformality of the FLASH treatment given the fixed horizontal beam geometry. Third, treatment was performed with a dose rate of 1500 Gy/s to decrease the overall time of irradiation as much as possible. This dose rate was 5 times higher than in our previous phase I clinical trial (300 Gy/s) and decreased the time of irradiation by tenfold. Ideally a single pulse of 30 Gy would have been selected based on previous mice experiments, but this was not technically feasible. Consequently the total dose was delivered in three pulses over 20 ms. As a result, we cannot formally exclude this slight increase in overall treatment time from being responsible, in part, for the observed bone toxicity. Whether the average dose rate was too low as compared with one pulse or too high as compared with 300 Gy/s remains uncertain. Fourth, interindividual variations may have led to a heightened radiosensitivity of the three cats with complications which cannot be excluded. In any case, at the tumor level the 30 Gy FLASH resulted in high local control, indicating that FLASH does not result in a protective effect on cancer cells, a theoretical (yet unsubstantiated) concern within the field.

Important lessons have been learned from these studies, highlighting the importance of longer-term investigations of late toxicity, a prerequisite for future clinical trials with domestic animals. Furthermore, implementation of state-of-the-art treatment planning systems for a FLASH beam seems to be mandatory, as defining volumes, visually estimated from gross tumor volume and based on passive dosimetry (alanine, film, and thermoluminescent) is suboptimal; see the information related to FLASH dosimetry in the Supplemental Material (207). Under the foregoing conditions used for the phase III cat trials electron distribution was problematic, as evidenced by the retrospective dose reconstruction performed in cats. eFLASH beams of intermediate energy (below 10 MeV) suffer from a dose distribution that is difficult to predict, especially when complex treatment geometries with cavities and tissue inhomogeneity are involved, and should not be selected for further clinical development. For clinical translation to humans, long-term toxicity follow-up is critical, and caution must be exercised before implementing FLASH at higher doses per fraction in human patients. Lastly, experiments under conventional fractionation at UHDR must be performed and are a priority for the clinical translation of FLASH. The rationale for this is straightforward because, if conventional fractionation is FLASH compatible, step-by-step dose per fraction escalation starting from the SoC would represent a safe and low-risk strategy for validating the benefits of FLASH in human patients. If conventional FLASH fractionation does not yield improved outcomes, other modest hypofractionated protocols could be investigated alongside hybrid protocols (delivering FLASH as a neo-adjuvant or boost).

B. Clinical application and implications

In contrast to the major improvements in the physical delivery of highly conformal image-guided radiation therapy, relatively few improvements in the biological therapeutic index of radiation therapy have translated to routine clinical care. The dominant approach over the past century has been fractionation of the radiation dose, dividing a large total dose into numerous small administrations (fractions), which exploits a biological differentiation of tumor and normal tissue response to radiation that allows preferential sparing of normal tissues. Agents that mitigate radiation injury to normal tissues (radioprotectors) or enhance tumor responses to radiation (radiosensitizers) have been difficult to translate to the clinic, though this remains an area of investigation with some promising candidates. Only a small number are in current use, for example, memantine to mitigate radiation-induced cognitive impairment from whole-brain radiation therapy (Brown *et al.*, 2013), and nimorazole to sensitize hypoxic tumor cells to radiation in some cancers of head and neck mucosal sites (Overgaard, 2011).

The recent preclinical observations of the FLASH effect have generated great interest because, if they are validated in humans, this would represent the first fundamental radiation intervention to improve the biological therapeutic index since fractionation. In fact, FLASH radiation therapy promises to increase the therapeutic index from both physical and biological perspectives. The speed of FLASH delivery addresses a universal challenge in physically precise and accurate radiation therapy: physiological motion of tumors and organs. Conventional radiation therapy delivery is on the order of minutes for current state-of-the-art technology, much longer than the timescale of physiological motion on the order of seconds to fractions of a second. Physiological motion is characteristic of all parts of the body and has a magnitude on the scale of millimeters to centimeters. Encompassing all tumor motion within the radiation target volume can lead to excessive irradiation of normal tissues. This necessitates complex, costly, and potentially error-prone "motion management" strategies (such as immobilization fixtures and/or beam gating or tracking) to compensate for the fundamental assumption that it takes longer to deliver radiation therapy than it does for any part of the body to move. Treatment completed in a fraction of a second would eliminate the opportunity for physiological motion and enable in principle the best possible physical targeting of highly conformal radiation therapy, provided that precise tumor localization can be realized. At the same time, *in vivo* biological research on FLASH has demonstrated selective sparing of normal tissues without compromising antitumor efficacy over a broad range of preclinical models. This promises an orthogonal approach to improving the therapeutic index, reaching scenarios in which normal tissue and cancer targets cannot be physically separated.

The nascent learning from preclinical FLASH research to date suggests several radiation therapy indications that may especially stand to benefit from FLASH RT. The clinical scenarios in which radiation therapy is most limited by a low therapeutic index also highlight high priority questions that must be answered about FLASH.

Currently the most extensive preclinical evidence for the sparing of normal organ integrity and function by FLASH is in the brain, intestine, skin, and lung: organs for which toxicity is frequently dose limiting in the clinical setting. FLASH effects have been demonstrated with multiple types of radiation used clinically, including electrons, x rays, protons, and carbon ions. This suggests that FLASH has the potential for broad applicability in clinical radiation therapy. However, the optimal clinical use of FLASH remains to be clarified within the limits of experimental data to date. Most of these studies have evaluated large single-fraction doses of radiation, and most have involved whole-organ irradiation (except for the skin). In general the observed DMF between FLASH and CONV on normal tissue sparing under these conditions has been approximately 1.2–1.3 (i.e., approximately 20%–30% more of a dose can be given in FLASH to produce the same toxicity as CONV). Normal tissue radiation dose responses are highly nonlinear and follow a sigmoidal relationship. Depending on the steepness of the response for a given organ and the specific dose, a DMF of 1.2–1.3 could produce either no clinical difference or a signficant near-binary separation between minimal and severe toxicity. The DMFs for normal tissues may also depend upon the specific tissue type, the partial volume effects (whole versus partial organ), and the dosing regimen (including the degree and timing of the fractionation), and thus remain to be characterized more broadly. In the end, isoeffect curves for acute (bone marrow and intestine) and late-responding (brain and lung) tissues have not been constructed for FLASH and will require time and significant research effort. Based on the DMF values reported to date and the established sensitivity of late-responding tissue to dose or fraction, one can presume a flattening of the isoeffect curves for FLASH, which may translate to the capability to deliver higher curative doses within limits while maintaining equal toxicity profiles. Furthermore, FLASH and CONV have demonstrated comparable tumor control across numerous preclinical tumor models as measured by tumor growth delay after irradiation. However, rigorous tests of noninferiority on *in vivo* tumor eradication are much more logistically challenging compared to tumor growth delay, and published data are lacking to date (Sørensen *et al.*, 2022).

The path to clinical translation of FLASH will be heavily influenced by two main factors: technological capabilities (existing and under development) and biological data. Existing technologies being used for FLASH preclinical research face substantial limitations in application to human patients. Electron beams of up to 20 MeV are currently used clinically for superficial targets, primarily tumors near the skin, because of their limited depth of penetration of up to a few centimeters. Existing clinical linear accelerators used to produce these electron beams can produce beam currents about 2 orders of magnitude higher than what has historically been used clinically. Simplistically, those indications currently treated using electrons are ripe for immediate clinical translation of FLASH. Existing proton therapy systems also have the capacity to increase beam current beyond what has typically been used clinically up to the FLASH range. The depth of penetration of protons with energy up to >200 MeV permits treatment of deep-seated targets. However, a key advantage of proton therapy over conventional x-ray therapy has been superior dose conformity, which is achieved through a combination of multiple intersecting beams and more spatially constrained dose deposition within the Bragg peak of the proton beam. Multiple intersecting beams are produced by mechanical rotation of a gantry-mounted beamline about the patient, which imposes a fundamental constraint on the delivery speed. Current pFLASH approaches therefore employ a single beam direction, which compromises dose conformity for FLASH, creating a trade-off between these means of achieving an improved therapeutic index. High-energy x rays in the energy range of 4–20 MV are the major staple of radiation therapy used for the large majority of patients and are the modality through which the previously described advancement in treatments and patient outcomes has primarily been achieved. Unlike electrons and protons, the existing clinical technologies for producing x rays have little margin to increase dose rate because the inefficiency of bremsstrahlung conversion from electrons requires these machines to be operated at near their maximum beam current. Preclinical x-ray FLASH research to date has been conducted

using large, highly specialized accelerator facilities such as synchrotron or free electron laser beamlines. Clinical x-ray FLASH within standard cancer treatment facilities requires entirely new technology; such developments are under way, as discussed in Sec. II.

Accordingly the first clinical trials of FLASH have focused on demonstrating feasibility and reliable delivery while considering the limitations of existing technologies as well as the potential risks in treating on timescales far shorter than are compatible with manual human intervention should an error occur. The University of Cincinnati completed accrual of FAST-01, a ten-patient feasibility study of pFLASH delivery for patients with painful metastatic tumors in the bones of extremities that was sponsored by Varian Medical Systems. The treatment comprised a palliative dose of 8 Gy, which is known to be a safe dose of CONV even when large volumes of normal tissues are included, delivering a 250 MeV proton beam from a single direction such that the dose roughly uniformly traverses the thickness of the body. As such, the trial assesses technical feasibility of delivering the dose at a nominal dose rate of 60 Gy/s, as well as pain relief and toxicity (which are expected to be similar to the historical results of CONV). As an initial step into clinical translation of FLASH, it does not attempt to test FLASH in indications beyond the boundaries of what can be done with a basic CONV treatment (Mascia *et al.*, 2023).

Enrollment has begun for the IMPULSE phase I clinical trial of electron FLASH for melanoma skin metastases conducted by CHUV. This is a dose escalation trial to determine the maximum tolerated dose of single-fraction electron FLASH (up to a dose of 34 Gy) for both large and small volume targets on the skin. This design affords an opportunity to determine whether FLASH doses can safely exceed limits encountered historically in clinical CONV using macroscopic observation and optical coherence imaging. Biological and translational end points are also included to explore the immune response and occurrence of the abscopal effect (i.e., systemic, out of radiation field effects).

Biological data to guide clinical translation are still developing. The most data with respect to normal organ sparing by FLASH have concentrated on a limited number of models, especially mice brain and intestine models. Most preclinical studies have been conducted using large single fractions of radiation, owing primarily to the logistical challenges of *in vivo* preclinical radiation research, though data on a limited number of fractionated treatment scenarios have begun to emerge. Furthermore, most have studied FLASH and CONV radiation as a single modality, whereas clinical radiation therapy is most often used as part of multimodality therapy, either concurrently or sequentially with systemic therapies.

As a thought exercise, we consider how one might design a clinical trial of FLASH guided by currently known biological observations and available technologies. Desirable features of such a trial would be (1) the indication is common enough that accrual could be completed in a reasonable time frame, (2) the toxicity and/or efficacy of standard treatment is poor enough that meaningful differences could be demonstrated with a reasonable number of patients, and (3) measurement of these end points is standardized and obtainable within a practical time frame. An additional feature desirable in an early trial would be that the treatment design be reasonably safe even if a FLASH effect is not elicited by the treatment regimen (i.e., the outcome would be acceptable even if FLASH behaves as CONV) or, alternatively, that a fallback plan be in place to mitigate toxicity should a FLASH effect not be elicited. The most robust design would be a randomized trial, which would require among other things that the trial have an adequate size.

Starting with the premise that the greatest breadth of preclinical data has been accumulated for cognitive sparing after whole-brain FLASH versus CONV in mice, one might envision a clinical trial of FLASH for brain metastases that would typically be treated with whole-brain radiation therapy (WBRT). Brain metastasis is a common manifestation of metastatic disease from a broad range of cancers and therefore impacts a large number of patients. Although WBRT for brain metastases has been declining in use with the trend of favoring stereotactic radiosurgery when possible, for a limited number of metastases a substantial proportion of patients have multiple brain metastases for which WBRT is still indicated. Toxicity from WBRT, particularly cognitive impairment, is common, is assessable by standardized metrics, and occurs in a relatively short time frame. In the benchmark trial NRG CC001 (a randomized trial comparing uniform WBRT with intensity-modulated radiation therapy treating the whole brain except with sparing of the hippocampus), cognitive function failure measured by a panel of neurocognitive tests occurred in 50%–60% of patients within four months of receiving WBRT despite receiving memantine for neurocognitive protection (Brown *et al.*, 2020). Furthermore, intracranial progression-free survival was a median of only about five months. Therefore, clinically significant improvements in either toxicity or (with dose escalation) intracranial tumor control with WBRT should be detectable within a practical trial size. In addition, WBRT is typically used as a single modality and not concurrently with anticancer systemic agents.

Considering the dose and fractionation regimen, a standard dose of conventional WBRT would be ten fractions of 3 Gy (total dose 30 Gy) as used in NRG CC001. This degree of fractionation and total dose was recently tested in preclinical FLASH experiments (Limoli *et al.*, 2023) and regimens comprising one fraction of 10 Gy, two fractions of 7 Gy (14 Gy in total), and three fractions of 10 Gy (30 Gy in total) have all demonstrated FLASH sparing of cognition compared to CONV without compromising tumor control in mouse brain tumor models (Montay-Gruel *et al.*, 2021), thus providing hope for generalizability to other fractionation schemes. However, if a threshold dose exceeding 3 Gy per fraction is required to obtain a FLASH effect, 30 Gy in ten fractions of 3 Gy would not achieve FLASH cognitive sparing. Adhering to the previously outlined principle, 30 Gy for ten fractions in FLASH would be reasonable to test against the same standard regimen in CONV since clinically significant FLASH cognitive sparing should be observable if present, but even if not the FLASH outcomes would be expected to be no different from those of standard CONV WBRT, and therefore would be acceptable. However, three fractions of 10 Gy FLASH produced superior tumor control than less intensive regimens without a measurable loss of cognitive function in a mouse model (Montay-Gruel *et al.*, 2021). However, such a regimen would not be tolerable in patients if delivered as CONV

WBRT, and using it could result in excessive toxicity should the FLASH effect not be replicated in humans at this dose and fractionation; this would arguably best be avoided during this early stage of FLASH clinical research.

Considering the technical perspective of FLASH delivery, FLASH WBRT should be possible to deliver with a single transmission proton beam on the plateau region of the dose distribution using techniques like those in the FAST-01 trial. This would produce a relatively homogeneous dose distribution throughout the volume of the whole brain. Techniques to use Bragg peak spot scanning and patient-specific ridge filters that are currently under development could in principle enable a degree of spatial intensity modulation of the dose to produce, for example, some dosimetric sparing of the hippocampus in conjunction with FLASH delivery. WBRT with hippocampal sparing through intensity-modulated radiation therapy (IMRT) was found to reduce the incidence of measurable cognitive dysfunction compared to homogeneous dose WBRT in NRG CC001. Therefore, it could be argued that the standard (control) arm against which FLASH should be compared is hippocampal-sparing WBRT, whereas the FLASH arm would have a homogeneous dose in the whole brain given the current state of technology. This raises the question of whether there would be equipoise between the arms: if there is no FLASH effect, the FLASH arm could produce inferior outcomes compared to the control arm. However, the demonstrated magnitude of benefit of hippocampal sparing on cognitive function was moderate (cognitive function failure at six months was reduced by about 25% overall and as much as 50% in specific domains), whereas in preclinical models cognitive function after FLASH WBRT is often the same as without any radiation (though this remains untested in humans).

The aforementioned exercise is intended to illustrate an example of the thought process considering the current state of technology development and radiobiological understanding for a rational FLASH clinical trial design. Vigorously debated topics remain on the requirements for broader clinical evaluations of FLASH. What degree of technical maturity should be required, particularly in real-time dose monitoring and control, to ensure that the intended dose and dose rate are delivered with a high degree of certainty? What are the minimum acceptable fail-safes and quality assurance standards to allow trials to proceed? How completely characterized must FLASH be in the preclinical setting before it can be employed in human trials? Must a biological mechanistic understanding of the FLASH effect come before further clinical studies are engaged in (the lack of which has not prevented other treatment modalities such as IMRT from moving into the clinical setting)? Could designing a trial that is biologically suboptimal because of a lack of understanding set it up for failure and prematurely curtail interest in the field?

Looking ahead we can consider what clinical indications may be of most benefit or even what new indications may be enabled by FLASH, assuming that initial trials demonstrate an improved therapeutic index in the clinical setting and how to deliver it optimally. In current practice, there are multiple cancers for which acute toxicities of radiation therapy impact a large proportion of patients. For example, radiation therapy for locally advanced mucosal cancers of the head and neck causes substantial mucositis during the course of treatment that produces morbidity including pain, weight loss, and temporary or sometimes prolonged dependence on feeding tubes for nutrition, commonly followed by multiple chronic side effects. This represents a scenario in which simply replacing CONV with FLASH while using the same dose and fractionation regimens could produce immediately measurable toxicity reductions that could be captured on a short timescale in clinical trials. Radiation therapy for a number of brain tumors in children has the potential to lead to long-term survival or a cure, and simultaneously a high risk of long-term neurological injury that may manifest as early as within several months of treatment. While there is generally a hesitation to test new treatments in children, particularly in the setting of a potential cure, this is a patient population in which the potential therapeutic index improvement of FLASH could have a large impact. Therefore, conducting trials of WBRT FLASH for brain metastases could pave the way for future pediatric trials should the results prove promising.

FLASH also promises to enable new or expanded uses of radiation therapy, where its use is currently limited because it is infeasible to give clinically meaningful doses of radiation. Pancreatic cancer has historically had poor outcomes even when localized, and ablative radiation is limited by tolerance of nearby sensitive organs such as the small intestine. Recent clinical data suggest that the ability to escalate the tumor dose safely through improved image-guided daily adaptive planning to reduce the dose to the adjacent bowel leads to higher overall survival, an outcome that has been notoriously recalcitrant to improvement in this disease (Rudra *et al.*, 2019). Reduced normal tissue toxicity with FLASH could enable a safe escalation of dosing for pancreatic and other cancers that are poorly controlled with conventional radiation regimens that are constrained by toxicity. Similarly, an emerging paradigm enabled by stereotactic ablative RT, which can sterilize limited, small volume metastatic (oligometastatic) disease, is expanding curative intent treatment to a patient population that has historically lacked potentially curative options (Iyengar *et al.*, 2018; Gomez *et al.*, 2019; Palma *et al.*, 2020). Nevertheless, more extensive metastatic disease with larger or more numerous metastatic tumors remains untreatable with ablative radiation approaches because of the excessive volume of normal tissues that would be damaged. In combination with emerging and more effective systemic therapies, FLASH has the potential to make a cure a realistic goal for many patients with metastatic cancer. Tumor recurrences at sites that have previously received high-dose radiation therapy represent a particularly challenging clinical situation. Reirradiation may be indicated when other salvage treatment approaches such as surgery are too risky but presents its own unique and potentially severe risks. For example, breakdowns of blood vessels leading to massive life-threatening bleeding or tissue breakdown leading to fistula formation between anatomic structures are recognized potential complications of high-dose reirradiation not commonly seen with an initial course of definitive radiation therapy. It remains to be studied whether FLASH can reduce the risk of severe radiation injury in organs that have previously received high-dose irradiation.

A consideration of future applications of FLASH highlights some areas in which more biology research and technology development are needed. Most radiation therapy is given with conventional fractionation (typically <3 Gy per fraction repeated >20 times in a course of treatment), often with concurrent chemotherapy and, increasingly, immunotherapy and small molecule drugs targeted at specific cellular signaling pathways. These are regimens for which preclinical data on FLASH are currently lacking, thus warranting research in this area. Highly conformal radiation therapy has made it safer in many cases to accelerate courses of radiation such that there has been a trend toward increasingly hypofractionated radiation courses, i.e., courses with a smaller number of treatments and a larger dose per fraction. Some preclinical studies have demonstrated FLASH effects with moderately hypofractionated courses, demonstrating at least that the biological advantage of FLASH persists in regimens with more than a single fraction (Montay-Gruel *et al.*, 2021; Liljedahl *et al.*, 2022). One preclinical study demonstrated that anti-PD-1 immune checkpoint inhibition given with FLASH produced superior antitumor efficacy over either treatment alone, while sparing of intestinal toxicity by FLASH was maintained with the combination therapy (Eggold *et al.*, 2022). Demonstrating FLASH effects in the context of cytotoxic chemotherapy agents as well as other systemic therapies will be important. Finally, because much of the improvements in radiation therapy outcomes in the current era are attributable to highly conformal radiation delivery, it stands to reason that the greatest potential benefit will be realized with highly conformal FLASH radiation therapy. Ultrarapid delivery with high conformity would ideally be delivered using beams from multiple different beam directions simultaneously or in rapid succession. Conventional technologies use mechanical motion of the radiation source relative to the patient (or in some cases movement of the patient relative to the source) to achieve multiple beam directions, which is inherently rate limiting. An approach using all-electronic beam intensity modulation and multiple integrated beam directions is under development (Maxim, Tantawi, and Loo, 2019).

VI. FUTURE AND CHALLENGES

In this review, we systematically reported and analyzed the current data available in the field of FLASH. Current consensus recognizes that FLASH has the potential to revolutionize the way radiation therapy is delivered. This optimism stems from its potential to widen the therapeutic window, thereby enhancing therapeutic outcomes and the quality of life of cancer patients suffering from a wide range of malignancies. To conclude this work, challenges and opportunities are identified that we anticipate the FLASH community will face in the future.

There is significant preclinical evidence that supports the clinical development of FLASH; see Secs. III and V. Although the results of more standardized fractionation protocols (lower doses over multiple fractions) implementing FLASH studies will become available, a preponderance of preclinical evidence suggests that the main advantage of FLASH would be realized under single-fraction or hypofractionated treatments given that long-term toxicity profiles have been identified. Either of these approaches would eliminate the uncertainties associated with motion management given accurate location of the tumor. Nonetheless, high single and/or hypofractionated approaches trigger adverse late complications, as recently reported in domestic animal trials (Rohrer Bley *et al.*, 2022; Børresen *et al.*, 2023). These reports demonstrated certain limitations of the FLASH effect. However, such an approach could be amenable in other models such as skin cancer with higher dose tolerances. In addition, the single beam direction used in the phase III cat trial was another confounding factor that limited conformal dose delivery, and it points to the need for developing highly conformal FLASH irradiators. Taking these limitations into account and using validated beams under optimized beam parameters able to deliver the FLASH effect, well-controlled phase I clinical trials should be launched. The results of such studies will be essential for patient safety and are prerequisites before embarking into larger, more costly clinical trials. Such studies can also be coupled with veterinary phase II and III randomized trials to hasten the evaluation of efficacy. Note that the therapeutic options for cat and dog patients are scarce and, since toxicities triggered by SoC are usually high with suboptimal efficacy, recruitment should be completed as rapidly as possible. This approach can streamline the process of demonstrating meaningful differences with a reasonable number of patients, with euthanasia remaining as an option if negative or adverse effects are encountered, an undesired yet default option most often taken by pet owners at diagnosis.

The ultimate realization of a robust and safe clinical transfer of FLASH will require multidisciplinary research teams at the interface of physics, chemistry, and biology. As shown in Sec. II, the FLASH effect has been observed using specific physical beam parameters that include dose rate, irradiation time, fractionation, pulse width and multiplicity (repetition frequency), total dose, and specific radiation geometry. Most of these parameters have been evaluated on small volumes of tissue using mice, providing the base line rationale for how to adjust certain parameters to the clinical setting. At present technology represents the main limitation for the field of FLASH, as practical solutions for implementation remain limited. For eFLASH and xFLASH modalities, conformality requires further development and, while pFLASH solutions seem poised for the clinic, high dose rates maintained in the plateau regions must be coupled with range modulators and PBS techniques to treat larger, deeper-seated tumors with the SOBP. Notwithstanding the progress that has been made in less than ten years, it has become possible to perform preclinical experiments in FLASH conditions with electrons, photons, and protons, with adaptations to each of these (for example, VHEE and laser driven linacs) well under way. Now each modality must await the necessary quality assurance for full clinical implementation, efforts that will require time and resources, as recently reviewed by Taylor *et al.* (2022).

Notwithstanding the importance of physical beam parameters, FLASH has and remains an *in vivo* effect, and characterization of the underlying mechanism of action remains a critical question in the field; see Secs. III–V. The fact that the FLASH effect has been reported across most organs and tissues in various organisms has defied identification of a unifying explanation, confounded further in that

FLASH retains antitumor efficacy across an equally broad range of neoplasms. Whether structural, molecular, cellular, or at larger global levels of physiological communication, the amplitude of the FLASH effect will likely be impacted by biochemical and intrinsic biological conditions that are incompletely understood. As more studies analyzing human tissues are forthcoming, we can expect more biological nuances, including volume effects, latency, tissue tolerances, and intrinsic tumor sensitivity to FLASH (Chabi *et al.*, 2021).

A final point to emphasize regards the more global and specific benefits to radiation oncology and radiation sciences that have resulted from the exciting revelations afforded by FLASH. For decades, radiation research and the resultant benefits to radiation oncology have been overshadowed by the economic interests of Big Pharma driving a profitable drug pipeline to the field of medical oncology. The promise of FLASH has provided an innovative boost to the entire interdisciplinary field that reunites the research activities of physicists, chemists, biologists, and clinicians. The result has been a rejuvenated development of world-class infrastructures to perform basic and clinical cancer research and conduct clinical trials. FLASH owes much of its initial support through academic grants provided by national funding agencies, France (Agence Nationale de la Recherche and Institut du Cancer) and Switzerland (Swiss National Science Foundation funds) have pioneered research in FLASH in an early and close collaboration with the U.S. (National Cancer Institute). Interest and funding in FLASH has spread worldwide and is now witnessing significant industrial commitment. In a few years, major linac suppliers have made meaningful investments in the technology required to implement FLASH and have partnered with the academic world. These efforts promise to hasten the needed investment in the use of radiation as an effective tool in the fight against cancer, which to date has been undervalued in comparison with other drug-based treatments that are often less effective. There can be little doubt about the marked impact that FLASH has had on the entire field of radiation sciences, and current developments will have a long-lasting and beneficial impact on academic research, infrastructure, and clinical oncology. In the end, resultant discoveries will promote educational and economic competitiveness in medical applications of radiation and related technologies, along with unique opportunities to train the next generation of scientists and physicians from various fields for translational research that will shape the future of oncology.

LIST OF SYMBOLS AND ABBREVIATIONS

AAPM	American Association of Physicists in Medicine
α/β	alpha-beta ratio
BED	biological equivalent dose
BCT	beam current transformer
clinac	clinical linac
DMF	dose modifying factor
eCONV	conventional dose rate delivery using electron beams
eFLASH	ultrahigh dose rate delivery using electron beams
ELBE	Electron Linac of High Brilliance and Low Emittance
ESRF	European Synchrotron Radiation Facility
eV	electron volt
FFF	flattening free filter
FWHM	full width at half maximum
Gy	gray
IAEA	International Atomic Energy Agency
ICRU	International Commission on Radiation Units and Measurements
IDL	isodose line
IORT	intraoperative radiotherapy
linac	linear accelerator
NMI	National Metrology Institute
NOR	novel object recognition
OSL	optically stimulated luminescence
PBS	pencil-beam scanning
pCONV	conventional dose rate delivery using proton beams
pFLASH	ultrahigh dose rate delivery using proton beams
PHASER	pluridirectional high-energy agile scanning electronic radiotherapy
PRF	pulse repetition frequencies
R50	half-value depth
rf	radio frequency
RP	radiation protection
RT	radiotherapy
SBRT	stereotactic body radiation therapy
SCC	squamous cell carcinoma
SLAC	Stanford Linear Accelerator Center
SoC	standard of care
SPHINX	scanning pencil-beam high-speed intensity-modulated x-ray source
SSB	DNA single-strand break
SSD	surface-to-source distance
TCD50	dose for 50% tumor control
TPS	treatment planning system
UHDR:	ultrahigh dose rate
VHEE	very high-energy electrons
xCONV	conventional dose rate delivery using photon beams
xFLASH	ultrahigh dose rate delivery using photon beams
ZF	zebrafish

ACKNOWLEDGMENTS

We thank Dr. V. Favaudon, who initiated research on FLASH, for his contribution to the scientific discussion and his critical reading of the manuscript. We thank the biology

team of the CHUV and UCI, especially H. Kacem, J. Ollivier, and B. Petit, and well as Drs. M. M. Acharya, Y. Alaghband B. Allen, J. E. Baulch, P. P. Montay-Gruel, and Ballesteros Zebadua for their past contributions to the FLASH project, and A. Almeida, O. G. G Drayson, and R. Kim for the help with figure preparation. We also thank Professors F. Bochud and J. Bourhis for their support, as well as Drs. T. Böhlen, T. Buchillier, L. Desorgher, P. Froidevaux, J. F. Germond, and V. Grilj for the fruitful scientific discussions. We thank the contributors to the FLASH radiation biology, medical physics, and accelerator-rf science program at Stanford Radiation Oncology and SLAC National Accelerator Laboratory, including E. Alemany, M. R Ashraf, M. Bazalova-Carter, K. Bush, K. M. Casey, F. Chavez, S. Chow, S. Dutt, M. Dworkin, J. T. Eggold, E. Engleman, E. E. Graves, V. Grover, B. Ha, N. Kapadia, R. B. Ko, A. C. Koong, F. M. Lartey, B. Lau, R. Lee, K. Levy, K. Liang, P. E. Loo, E. Nanni, R. Manjappa, S. Melemenidis, C. Nantista, S. Natarajan, H. Joshua No, G. Pratx, E. B. Rankin, S. Rokni, A. Rosenstrom, M. Santana, E. Schueler, M. Shumail, D. Simmons, L. Skinner, E. Snively, L. A. Soto, S. Strober, M. Surucu, A. Tremaine, V. Viswanathan, J. Wang, L. Wang, B. Whelan, Y. (Fred) Wu, and A. S. Yu. We are grateful for the support of the Stanford Department of Radiation Oncology and Dr. Q. T. Le. The studies were supported by a Sinergia grant from the Swiss National Science Foundation (SNSF) (Grant No. CRS II5_186369) (M.-C. V), a Spirit grant from SNSF Grant No. IZSTZ0_198747/1 (M.-C. V.), Swiss Cancer Research (Oncosuisse) Grant No. KFS-4438-02-2018 (M.-C. V.), NIH program Project Grant No. PO1CA244091 (M.-C. V., B. W. L., P. M., D. R. S., and C. L. L.), NIH Grant No. R01CA254892 (M.-C. V. and C. L. L.), National Institutes of Allergy and Infectious Diseases Grants No. R01CA233958 and No. R01CA266673 (B. W. L.), and NIH Grant No. R44CA217607 (B. W. L.). We gratefully acknowledge the support of the ISREC Foundation (2016–2020) thanks to a donation from the Biltema Foundation (M.-C. V.), as well as the partnership of philanthropic donors to Stanford Radiation Oncology supporting the FLASH research program (B. W. L.).

REFERENCES

Adrian, G., E. Konradsson, S. Beyer, A. Wittrup, K. T. Butterworth, S. J. McMahon, M. Ghita, K. Petersson, and C. Ceberg, 2021, "Cancer cells can exhibit a sparing FLASH effect at low doses under normoxic *in vitro*-conditions," Front. Oncol. **11**, 686142.

Adrian, G., E. Konradsson, M. Lempart, S. Back, C. Ceberg, and K. Petersson, 2020, "The FLASH effect depends on oxygen concentration," Br. J. Radiol. **93**, 20190702.

Adrian, G., J. L. Ruan, S. Paillas, C. R. Cooper, and K. Petersson, 2022, "*In vitro* assays for investigating the FLASH effect," Expert Rev. Mol. Med. **24**, e10.

Agmon, E., J. Solon, P. Bassereau, and B. R. Stockwell, 2018, "Modeling the effects of lipid peroxidation during ferroptosis on membrane properties," Sci. Rep. **8**, 5155.

Alaghband, Y., *et al.*, 2020, "Neuroprotection of radiosensitive juvenile mice by ultra-high dose rate FLASH irradiation," Cancers **12**, 1671.

Alexander, M. S., *et al.*, 2018, "Pharmacologic ascorbate reduces radiation-induced normal tissue toxicity and enhances tumor radiosensitization in pancreatic cancer," Cancer Res. **78**, 6838–6851.

Allen, B. D., M. M. Acharya, P. Montay-Gruel, P. G. Jorge, C. Bailat, B. Petit, M. C. Vozenin, and C. Limoli, 2020, "Maintenance of tight junction integrity in the absence of vascular dilation in the brain of mice exposed to ultra-high-dose-rate FLASH irradiation," Radiat. Res. **194**, 625–635.

Almeida, A., *et al.*, 2024, "Dosimetric and biologic intercomparison between electron and proton FLASH beams," Radiother. Oncol. **190**, 109953.

Atun, R., *et al.*, 2015, "Expanding global access to radiotherapy," Lancet Oncol. **16**, 1153–1186.

Auer, S., V. Hable, C. Greubel, G. A. Drexler, T. E. Schmid, C. Belka, G. Dollinger, and A. A. Friedl, 2011, "Survival of tumor cells after proton irradiation with ultra-high dose rates," Radiat. Oncol. **6**, 139.

Aykin-Burns, N., I. M. Ahmad, Y. Zhu, L. W. Oberley, and D. R. Spitz, 2009, "Increased levels of superoxide and H_2O_2 mediate the differential susceptibility of cancer cells versus normal cells to glucose deprivation," Biochem. J. **418**, 29–37.

Badgley, M. A., *et al.*, 2020, "Cysteine depletion induces pancreatic tumor ferroptosis in mice," Science **368**, 85–89.

Baldacchino, G., E. Brun, I. Denden, S. Bouhadoun, R. Roux, H. Khodja, and C. Sicard-Roselli, 2019. "Importance of radiolytic reactions during high-LET irradiation modalities: LET effect, role of O_2 and radiosensitization by nanoparticles," Cancer Nanotechnol. **10**, 3.

Barghouth, P. G., *et al.*, 2023, "FLASH-RT does not affect chromosome translocations and junction structures beyond that of CONV-RT dose-rates," Radiother. Oncol. **188**, 109906.

Bayart, E., A. Flacco, O. Delmas, L. Pommarel, D. Levy, M. Cavallone, F. Megnin-Chanet, E. Deutsch, and V. Malka, 2019, "Fast dose fractionation using ultra-short laser accelerated proton pulses can increase cancer cell mortality, which relies on functional PARP1 protein," Sci. Rep. **9**, 10132.

Bazalova-Carter, M., and N. Esplen, 2019, "On the capabilities of conventional x-ray tubes to deliver ultra-high (FLASH) dose rates," Med. Phys. **46**, 5690–5695.

Berne, A., K. Petersson, I. D. C. Tullis, R. G. Newman, and B. Vojnovic, 2021, "Monitoring electron energies during FLASH irradiations," Phys. Med. Biol. **66**, 045015.

Berry, R. J., E. J. Hall, D. W. Forster, T. H. Storr, and M. J. Goodman, 1969, "Survival of mammalian cells exposed to x rays at ultra-high dose-rates," Br. J. Radiol. **42**, 102–107.

Beyreuther, E., M. Brand, S. Hans, K. Hideghety, L. Karsch, E. Lessmann, M. Schurer, E. R. Szabo, and J. Pawelke, 2019, "Feasibility of proton FLASH effect tested by zebrafish embryo irradiation," Radiother. Oncol. **139**, 46–50.

Børresen, B., M. L. Arendt, E. Konradsson, K. Bastholm Jensen, S. A. Back, P. Munck af Rosenschöld, C. Ceberg, and K. Petersson, 2023, "Evaluation of single-fraction high dose FLASH radiotherapy in a cohort of canine oral cancer patients," Front. Oncol. **13**, 1256760.

Boscolo, D., E. Scifoni, M. Durante, M. Krämer, and M. C. Fuss, 2021, "May oxygen depletion explain the FLASH effect? A chemical track structure analysis," Radiother. Oncol. **162**, 68–75.

Bourhis, J., *et al.*, 2019, "Treatment of a first patient with FLASH-radiotherapy," Radiother. Oncol. **139**, 18–22.

Brauer-Krisch, E., *et al.*, 2015, "Medical physics aspects of the synchrotron radiation therapies: Microbeam radiation therapy (MRT) and synchrotron stereotactic radiotherapy (SSRT)," Phys. Med. **31**, 568–583.

Breitkreutz, D. Y., M. Shumail, K. K. Bush, S. G. Tantawi, P. G. Maxime, and B. W. Loo, Jr., 2020, "Initial steps towards a clinical FLASH radiotherapy system: Pediatric whole brain irradiation with 40 MeV electrons at FLASH dose rates," Radiat. Res. **194**, 594–599.

Brown, P. D., *et al.*, 2013, "Memantine for the prevention of cognitive dysfunction in patients receiving whole-brain radiotherapy: A randomized, double-blind, placebo-controlled trial," Neuro-Oncology **15**, 1429–1437.

Brown, P. D., *et al.*, 2020, "Hippocampal avoidance during whole-brain radiotherapy plus memantine for patients with brain metastases: Phase III trial NRG oncology CC001," J. Clin. Oncol. **38**, 1019–1029.

Buchsbaum, J. C., C. N. Coleman, M. G. Espey, P. G. S. Prasanna, J. Capala, M. M. Ahmed, J. A. Hong, and C. Obcemea, 2021, "FLASH radiation therapy: New technology plus biology required," Int. J. Radiat. Oncol. Biol. Phys. **110**, 1248–1249.

Buonanno, M., V. Grilj, and D. J. Brenner, 2019, "Biological effects in normal cells exposed to FLASH dose rate protons," Radiother. Oncol. **139**, 51–55.

Cao, X., *et al.*, 2021, "Quantification of oxygen depletion during FLASH irradiation *in vitro* and *in vivo*," Int. J. Radiat. Oncol. Biol. Phys. **111**, 240–248.

Cecchi, D. D., F. Therriault-Proulx, S. Lambert-Girard, A. Hart, A. Macdonald, M. Pfleger, M. Lenckowski, and M. Bazalova-Carter, 2021, "Characterization of an x-ray tube-based ultrahigh dose-rate system for *in vitro* irradiations," Med. Phys. **48**, 7399–7409.

Chabi, S., *et al.*, 2021, "Ultra-high-dose-rate FLASH and conventional-dose-rate irradiation differentially affect human acute lymphoblastic leukemia and normal hematopoiesis," Int. J. Radiat. Oncol. Biol. Phys. **109**, 819–829.

Cunningham, S., *et al.*, 2021, "FLASH proton pencil beam scanning irradiation minimizes radiation-induced leg contracture and skin toxicity in mice," Cancers **13**, 1012.

Dal Bello, R., *et al.*, 2023, "Enabling ultra-high dose rate electron beams at a clinical linear accelerator for isocentric treatments," Radiother. Oncol. **187**, 109822.

Daugherty, E. C., *et al.*, 2023, "FLASH radiotherapy for the treatment of symptomatic bone metastases (FAST-01): Protocol for the first prospective feasibility study," JMIR Res. Protoc. **12**, e41812.

Dayal, D., S. M. Martin, C. L. Limoli, and D. R. Spitz, 2008, "Hydrogen peroxide mediates the radiation-induced mutator phenotype in mammalian cells," Biochem. J. **413**, 185–191.

Dayal, D., *et al.*, 2009, "Mitochondrial complex II dysfunction can contribute significantly to genomic instability after exposure to ionizing radiation," Radiat. Res. **172**, 737–745.

Delanian, S., and J. L. Lefaix, 2007, "Current management for late normal tissue injury: Radiation-induced fibrosis and necrosis," Semin. Radiat. Oncol. **17**, 99–107.

DesRosiers, C., V. Moskvin, A. F. Bielajew, and L. Papiez, 2000, "150–250 MeV electron beams in radiation therapy," Phys. Med. Biol. **45**, 1781.

DesRosiers, C., V. Moskvin, M. Cao, C. Joshi, and M. Langer, 2008, "Lung tumor treatment with very high energy electron beams of 150–250 MeV as compared to conventional megavoltage photon beams," Int. J. Radiat. Oncol. Biol. Phys. **72**, S612.

Diffenderfer, E. S., B. S. Sørensen, A. Mazal, and D. J. Carlson, 2022, "The current status of preclinical proton FLASH radiation and future directions," Med. Phys. **49**, 2039–2054.

Diffenderfer, E. S., *et al.*, 2020, "Design, implementation, and *in vivo* validation of a novel proton FLASH radiation therapy system," Int. J. Radiat. Oncol. Biol. Phys. **106**, 440–448.

Di Martino, F., *et al.*, 2020, "FLASH radiotherapy with electrons: Issues related to the production, monitoring, and dosimetric characterization of the beam," Front. Phys. **8**, 481.

Doll, S., *et al.*, 2017, "ACSL4 dictates ferroptosis sensitivity by shaping cellular lipid composition," Nat. Chem. Biol. **13**, 91–98.

Eggold, J. T., *et al.*, 2022, "Abdominopelvic FLASH irradiation improves PD-1 immune checkpoint inhibition in preclinical models of ovarian cancer," Mol. Cancer Ther. **21**, 371–381.

Eling, L., A. Bouchet, C. Nemoz, V. Djonov, J. Balosso, J. Laissue, E. Bräuer-Krisch, J. F. Adam, and R. Serduc, 2019, "Ultra high dose rate synchrotron microbeam radiation therapy. Preclinical evidence in view of a clinical transfer," Radiother. Oncol. **139**, 56–61.

El Khatib, M., *et al.*, 2022, "Ultrafast tracking of oxygen dynamics during proton FLASH," Int. J. Radiat. Oncol. Biol. Phys. **113**, 624–634.

Epp, E. R., H. Weiss, B. Djordjevic, and A. Santomasso, 1972, "The radiosensitivity of cultured mammalian cells exposed to single high intensity pulses of electrons in various concentrations of oxygen," Radiat. Res. **52**, 324–332.

Epp, E. R., H. Weiss, and A. Santomasso, 1968, "The oxygen effect in bacterial cells irradiated with high-intensity pulsed electrons," Radiat. Res. **34**, 320–325.

Esplen, N., L. Egoriti, B. Paley, T. Planche, C. Hoehr, A. Gottberg, and M. Bazalova-Carter, 2022, "Design optimization of an electron-to-photon conversion target for ultra-high dose rate x-ray (FLASH) experiments at TRIUMF," Phys. Med. Biol. **67**, 105003.

Evans, T., J. Cooley, M. Wagner, T. N. Yu, and T. Zwart, 2022, "Demonstration of the FLASH effect within the spread-out Bragg peak after abdominal irradiation of mice," Int. J. Part. Ther. **8**, 68–75.

Farr, J., V. Grilj, V. Malka, S. Sudharsan, and M. Schippers, 2022, "Ultra-high dose rate radiation production and delivery systems intended for FLASH," Med. Phys. **49**, 4875–4911.

Farr, J. B., K. Parodi, and D. J. Carlson, 2022, "FLASH: Current status and the transition to clinical use," Med. Phys. **49**, 1972–1973.

Favaudon, V., R. Labarbe, and C. L. Limoli, 2022, "Model studies of the role of oxygen in the FLASH effect," Med. Phys. **49**, 2068–2081.

Favaudon, V., J.-M. Lentz, S. Heinrich, A. Patriarca, L. de Marzi, C. Fouillade, and M. Dutreix, 2019, "Time-resolved dosimetry of pulsed electron beams in very high dose-rate, FLASH irradiation for radiotherapy preclinical studies," Nucl. Instrum. Methods Phys. Res., Sect. A **944**, 162537.

Favaudon, V., *et al.*, 2014, "Ultrahigh dose-rate FLASH irradiation increases the differential response between normal and tumor tissue in mice," Sci. Transl. Med. **6**, 245ra293.

Field, S. B., and D. K. Bewley, 1974, "Effects of dose-rate on the radiation response of rat skin," Int. J. Radiat. Biol. Relat. Stud. Phys. Chem. Med. **26**, 259–267.

Fiorini, F., *et al.*, 2011, "Dosimetry and spectral analysis of a radiobiological experiment using laser-driven proton beams," Phys. Med. Biol. **56**, 6969–6982.

Folkerts, M. M., E. Abel, S. Busold, J. R. Perez, V. Krishnamurthi, and C. C. Ling, 2020, "A framework for defining FLASH dose rate for pencil beam scanning," Med. Phys. **47**, 6396–6404.

Forrest, L. J., T. R. Mackie, K. Ruchala, M. Turek, J. Kapatoes, H. Jaradat, S. Hui, J. Balog, D. M. Vail, and M. P. Mehta, 2004, "The utility of megavoltage computed tomography images from a helical tomotherapy system for setup verification purposes," Int. J. Radiat. Oncol. Biol. Phys. **60**, 1639–1644.

Fouillade, C., *et al.*, 2020, "FLASH irradiation spares lung progenitor cells and limits the incidence of radio-induced senescence," Clin. Cancer Res. **26**, 1497–1506.

Franzi, M., J. W. Wang, V. Dolgashev, and S. Tantawi, 2016, "Compact rf polarizer and its application to pulse compression systems," Phys. Rev. Accel. Beams **19**, 062002.

Froidevaux, P., V. Grilj, C. Bailat, W. R. Geyer, F. Bochud, and M. C. Vozenin, 2023, "FLASH irradiation does not induce lipid peroxidation in lipids micelles and liposomes," Radiat. Phys. Chem. **205**, 110733.

Gaide, O., *et al.*, 2022, "Comparison of ultra-high versus conventional dose rate radiotherapy in a patient with cutaneous lymphoma," Radiother. Oncol. **174**, 87–91.

Gao, F., *et al.*, 2022, "First demonstration of the FLASH effect with ultrahigh dose rate high-energy x-rays," Radiother. Oncol. **166**, 44–50.

Gardner, H. L., J. M. Fenger, and C. A. London, 2016, "Dogs as a model for cancer," Annu. Rev. Anim. Biosci. **4**, 199–222.

Gasymova, E., V. Meier, F. Guscetti, S. Cancedda, M. Roos, and C. Rohrer Bley, 2017, "Retrospective clinical study on outcome in cats with nasal planum squamous cell carcinoma treated with an accelerated radiation protocol," BMC Vet. Res. **13**, 86.

Gomez, D. R., *et al.*, 2019, "Local consolidative therapy vs. maintenance therapy or observation for patients with oligometastatic non-small-cell lung cancer: Long-term results of a multi-institutional, phase II, randomized study," J. Clin. Oncol. **37**, 1558–1565.

Gonçalves Jorge, P., *et al.*, 2022, "Design and validation of a dosimetric comparison scheme tailored for ultra-high dose-rate electron beams to support multicenter FLASH preclinical studies," Radiother. Oncol. **175**, 203–209.

Greenberger, J. S., and M. W. Epperly, 2007, "Review. Antioxidant gene therapeutic approaches to normal tissue radioprotection and tumor radiosensitization," In Vivo **21**, 141–146, https://iv.iiarjournals.org/content/invivo/21/2/141.full.pdf.

Griffin, R. J., *et al.*, 2020, "Understanding high-dose, ultra-high dose rate, and spatially fractionated radiation therapy," Int. J. Radiat. Oncol. Biol. Phys. **107**, 766–778.

Grilj, V., M. Buonanno, D. Welch, and D. J. Brenner, 2020, "Proton irradiation platforms for preclinical studies of high-dose-rate (FLASH) effects at RARAF," Radiat. Res. **194**, 646–655.

Guo, Z., M. Buonanno, A. Harken, G. Zhou, and T. K. Hei, 2022, "Mitochondrial damage response and fate of normal cells exposed to FLASH irradiation with protons," Radiat. Res. **197**, 569–582.

Hall, E. J., and A. J. Giaccia, 2012, *Radiobiology for the Radiologist* (Lippincott Williams & Wilkins, Philadelphia).

Hanton, F., *et al.*, 2019, "DNA DSB repair dynamics following irradiation with laser-driven protons at ultra-high dose rates," Sci. Rep. **9**, 4471.

Harris, I. S., and G. M. DeNicola, 2020, "The complex interplay between antioxidants and ROS in cancer," Trends Cell Biol. **30**, 440–451.

Hayes, J. D., and A. T. Dinkova-Kostova, 2014, "The Nrf2 regulatory network provides an interface between redox and intermediary metabolism," Trends Biochem. Sci. **39**, 199–218.

Hayes, J. D., A. T. Dinkova-Kostova, and K. D. Tew, 2020, "Oxidative stress in cancer," Cancer Cell **38**, 167–197.

Hendry, J. H., J. V. Moore, B. W. Hodgson, and J. P. Keene, 1982, "The constant low oxygen concentration in all the target cells for mouse tail radionecrosis," Radiat. Res. **92**, 172–181.

Hiroki, A., S. M. Pimblott, and J. A. LaVerne, 2002, "Hydrogen peroxide production in the radiolysis of water with high radical scavenger concentrations," J. Phys. Chem. A **106**, 9352–9358.

Hong, J. H., C. S. Chiang, I. L. Campbell, J. R. Sun, H. R. Withers, and W. H. McBride, 1995, "Induction of acute phase gene expression by brain irradiation," Int. J. Radiat. Oncol. Biol. Phys. **33**, 619–626.

Hopewell, J. W., and K. R. Trott, 2000, "Volume effects in radiobiology as applied to radiotherapy," Radiother. Oncol. **56**, 283–288.

Hopewell, J. W., and G. J. van den Aardweg, 1988, "Current concepts of dose fractionation in radiotherapy. Normal tissue tolerance," Br. J. Radiol. Suppl. **22**, 88–94.

Hornsey, S., and D. K. Bewley, 1971, "Hypoxia in mouse intestine induced by electron irradiation at high dose-rates," Int. J. Radiat. Biol. Relat. Stud. Phys. Chem. Med. **19**, 479–483.

Inada, T., H. Nishio, S. Amino, K. Abe, and K. Saito, 1980, "High dose-rate dependence of early skin reaction in mouse," Int. J. Radiat. Biol. Relat. Stud. Phys. Chem. Med. **38**, 139–145.

Iturri, L., *et al.*, 2023, "Oxygen supplementation in anesthesia can block FLASH effect and anti-tumor immunity in conventional proton therapy," Commun. Med. **3**, 183.

Iyengar, P., *et al.*, 2018, "Consolidative radiotherapy for limited metastatic non-small-cell lung cancer: A phase 2 randomized clinical trial," JAMA Oncol. **4**, e173501.

Jaccard, M., M. T. Durán, K. Petersson, J.-F. Germond, P. Liger, M.-C. Vozenin, J. Bourhis, F. Bochud, and C. Bailat, 2018, "High dose-per-pulse electron beam dosimetry: Commissioning of the Oriatron eRT6 prototype linear accelerator for preclinical use," Med. Phys. **45**, 863–874.

Jaccard, M., K. Petersson, T. Buchillier, J. F. Germond, M. T. Durán, M. C. Vozenin, J. Bourhis, F. O. Bochud, and C. Bailat, 2017, "High dose-per-pulse electron beam dosimetry: Usability and dose-rate independence of EBT3 Gafchromic films," Med. Phys. **44**, 725–735.

Jansen, J., J. Knoll, E. Beyreuther, J. Pawelke, R. Skuza, R. Hanley, S. Brons, F. Pagliari, and J. Seco, 2021, "Does FLASH deplete oxygen? Experimental evaluation for photons, protons, and carbon ions," Med. Phys. **48**, 3982–3990.

Jensen, A., J. Neilson, and S. Tantawi, 2015, "*X*-band multi-beam klystron design and progress report," in *Proceedings of the 2015 IEEE International Vacuum Electronics Conference (IVEC), Beijing, 2015* (IEEE, New York), pp. 1–2.

Joiner, M. C. E., and A. E. van der Kogel, 2018, Eds., *Basic Clinical Radiobiology*, 5th ed. (CRC Press, Boca Raton).

Jorge, P. G., *et al.*, 2019, "Dosimetric and preparation procedures for irradiating biological models with pulsed electron beam at ultra-high dose-rate," Radiother. Oncol. **139**, 34–39.

Kacem, H., A. Almeida, N. Cherbuin, and M. C. Vozenin, 2022, "Understanding the FLASH effect to unravel the potential of ultra-high dose rate irradiation," Int. J. Radiat. Biol. **98**, 506–516.

Kacem, H., *et al.*, 2022, "Comparing radiolytic production of H_2O_2 and development of zebrafish embryos after ultra high dose rate exposure with electron and transmission proton beams," Radiother. Oncol. **175**, 197–202.

Karsch, L., *et al.*, 2022, "Beam pulse structure and dose rate as determinants for the FLASH effect observed in zebrafish embryo," Radiother. Oncol. **173**, 49–54.

Khan, S., M. Bassenne, J. Wang, R. Manjappa, S. Melemenidis, D. Y. Breitkreutz, P. G. Maxim, L. Xing, B. W. Loo, Jr., and G. Pratx, 2021, "Multicellular spheroids as *in vitro* models of oxygen depletion during FLASH irradiation," Int. J. Radiat. Oncol. Biol. Phys. **110**, 833–844.

Kim, M. M., *et al.*, 2021, "Comparison of FLASH proton entrance and the spread-out Bragg peak dose regions in the sparing of mouse intestinal crypts and in a pancreatic tumor model," Cancers **13**, 4244.

Kim, Y.-E., *et al.*, 2021, "Effects of ultra-high doserate FLASH irradiation on the tumor microenvironment in Lewis lung carcinoma: Role of myosin light chain," Int. J. Radiat. Oncol. Biol. Phys. **109**, 1440–1453.

Konradsson, E., M. L. Arendt, K. Bastholm Jensen, B. Børresen, A. E. Hansen, S. Bäck, A. T. Kristensen, P. Munck af Rosenschöld , C. Ceberg, and K. Petersson, 2021, "Establishment and initial experience of clinical FLASH radiotherapy in canine cancer patients," Front. Oncol. **11**, 658004.

Krieger, M., S. van de Water, M. M. Folkerts, A. Mazal, S. Fabiano, N. Bizzocchi, D. C. Weber, S. Safai, and A. J. Lomax, 2022, "A quantitative FLASH effectiveness model to reveal potentials and pitfalls of high dose rate proton therapy," Med. Phys. **49**, 2026–2038.

Kutsaev, S. V., *et al.*, 2021, "Linear accelerator for security, industrial and medical applications with rapid beam parameter variation," Radiat. Phys. Chem. **183**, 109398.

Laissue, J. A., *et al.*, 2013, "Response of the rat spinal cord to x-ray microbeams," Radiother. Oncol. **106**, 106–111.

Lang, X. T., *et al.*, 2019, "Radiotherapy and immunotherapy promote tumoral lipid oxidation and ferroptosis via synergistic repression of SLC7A11," Cancer Discovery **9**, 1673–1685.

Lansonneur, P., V. Favaudon, S. Heinrich, C. Fouillade, P. Verrelle, and L. De Marzi, 2019, "Simulation and experimental validation of a prototype electron beam linear accelerator for preclinical studies," Phys. Med. **60**, 50–57.

Lee, G., *et al.*, 2016, "Oxidative dimerization of PHD2 is responsible for its inactivation and contributes to metabolic reprogramming via HIF-1α activation," Sci. Rep. **6**, 18928.

Lefaix, J. L., and F. Daburon, 1998, "Diagnosis of acute localized irradiation lesions: Review of the French experimental experience," Health Phys. **75**, 375–384.

Lei, G., C. Mao, Y. L. Yan, L. Zhuang, and B. Y. Gan, 2021, "Ferroptosis, radiotherapy, and combination therapeutic strategies," Protein Cell **12**, 836–857.

Lempart, M., B. Blad, G. Adrian, S. Back, T. Knoos, C. Ceberg, and K. Petersson, 2019, "Modifying a clinical linear accelerator for delivery of ultra-high dose rate irradiation," Radiother. Oncol. **139**, 40–45.

Levy, K., *et al.*, 2020, "Abdominal FLASH irradiation reduces radiation-induced gastrointestinal toxicity for the treatment of ovarian cancer in mice," Sci. Rep. **10**, 21600.

Lievens, Y., J. M. Borras, and C. Grau, 2015, "Cost calculation: A necessary step towards widespread adoption of advanced radiotherapy technology," Acta Oncol. **54**, 1275–1281.

Liljedahl, E., E. Konradsson, E. Gustafsson, K. F. Jonsson, J. K. Olofsson, C. Ceberg, and H. N. Redebrandt, 2022, "Long-term anti-tumor effects following both conventional radiotherapy and FLASH in fully immunocompetent animals with glioblastoma," Sci. Rep. **12**, 12285.

Limoli, C. L., E. A. Kramar, A. Almeida, B. Petit, V. Grilj, J. E. Baulch, P. Ballesteros-Zebadua, B. W. Loo, Jr., M. A. Wood, and M. C. Vozenin, 2023, "The sparing effect of FLASH-RT on synaptic plasticity is maintained in mice with standard fractionation," Radiother. Oncol. **186**, 109767.

Limoli, C. L., P. Montay-Gruel, C. Bailat, and M. C. Vozenin, 2020, "The biology of FLASH radiotherapy," in *The Modern Technology of Radiation Oncology*, Vol. 4, edited by J. Van Dyk (Medical Physics Publishing, Madison, WI).

Limoli, C. L., and M.-C. Vozenin, 2023, "Reinventing radiobiology in the light of FLASH radiotherapy," Annu. Rev. Cancer Biol. **7**, 1–21.

Ling, C. C., H. B. Michaels, E. R. Epp, and E. C. Peterson, 1978, "Oxygen diffusion into mammalian cells following ultrahigh dose rate irradiation and lifetime estimates of oxygen-sensitive species," Radiat. Res. **76**, 522–532.

Liu, F., *et al.*, 2023, "Development of a compact linear accelerator to generate ultrahigh dose rate high-energy x-rays for FLASH radiotherapy applications," Med. Phys. **50**, 1680–1698.

Lomax, A. J., T. Bortfeld, G. Goitein, J. Debus, C. Dykstra, P. A. Tercier, P. A. Coucke, and R. O. Mirimanoff, 1999, "A treatment planning inter-comparison of proton and intensity modulated photon radiotherapy," Radiother. Oncol. **51**, 257–271.

Loo, Jr., B. W., E. Schueler, F. Lartey, M. Rafat, G. J. King, S. Trovatin, A. C. Kroong, and P. G. Maxim, 2017, "Delivery of ultra-rapid FLASH radiation therapy and demonstration of normal tissue sparing after abdominal irradiation of mice," Int. J. Radiat. Oncol. Biol. Phys. **98**, E16.

Lu, X., Z. Li, V. Dolgashev, G. Bowden, A. Sy, S. Tantawi, and E. A. Nanni, 2021, "A proton beam energy modulator for rapid proton therapy," Rev. Sci. Instrum. **92**, 024705.

Marconato, L., M. Weyland, N. Tresch, F. Rossi, V. Leone, and C. Rohrer Bley, 2020, "Toxicity and outcome in cats with oral squamous cell carcinoma after accelerated hypofractionated radiotherapy and concurrent systemic treatment," Vet. Comp. Oncol. **18**, 362–369.

Mascia, A. E., *et al.*, 2023, "Proton FLASH radiotherapy for the treatment of symptomatic bone metastases: The FAST-01 nonrandomized trial," JAMA Oncol. **9**, 62–69.

Maxim, P. G., P. Keall, and J. Cai, 2019, "FLASH radiotherapy: Newsflash or flash in the pan?," Med. Phys. **46**, 4287–4290.

Maxim, P. G., S. G. Tantawi, and B. W. Loo, 2019, "PHASER: A platform for clinical translation of FLASH cancer radiotherapy," Radiother. Oncol. **139**, 28–33.

Melzer, K., F. Guscetti, C. Rohrer Bley, A. Sumova, M. Roos, and B. Kaser-Hotz, 2006, "Ki67 reactivity in nasal and periocular squamous cell carcinomas in cats treated with electron beam radiation therapy," Vet. Intern. Med. **20**, 676–681.

Michaels, H. B., E. R. Epp, C. C. Ling, and E. C. Peterson, 1978, "Oxygen sensitization of CHO cells at ultrahigh dose rates: Prelude to oxygen diffusion studies," Radiat. Res. **76**, 510–521.

Miles, D., *et al.*, 2023, "FLASH effects induced by orthovoltage x-rays," Int. J. Radiat. Oncol. Biol. Phys. **117**, 1018–1027.

Moeckli, R., P. Gonçalves Jorge, V. Grilj, R. Oesterle, N. Cherbuin, J. Bourhis, M. C. Vozenin, J. F. Germond, F. Bochud, and C. Bailat, 2021, "Commissioning of an ultra-high dose rate pulsed electron beam medical LINAC for FLASH RT preclinical animal experiments and future clinical human protocols," Med. Phys. **48**, 3134–3142.

Montay-Gruel, P., G. Boivin, and M. C. Vozenin, 2016, "Novel strategies to prevent, mitigate or reverse radiation injury and fibrosis," in *Strategies to Enhance the Therapeutic Ratio of Radiation as a Cancer Treatment*, edited by M. S. Anscher and K. Valerie (Springer, New York).

Montay-Gruel, P., S. Corde, J. A. Laissue, and M. Bazalova-Carter, 2022, "FLASH radiotherapy with photon beams," Med. Phys. **49**, 2055–2067.

Montay-Gruel, P., *et al.*, 2017, "Irradiation in a flash: Unique sparing of memory in mice after whole brain irradiation with dose rates above 100 Gy/s," Radiother. Oncol. **124**, 365–369.

Montay-Gruel, P., *et al.*, 2018, "X-rays can trigger the FLASH effect: Ultra-high dose-rate synchrotron light source prevents normal brain injury after whole brain irradiation in mice," Radiother. Oncol. **129**, 582–588.

Montay-Gruel, P., *et al.*, 2019, "Long-term neurocognitive benefits of FLASH radiotherapy driven by reduced reactive oxygen species," Proc. Natl. Acad. Sci. U.S.A. **116**, 10943–10951.

Montay-Gruel, P., *et al.*, 2020, "Ultra-high-dose-rate FLASH irradiation limits reactive gliosis in the brain," Radiat. Res. **194**, 636–645.

Montay-Gruel, P., *et al.*, 2021, "Hypofractionated FLASH-RT as an effective treatment against glioblastoma that reduces neurocognitive side effects in mice," Clin. Cancer Res. **27**, 775–784.

Moon, E. J., K. Petersson, and M. M. Olcina, 2022, "The importance of hypoxia in radiotherapy for the immune response, metastatic potential and FLASH-RT," Int. J. Radiat. Biol. **98**, 439–451.

Nantista, C. D., and S. G. Tantawi, 2000, "A compact, planar, eight-port waveguide power divider/combiner: The cross potent super-hybrid," IEEE Microwave Guided Wave Lett. **10**, 520–522.

Nolan, M. W., M. S. Kent, and M. K. Boss, 2019, "Emerging translational opportunities in comparative oncology with companion canine cancers: Radiation oncology," Front. Oncol. **9**, 1291.

Overgaard, J., 2011, "Hypoxic modification of radiotherapy in squamous cell carcinoma of the head and neck—A systematic review and meta-analysis," Radiother. Oncol. **100**, 22–32.

Palma, B., M. Bazalova-Carter, B. Hardemark, E. Hynning, B. Qu, B. W. Loo, Jr., and P. G. Maxim, 2016, "Assessment of the quality of very high-energy electron radiotherapy planning," Radiother. Oncol. **119**, 154–158.

Palma, D. A., *et al.*, 2020, "Stereotactic ablative radiotherapy for the comprehensive treatment of oligometastatic cancers: Long-term results of the SABR-COMET phase II randomized trial," J. Clin. Oncol. **38**, 2830–2838.

Papiez, L., C. DesRosiers, and V. Moskvin, 2002, "Very high energy electrons (50–250 MeV) and radiation therapy," Technol. Cancer Res. Treat. **1**, 105–110.

Patterson, A. D., B. A. Carlson, F. Li, J. A. Bonzo, M. H. Yoo, K. W. Krausz, M. Conrad, C. Chen, F. J. Gonzalez, and D. L. Hatfield, 2013, "Disruption of thioredoxin reductase 1 protects mice from acute acetaminophen-induced hepatotoxicity through enhanced NRF2 activity," Chem. Res. Toxicol. **26**, 1088–1096.

Pawelke, J., M. Brand, S. Hans, K. Hideghety, L. Karsch, E. Lessmann, S. Lock, M. Schurer, E. R. Szabo, and E. Beyreuther, 2021, "Electron dose rate and oxygen depletion protect zebrafish embryos from radiation damage," Radiother. Oncol. **158**, 7–12.

Pelka, J. B., 2008, "Synchrotron radiation in biology and medicine," Acta Phys. Pol. A **114**, 309–329.

Petersson, K., G. Adrian, K. Butterworth, and S. J. McMahon, 2020, "A quantitative analysis of the role of oxygen tension in FLASH radiation therapy," Int. J. Radiat. Oncol. Biol. Phys. **107**, 539–547.

Petersson, K., M. Jaccard, J. F. Germond, T. Buchillier, F. Bochud, J. Bourhis, M. C. Vozenin, and C. Bailat, 2017, "High dose-per-pulse electron beam dosimetry—A model to correct for the ion recombination in the Advanced Markus ionization chamber," Phys. Med. **44**, 1157–1167.

Pistenmaa, D. A., M. Dosanjh, U. Amaldi, D. Jaffray, E. Zubizarreta, K. Holt, Y. Lievens, Y. Pipman, C. N. Coleman, and P. Workshop, 2018, "Changing the global radiation therapy paradigm," Radiother. Oncol. **128**, 393–399.

Poirier, V. J., B. Kaser-Hotz, D. M. Vail, and R. C. Straw, 2013, "Efficacy and toxicity of an accelerated hypofractionated radiation therapy protocol in cats with oral squamous cell carcinoma," Vet. Radiol. Ultrasound **54**, 81–88.

Ponette, V., N. Giocanti, H. Tourbez, J. Balosso, C. Hennequin, and V. Favaudon, 1996, "Pulse exposure to ionizing radiation elicits rapid changes in cellular radiosensitivity," C.R. Acad. Sci., Ser. III **319**, 505–509.

Prezado, Y., 2021, "Spatially fractionated radiotherapy," Radiother. Oncol. **161**, S554–S554.

Prezado, Y., S. Sarun, S. Gil, P. Deman, A. Bouchet, and G. Le Duc, 2012, "Increase of lifespan for glioma-bearing rats by using minibeam radiation therapy," J. Synchrotron Radiat. **19**, 60–65.

Rahman, M., M. R. Ashraf, R. Zhang, D. J. Gladstone, X. Cao, B. B. Williams, P. Jack Hoopes, B. W. Pogue, and P. Bruza, 2021, "Spatial and temporal dosimetry of individual electron FLASH beam pulses using radioluminescence imaging," Phys. Med. Biol. **66**, 135009.

Rahman, M., *et al.*, 2021, "Electron FLASH delivery at treatment room isocenter for efficient reversible conversion of a clinical LINAC," Int. J. Radiat. Oncol. Biol. Phys. **110**, 872–882.

Rahman, M., *et al.*, 2023, "Characterization of a newly designed diode dosimeter for UHDR FLASH radiotherapy," Med. Phys. **50**, 5875–5883.

Rezaee, M., I. Iordachita, and J. W. Wong, 2021, "Ultrahigh dose-rate (FLASH) x-ray irradiator for pre-clinical laboratory research," Phys. Med. Biol. **66**, 095006.

Rohrer Bley, C., *et al.*, 2022, "Dose- and volume-limiting late toxicity of FLASH radiotherapy in cats with squamous cell carcinoma of the nasal planum and in mini pigs," Clin. Cancer Res. **28**, 3814–3823.

Romano, F., C. Bailat, P. G. Jorge, M. L. F. Lerch, and A. Darafsheh, 2022, "Ultra-high dose rate dosimetry: Challenges and opportunities for FLASH radiation therapy," Med. Phys. **49**, 4912–4932.

Rosenblatt, E., J. Izewska, Y. Anacak, Y. Pynda, P. Scalliet, M. Boniol, and P. Autier, 2013, "Radiotherapy capacity in European countries: An analysis of the Directory of Radiotherapy Centres (DIRAC) database," Lancet Oncol. **14**, e79–86.

Ruan, J. L., *et al.*, 2021, "Irradiation at ultra-high (FLASH) dose rates reduces acute normal tissue toxicity in the mouse gastrointestinal system," Int. J. Radiat. Oncol. Biol. Phys. **111**, 1250–1261.

Rudra, S., *et al.*, 2019, "Using adaptive magnetic resonance image-guided radiation therapy for treatment of inoperable pancreatic cancer," Cancer Med. **8**, 2123–2132.

Sampayan, S. E., K. C. Sampayan, G. J. Caporaso, Y. J. Chen, S. Falabella, S. A. Hawkins, J. Hearn, J. A. Watson, and J. M. Zentler, 2021, "Megavolt bremsstrahlung measurements from linear induction accelerators demonstrate possible use as a FLASH radiotherapy source to reduce acute toxicity," Sci. Rep. **11**, 17104.

Schachtschneider, K. M., *et al.*, 2017, "The Oncopig cancer model: An innovative large animal translational oncology platform," Front. Oncol. **7**, 190.

Schneider, T., C. Fernandez-Palomo, A. Bertho, J. Fazzari, L. Iturri, O. A. Martin, V. Trappetti, V. Djonov, and Y. Prezado, 2022, "Combining FLASH and spatially fractionated radiation therapy: The best of both worlds," Radiother. Oncol. **175**, 169–177.

Schoenfeld, J. D., *et al.*, 2017, "O_2^- and H_2O_2-mediated disruption of Fe metabolism causes the differential susceptibility of NSCLC and GBM cancer cells to pharmacological ascorbate," Cancer Cell **31**, 487–500.

Schueler, E., M. Acharya, P. Montay-Gruel, B. W. Loo, Jr., M. C. Vozenin, and P. G. Maxim, 2022, "Ultra-high dose rate electron beams and the FLASH effect: From preclinical evidence to a new radiotherapy paradigm," Med. Phys. **49**, 2082–2095.

Schueler, E., K. Eriksson, E. Hynning, S. L. Hancock, S. M. Hiniker, M. Bazalova-Carter, T. Wong, Q. T. Le, B. W. Loo, Jr., and P. G. Maxim, 2017, "Very high-energy electron (VHEE) beams in radiation therapy; treatment plan comparison between VHEE, VMAT, and PPBS," Med. Phys. **44**, 2544–2555.

Schueler, E., S. Trovati, G. King, F. Lartey, M. Rafat, M. Villegas, A. J. Praxel, B. W. Loo, Jr., and P. G. Maxim, 2017, "Experimental platform for ultra-high dose rate FLASH irradiation of small

animals using a clinical linear accelerator," Int. J. Radiat. Oncol. Biol. Phys. **97**, 195–203.
Schüller, A., *et al.*, 2020, "The European joint research project UHDpulse—Metrology for advanced radiotherapy using particle beams with ultra-high pulse dose rates," Phys. Med. **80**, 134–150.
Schulte, R., *et al.*, 2023, "Transformative technology for FLASH radiation therapy," Appl. Sci. **13**, 5021.
Simakov, E. I., V. A. Dolgashev, and S. G. Tantawi, 2018, "Advances in high gradient normal conducting accelerator structures," Nucl. Instrum. Methods Phys. Res., Sect. A **907**, 221–230.
Simmons, D. A., *et al.*, 2019, "Reduced cognitive deficits after FLASH irradiation of whole mouse brain are associated with less hippocampal dendritic spine loss and neuroinflammation," Radiother. Oncol. **139**, 4–10.
Singers Sørensen, B., M. Krzysztof Sitarz, C. Ankjaergaard, J. Johansen, C. E. Andersen, E. Kanouta, C. Overgaard, C. Grau, and P. Poulsen, 2022, "*In vivo* validation and tissue sparing factor for acute damage of pencil beam scanning proton FLASH," Radiother. Oncol. **167**, 109–115.
Smyth, L. M. L., J. F. Donoghue, J. A. Ventura, J. Livingstone, T. Bailey, L. R. J. Day, J. C. Crosbie, and P. A. W. Rogers, 2018, "Comparative toxicity of synchrotron and conventional radiation therapy based on total and partial body irradiation in a murine model," Sci. Rep. **8**, 12044.
Sørensen, B. S., M. K. Sitarz, C. Ankjaergaard, J. G. Johansen, C. E. Andersen, E. Kanouta, C. Grau, and P. Poulsen, 2022, "Pencil beam scanning proton FLASH maintains tumor control while normal tissue damage is reduced in a mouse model," Radiother. Oncol. **175**, 178–184.
Soto, L. A., *et al.*, 2020, "FLASH irradiation results in reduced severe skin toxicity compared to conventional-dose-rate irradiation," Radiat. Res. **194**, 618–624.
Spitz, D. R., E. I. Azzam, J. J. Li, and D. Gius, 2004, "Metabolic oxidation/reduction reactions and cellular responses to ionizing radiation: A unifying concept in stress response biology," Cancer Metastasis Rev. **23**, 311–322.
Spitz, D. R., G. R. Buettner, M. S. Petronek, J. J. St-Aubin, R. T. Flynn, T. J. Waldron, and C. L. Limoli, 2019, "An integrated physico-chemical approach for explaining the differential impact of FLASH versus conventional dose rate irradiation on cancer and normal tissue responses," Radiother. Oncol. **139**, 23–27.
Stephan, F., *et al.*, 2022, "FLASHlab@PITZ: New R&D platform with unique capabilities for electron FLASH and VHEE radiation therapy and radiation biology under preparation at PITZ," Phys. Med. **104**, 174–187.
Stockwell, B. R., *et al.*, 2017, "Ferroptosis: A regulated cell death nexus linking metabolism, redox biology, and disease," Cell **171**, 273–285.
Tantawi, S., M. Nasr, Z. H. Li, C. Limborg, and P. Borchard, 2020, "Design and demonstration of a distributed-coupling linear accelerator structure," Phys. Rev. Accel. Beams **23**, 092001.
Tantawi, S. G., C. D. Nantista, V. A. Dolgashev, C. Pearson, J. Nelson, K. Jobe, J. Chan, K. Fant, J. Frisch, and D. Atkinson, 2005, "High-power multimode *X*-band rf pulse compression system for future linear colliders," Phys. Rev. ST Accel. Beams **8**, 042002.
Taylor, P. A., J. M. Moran, D. A. Jaffray, and J. C. Buchsbaum, 2022, "A roadmap to clinical trials for FLASH," Med. Phys. **49**, 4099–4108.
Tinganelli, W., *et al.*, 2022a, "Ultra-high dose rate (FLASH) carbon ion irradiation: Dosimetry and first cell experiments," Int. J. Radiat. Oncol. Biol. Phys. **112**, 1012–1022.
Tinganelli, W., *et al.*, 2022b, "FLASH with carbon ions: Tumor control, normal tissue sparing, and distal metastasis in a mouse osteosarcoma model," Radiother. Oncol. **175**, 185–190.
Town, C. D., 1967, "Radiobiology. Effect of high dose rates on survival of mammalian cells," Nature (London) **215**, 847–848.
Traver, D., A. Winzeler, H. M. Stern, E. A. Mayhall, D. M. Langenau, J. L. Kutok, A. T. Look, and L. I. Zon, 2004, "Effects of lethal irradiation in zebrafish and rescue by hematopoietic cell transplantation," Blood **104**, 1298–1305.
Valdes Zayas, A., *et al.*, 2023, "Independent reproduction of the FLASH effect on the gastrointestinal tract: A multi-institutional comparative study," Cancers **15**, 2121.
van der Reest, J., S. Lilla, L. Zheng, S. Zanivan, and E. Gottlieb, 2018, "Proteome-wide analysis of cysteine oxidation reveals metabolic sensitivity to redox stress," Nat. Commun. **9**, 1581.
van Marlen, P., M. Dahele, M. Folkerts, E. Abel, B. J. Slotman, and W. Verbakel, 2020, "Bringing FLASH to the clinic: Treatment planning considerations for ultrahigh dose-rate proton beams," Int. J. Radiat. Oncol. Biol. Phys. **106**, 621–629.
Velalopoulou, A., *et al.*, 2021, "FLASH proton radiotherapy spares normal epithelial and mesenchymal tissues while preserving sarcoma response," Cancer Res. **81**, 4808–4821.
Venkatesulu, B. P., A. Sharma, J. M. Pollard-Larkin, R. Sadagopan, J. Symons, S. Neri, P. K. Singh, R. Tailor, S. H. Lin, and S. Krishnan, 2019, "Ultra high dose rate (35 Gy/ sec) radiation does not spare the normal tissue in cardiac and splenic models of lymphopenia and gastrointestinal syndrome," Sci. Rep. **9**, 17180.
Venkatesulu, B. P., A. Sharma, J. M. Pollard-Larkin, R. Sadagopan, J. Symons, S. Neri, P. K. Singh, R. Tailor, S. H. Lin, and S. Krishnan, 2020, "Author correction: Ultra high dose rate (35 Gy/ sec) radiation does not spare the normal tissue in cardiac and splenic models of lymphopenia and gastrointestinal syndrome," Sci. Rep. **10**, 11018.
Vozenin, M. C., J. Bourhis, and M. Durante, 2022, "Towards clinical translation of FLASH radiotherapy," Nat. Rev. Clin. Oncol. **19**, 791–803.
Vozenin, M. C., J. H. Hendry, and C. L. Limoli, 2019, "Biological benefits of ultra-high dose rate FLASH radiotherapy: Sleeping beauty awoken," Clin. Oncol. **31**, 407–415.
Vozenin, M. C., *et al.*, 2019, "The advantage of FLASH radiotherapy confirmed in mini-pig and cat-cancer patients," Clin. Cancer Res. **25**, 35–42.
Wasselin-Trupin, V., G. Baldacchino, S. Bouffard, and B. Hickel, 2002, "Hydrogen peroxide yields in water radiolysis by high-energy ion beams at constant LET," Radiat. Phys. Chem. **65**, 53–61.
Whelan, B., *et al.*, 2022, "Bayesian optimization to design a novel x-ray shaping device," Med. Phys. **49**, 7623–7637.
Wiernicki, B., H. Dubois, Y. Y. Tyurina, B. Hassannia, H. Bayir, V. E. Kagan, P. Vandenabeele, A. Wullaert, and T. Vanden Berghe, 2020, "Excessive phospholipid peroxidation distinguishes ferroptosis from other cell death modes including pyroptosis," Cell Death Dis. **11**, 922.
Winter, J., M. Galek, C. Matejcek, J. J. Wilkens, K. Aulenbacher, S. E. Combs, and S. Bartzsch, 2020, "Clinical microbeam radiation therapy with a compact source: Specifications of the line-focus x-ray tube," Phys. Imaging Radiat. Oncol. **14**, 74–81.
Withers, H. R., *et al.*, 1995, "Late normal tissue sequelae from radiation therapy for carcinoma of the tonsil: Patterns of fractionation study of radiobiology," Int. J. Radiat. Oncol. Biol. Phys. **33**, 563–568.
Yamamoto, M., T. W. Kensler, and H. Motohashi, 2018, "The KEAP1-NRF2 system: A thiol-based sensor-effector apparatus for maintaining redox homeostasis," Physiol. Rev. **98**, 1169–1203.

Yarnold, J., and M. C. Brotons, 2010, "Pathogenetic mechanisms in radiation fibrosis," Radiother. Oncol. **97**, 149–161.

Zhang, Q., E. Cascio, C. Li, Q. Yang, L. E. Gerweck, P. Huang, B. Gottschalk, J. Flanz, and J. Schuemann, 2020, "FLASH investigations using protons: Design of delivery system, preclinical setup and confirmation of FLASH effect with protons in animal systems," Radiat. Res. **194**, 656–664.

Zhu, Y., A. E. Dean, N. Horikoshi, C. Heer, D. R. Spitz, and D. Gius, 2018, "Emerging evidence for targeting mitochondrial metabolic dysfunction in cancer therapy," J. Clin. Invest. **128**, 3682–3691.

Zlobinskaya, O., G. Dollinger, D. Michalski, V. Hable, C. Greubel, G. Du, G. Multhoff, B. Roper, M. Molls, and T. E. Schmid, 2012, "Induction and repair of DNA double-strand breaks assessed by gamma-H2AX foci after irradiation with pulsed or continuous proton beams," Radiat. Environ. Biophys. **51**, 23–32.

Zou, W., *et al.*, 2021, "Current delivery limitations of proton PBS for FLASH," Radiother. Oncol. **155**, 212–218.

See Supplemental Material at http://link.aps.org/supplemental/10.1103/RevModPhys.96.035002 for metrology and medical physics requirements to support clinical application of FLASH.